Surface protection of steel CR4 by using *N-acyl* sarcosine derivatives in salt water

by

Saad Elias Kaskah

from Baghdad - Iraq

Accepted Dissertation thesis for the partial fulfilment of the requirements for a

Doctor of Natural Sciences

Fachbereich 3: Mathematik/Naturwissenschaften

Universität Koblenz-Landau

Reviewer:

Dr. Christian B. Fischer

Prof. Dr. Jörg Gollnick

Examiner:

Dr. Christian B. Fischer

Prof. Dr. Jörg Gollnick

Prof. Dr. Wolfgang Imhof

Date of the oral examination: 31st August 2018

Abstract in English

Different techniques (weight loss, electrochemical, and spray corrosion measurements) have been used to evaluate four sarcosine derivatives to inhibit corrosion and one commercial compound as synergist. The basic metal was low carbon steel CR4 tested at different conditions. As working media mainly neutral water and 0.1 M NaCl was applied. The protective film was formed on the steel surface via direct absorption of the tested substances during the immersion process.

A highly improved corrosion protection with direct correlation to the molecular weight and carbon chain length of the tested compounds was detected. The protection of steel CR4 against corrosion in 0.1 M NaCl enhanced with increasing concentration of selected sarcosine compounds. The best inhibitor throughout all tested concentrations and all evaluation systems was Oleoylsarcosine (O) with efficiencies up to 97 % in potentiodynamic polarization (PP), 83 % electrochemical impedance spectroscopy (EIS), and 85 % weight loss (WL) at 100 mmol/L as highest concentration tested here. The second best inhibitor was Myristoylsarcosine (M) with efficiencies up to 82 % in PP, 69 % in EIS, and 75 % in WL at highest concentration. The inhibitor with the shortest hydrocarbon chain in this series is Lauroylsarcosine (L). It showed lowest effects to inhibit corrosion compared to O and M. The efficiencies of L were a bit more than 50 % at 75 and 100 mmol/L and less than 50 % at 25 and 50 mmol/L in all used evaluation systems. Furthermore, the overall efficiency is promoted with longer dip coating times during the steel CR4 immersion as shown for 50 mmol/L for all present derivatives. This survey indicated 10 min as best time in respect of cost and protection efficiency.

The commercial inhibitor Oley-Imidazole (OI) improved significantly the effectiveness of compound Cocoylsarcosine (C), which contains the naturally mixture of carbon chain lengths from coconut oil (C_8 - C_{18}), and enhanced protection when used in combination (C+OI, 1:1 molar ration). In this system the efficiency increased from 47 % to 91 % in PP, from 40 % to 84 % in EIS, and from 45 % to 82 % in WL at highest concentration.

Spray corrosion tests were used to evaluate all present sarcosine substances on steel CR4 in a more realistic system. The best inhibitor after a 24 h test was O followed by the combination C+OI and M with efficiencies up to 99 %, 80 %, and 79 %, respectively. The obtained results indicate a good stability of the protective film formed by the present inhibitors even after 24 h.

All evaluation systems used in the current investigation were in good agreement and resulted in the same inhibitor sequence. Furthermore, the adsorption process of the tested compounds is assumed to follow the Langmuir type isotherm.

Response surface methodology (RSM) is an optimization method depending on Box-Behnken Design (BBD). It was used in the current system to find the optimum efficiency for inhibitor O to protect steel CR4 against corrosion in salt water. Four independent variables were used here: inhibitor concentration (A), dip coating time (B), temperature (C), and NaCl concentration (D); each with three respective levels: lower (-1), mid (0), and upper (+1). According to the present result, temperature has the greatest effect on the protection process as individual parameter followed by the inhibitor concentration itself. In this investigation an optimum efficiency of 99 % is calculated by the following parameter and level combination: upper level (+1) for inhibitor concentration, dip coating time, and NaCl concentration while lower level (-1) for temperature.

Abstract auf Deutsch

Verschiedene Methoden (Gewichtsverlust, elektrochemische und Sprühkorrosions-messungen) wurden eingesetzt, um die Korrosionsinhibierung von vier Sarkosinderivaten und einer kommerziellen Verbindung als Synergist zu bewerten. Das Basismetall war kohlenstoffarmer Stahl CR4, der unter verschiedenen Bedingungen getestet wurde. Als Arbeitsmedien wurden hauptsächlich neutrales Wasser und 0.1 M NaCl eingesetzt. Der Schutzfilm wurde auf der Stahloberfläche durch direkte Apsorption der Prüfsubstanzen während des Eintauchprozesses gebildet.

Ein stark verbesserter Korrosionsschutz mit direkter Korrelation zwischen Molekulargewicht und Kohlenstoffkettenlänge der Prüfsubstanzen konnte nachgewiesen werden. Die Schutzwirkung der ausgewählten Sarkosinverbindungen auf Stahl CR4 erhöht sich in 0.1 M NaCl mit zunehmender Konzentration. In allen getesteten Methoden und Konzentrationen erwies sich Oleoylsarcosin (O) als bester Inhibitor. Es wurden Wirksamkeiten bis zu 97 % in der potentiodynamischen Polarisation (PP), 83 % bei der elektrochemische Impedanz-spektroskopie (EIS) und 85 % in der Gewichtsabnahme (WL) bei 100 mmol/L als höchster hier getesteten Konzentration erzielt. Der zweitbeste Inhibitor ist Myristoylsarcosin (M) mit Effektivitäten bis zu 82 % in PP, 69 % in EIS und 75 % in WL ebenfalls bei der höchsten Konzentration. Der Inhibitor mit der kürzesten Kette in dieser Testreihe ist Lauroylsarcosin (L). L ergab Schutzwirkungen von etwas über 50 % bei 75 und 100 mmol/L und unter 50 % bei 25 und 50 mmol/L in allen angewandten Methoden. Zudem werden die Gesamteffizienzen aller verwendeten Prüfsubstanzen durch längere Einwirkzeiten beim Eintauchen der CR4 Stahlproben erhöht, wie für 50 mmol/L gezeigt werden konnte. Die Untersuchung ergab 10 Minuten als beste Zeit bezüglich Kosten- und Schutzeffizienz.

Der kommerzielle Inhibitor Oley-Imidazol (OI) verbesserte die Wirksamkeit von Cocoylsarcosin (C), der natürlichen Mischung aus Kokosnussöl mit Kohlenstoffkettenlängen von C8 - C18, und verbesserte den Schutz in einer 1:1 (mol) Kombination (C+OI). Hierbei stieg der Wirkungsgrad von 47 % auf 91 % in PP, von 40 % auf 84 % in EIS und von 45 % auf 82 % in WL bei der höchsten Konzentration.

Mit Hilfe von Sprühkorrosionstests wurden alle vorliegenden Sarkosinsubstanzen auf Stahl CR4 in einem realistischeren System untersucht. Der beste Inhibitor nach einem 24-Stunden-Test war O, gefolgt von der Kombination C+OI und M mit entsprechenden Wirkungsgraden von bis zu 99 % (O), 80 % (C+OI) bzw. 79 % (M). Die erhaltenen Ergebnisse zeigen eine gute Stabilität der Prüfsubstanzen bezüglich des gebildeten Schutzfilms auch nach 24 h.

Alle verwendeten Methoden ergaben in der aktuellen Untersuchung übereinstimmende Ergebnisse und die gleiche Reihenfolg der Inhibitoren. Darüber hinaus wird angenommen, dass der Adsorptionsprozess der Prüfsubstanzen der Langmuir-Isotherme folgt.

Die Response Surface Methodik (RSM) ist eine vom Box-Behnken Design (BBD) abhängige Optimierungsmethode. Diese wurde im aktuellen System angewandt, um die optimale Effektivität für Inhibitor O beim Korrosionsschutz von Stahl CR4 in Salzwasser zu ermitteln. Hierfür wurden vier unabhängige Variablen benutzt: Inhibitorkonzentration (A), Tauchbeschichtungszeit (B), Temperatur (C) und NaCl-Konzentration (D); jeweils in drei Stufen: untere (-1), mittlere (0) und obere (+1). Nach dem vorliegenden Ergebnis hat die Temperatur als Einzelparameter den größten Einfluss auf den Schutzprozess, gefolgt von der Inhibitorkonzentration. Anhand der Berechnung ergibt sich ein optimaler Wirkungsgrad von 99 % durch folgende Parameter- und Pegelkombination: oberer Wert (+1) jeweils für Inhibitorkonzentration, Tauchbeschichtungszeit und NaCl-Konzentration sowie ein unterer Wert (-1) für die Temperatur.

Index

Index

Symbols and abbreviations

List of symbols and abbreviations

Symbol	Details
CR4	Low carbon steel grade CR4 (also denoted as 1.0330 or DC01)
C	Cocoylsarcosine
L	Lauroylsarcosine
M	Myristoylsarcosine
O	Oleoylsarcosine
OI	Oleyl-Imidazoline
MI	Methyl-Imidazole
C+OI	Combination of Cocoylsarcosine and Oleyl Imidazoline
OCP	Open circuit potential
EIS	Electrochemical impedance spectroscopy
WE	Working electrode
RE	Reference electrode
AE	Auxiliary electrode
E_{corr}	Corrosion potential
i_{corr}	Corrosion current density
Θ	Surface coverage
IE	Inhibitor efficiency
i_{inh}	Corrosion current density of present inhibitor
β_a	Anodic Tafel slope
β_c	Cathodic Tafel slope
CR	Corrosion rate
ΔW	Weight loss of steel CR4 in absence inhibitor
ΔW_{inh}	Weight loss of steel CR4 in presence inhibitor
A	Total area of sample
t	Relevant immersion time of the coupon in the 0.1 N NaCl test solution.
C_{inh}	Concentration of inhibitor
R_{ct}	Charge transfer in absence inhibitor
R_{inh}	Charge transfer in presence inhibitor
K	Adsorption constant

Symbols and abbreviations

ΔG_{ads}	Standard of free energy of adsorption
R^2	Square regression coefficient
A_1	Relative corrosion area in absence inhibitor
A_2	Relative corrosion area in presence inhibitor

List of symbols and abbreviations - Optimization

Symbol	Details
DOE	Design of experiment
BBD	Box-Behnken Design
RSM	Response surface methodology
Y	Dependent response (efficiency of inhibitor O to protect steel CR4 in salt water)
A	Inhibitor concentration
B	Immersed time of steel CR4 probes in inhibitor stock
C	Temperature
D	NaCl content in test solution
β	Regression coefficient
S	Number of experiments
L	Number of levels
k	Number of independent variables
ℓH	Higher value of effect
ℓL	Lower value of effect
E_f	Estimated effect

Chapter one

Introduction

1.1 Preface

Corrosion is a deterioration of a material when it reacts with its environment through chemical or electrochemical processes and it is a natural phenomenon [1-4]. Several parameters may are included in the corrosive environment like moisture, oxygen, temperature, high pressure, chlorides, inorganic and organic acids [2]. Metals and alloys show the tendency to be more stable thermodynamically by releasing the energy added to the ores during spontaneously reaction of corrosion [5]. Corrosion occurs in different conditions when metals and alloys are exposed in electrolytes or in presence of moisture on the metal surface [2]. In the case of steel, electrochemical process consists of three main parts: Anode which is the side that the oxidation reaction occurs, cathode where the reduction reaction occurs, solution of the work as environment (Fig. 1) [1-3]. The dissolution of metal takes place on anodic side giving electrons while reduction of hydrogen or oxygen locates at the cathode [2]. Fig. 1 represents a real corrosion system that shows the electron flow from anode to cathode regions when steel surface in contact with a drop of water.

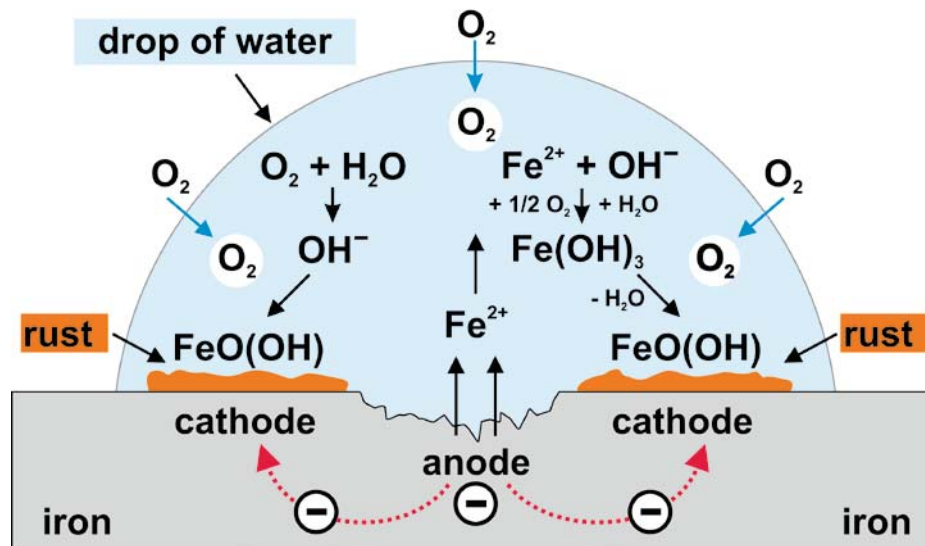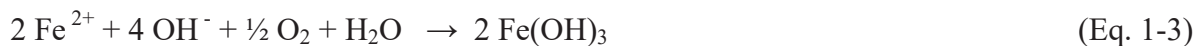**Fig. 1-1:** Scheme of local corrosion cell shows anode and cathode regions on iron surface when it is contact with a drop of water [6].

At the region of steel surface (anode) iron oxidizes to Fe^{2+} ions (Eq. 1-1) and at the other place on the surface (cathode) oxygen reduces under formation of OH^- ions (Eq. 1-2).

$$2\ Fe \quad \rightarrow \quad 2\ Fe^{2+} + 4\ e^- \qquad\qquad\qquad Oxidation\ (Anode) \quad (Eq.\ 1\text{-}1)$$

$$2\,H_2O \;+\; O_2 \;+\; 4\,e^- \quad\rightarrow\quad 4\,OH^- \qquad\qquad \text{Reduction (Cathode)} \quad (Eq.\ 1\text{-}2)$$

The formed Fe^{2+} and OH^- ions move through the water to form $Fe(OH)_3$ (Eq. 1-3) which contains a certain amount of water and is unstable when in contact with oxygen. It changes via the deposit of $FeO(OH)$ (Eq. 1-4). When water is present with $Fe_2O_3 \cdot xH_2O$ representing the genuine form of rust (Eq. 1-5). The term of ″rust″ comprises in overall more than 30 different iron compounds that are formed and modified depending on the environmental conditions [4,7,8].

$$2\,Fe^{2+} + 4\,OH^- + \tfrac{1}{2}\,O_2 + H_2O \;\rightarrow\; 2\,Fe(OH)_3 \qquad\qquad\qquad (Eq.\ 1\text{-}3)$$

$$Fe(OH)_3 \qquad\rightarrow\qquad FeO(OH) \;+\; H_2O \qquad\qquad\qquad (Eq.\ 1\text{-}4)$$

$$2\,FeO(OH) \;=\; Fe_2O_3 \cdot x\,H_2O \;+\; y\,H_2O \qquad\qquad\qquad (Eq.\ 1\text{-}5)$$

1.2 Electrochemical polarization

Corrosion reaction of metal can be chemical or electrochemical depending on work conditions and overall it is an electrochemical process. Many types of reactions occur when steel is submerged in a solution. Metal forms its ions by the loss of electrons or obtain electrons and enter the solid metal state during reduction reaction [2]. The parity of the partial Gibbs free-energy or chemical potentials on either side of the electrode determines the equilibrium to identify which reaction occur across the metal-solution interface [2,3]. During immersion the metal in the electrolyte, thermodynamics tendency to interfacial electron transfer until the electrochemical potentials on both sides are balanced and the net current is zero [2,9]. The shift that results by a changed net current between anode and cathode electrodes is called polarization [10]. The net equivalent current that flows across the interface per unit surface area when there is no external current source is known as the exchange current density (i_{corr}). Polarization of the corroding electrode in the specific medium is control the system when it can be anodic or cathodic polarization [2]. Both oxidation and reduction reactions have a respective slope in the polarization curve known as anodic and cathodic Tafel slope [2]. There are specific parameters like exchange current density (i_{corr}), potential of electrode (E), and transfer coefficient of anodic and cathodic reactions affect on the Tafel slope [2]. The system is anodically in equilibrium when Tafel

slope for anode is higher than cathode and it is cathodically in equilibrium when Tafel slope for cathode is larger than anode [2]. Corresponding on the corrosion potential E_{corr} and corrosion current density i_{corr} per area A (i_{corr} = I_{corr}/A), there are four types of polarization: activation, concentration, combined, and resistance polarization [3].

Electrochemical evaluation can be used to estimate the corrosion rate of metals when both oxidation and reduction processes occur on metal surface during immersion in a corrosive medium [2,11-14].

Corrosion rate (CR) can be expressed by different ways depending on the method of evaluation used. In present work different evaluation techniques are used to find the corrosion rate, in weight loss measurement it is determined according to mass loss during test while in electrochemical tests it is calculated depending on exchange current density (i_{corr}) and in spray corrosion test it is estimated from the corroded metal surface area (A).

1.3 Corrosion protection by the use of inhibitors

The prevention from corrosion is the main consideration to enhance safety, better performance, and economic impact by reduce the loss of materials [3,10,15]. The protection of metals, especially low carbon steel against corrosion is an important task because it is widely used in industry and in various applications for its mechanical and physical properties [4,7].

Several ways exist to prevent metals from corrosion and one of the most effective and lower cost protection method in many applications is the use of inhibitors [8,16-21]. To prevent materials degradation, which in particular proceeds on the metal surface, the application of corrosion inhibitors is considered to be the first line of defense against beginning corrosion, especially in the oil and processing industries [21,22]. In general, an inhibitor can be defined as a chemical substance that suppresses corrosion when added to corrosive environments containing a metal or an alloy [2,23-26]. Inhibitors can also apply in the protection system when they are added as dissolvable pigments in organic coatings or paint [27]. These compounds effect to retard corrosion of metals and alloys immersed in corrosive solution via different mechanisms depending on the basic metal, type of working media, and nature of inhibitor [2]. These mechanisms decrease corrosion by (i) adsorption of inhibitor anion by metal surface, (ii) close the pores of the passive oxide film, (iii) improving passive film by reparation of damaged oxide film, and (iv) reducing the dissolution of metal [2,28]. In

general, inhibitors are classified into two types environmental conditioners which decrease corrosivity of the medium and interface inhibitor that reduce corrosion by forming a barrier film at the metal surface towards the environment [29]. Interface inhibitors are sub classified to vapour and liquid type (Fig. 1-2) [29].

Inhibitors are classified depending on their chemical nature into organic (grease, wax, paints) and inorganic non-metallic (oxides, phosphates, enamel) inhibitors [8,17]. They are classified also according to their effect on anodic and cathodic reactions as anodic, cathodic, or mixed inhibitor [30-35]. The hierarchy in Fig. 1-2 summarizes the respective classification of inhibitors [29].
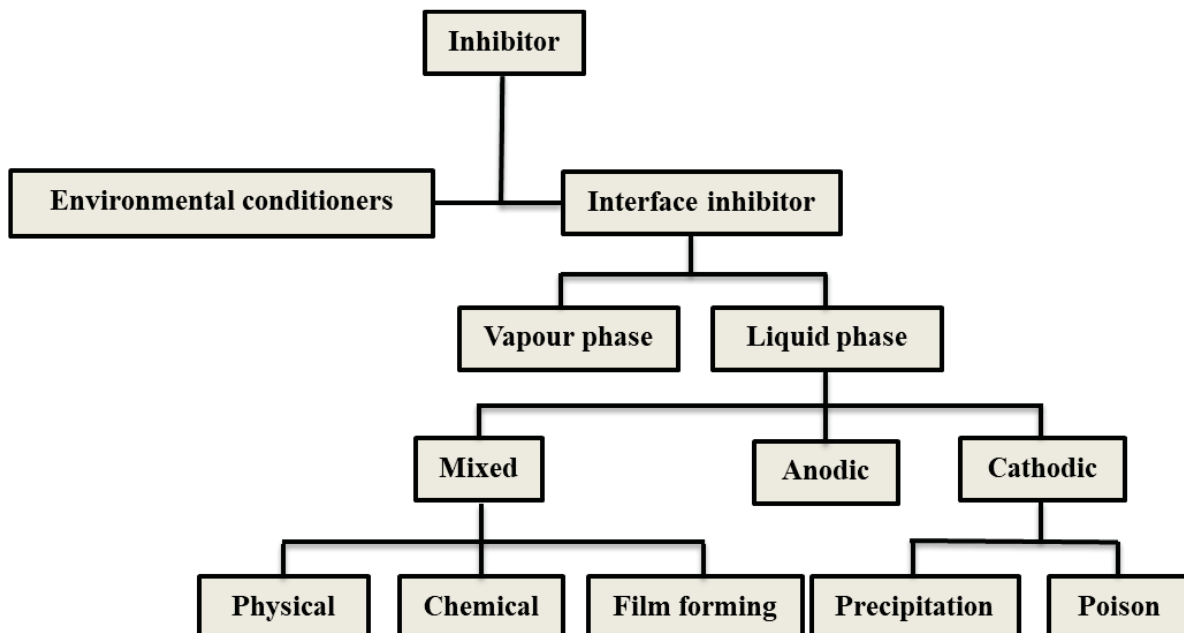

Fig. 1-2: Hierarchy for classification of inhibitors [29].

Nevertheless, the application of chemical inhibitors is one of the most efficient approaches to reduce corrosion [36,37]. Some of these chemical inhibitors like nitrate, chromate, and dichromate have toxic and hazardous risks to both humans and the environment [2,23,38]. Furthermore, environmental regulations require non-toxic and sustainable inhibitor substances for corrosion protection without causing any environmental damage [39]. An efficient inhibitor would be preferably environmentally friendly and of low cost in application as well [21,39]. Organic compounds that have sulfur, nitrogen, and oxygen atoms or heterocyclic compounds containing polar groups are used as alternative corrosion inhibitor instead of chemical one [2,40-44]. The whole surface area of corroding metal is covered with

a protective film comprising of several monolayers that are formed by the organic inhibitor. This barrier film changes the structure of the double layer at the metal interface and decreases the depolarization rate [2]. The initially physisorbed film formed by charged ionic species of inhibitor through van Der Waals forces then stabilized through chemisorption [45]. Adsorption of organic molecules via metal surface can be proceeding by physorption when the activation energy is low or by chemisorption with high activation energy [2]. In physorption the adsorption of attractive forces between the charged surface of the metal and organic ions or dipoles results as electrostatic adsorption while in chemisorption the interaction between unshared electron pairs or "P" electrons from organic substances and the metal orbitals leads to form a "coordinate-type" bond [2].

Several recent studies investigated organic compounds like amino acids, derivatives of amino carboxylic acids, monocarboxylic, dicarboxylic acids, and many others as corrosion inhibitor to protect steel [46-62]. Additional researches detected a synergistic behavior for a combination of fatty amines containing an Oleoyl residue together with phosphor containing carboxylic acids for carbon steel protection with a mixed type inhibitor effect in basic surrounding [63-65]. There are different mechanisms to accomplish the corrosion inhibition. Some inhibitors interact with metal surface and forming a barrier film on the surface like organic amines and imidazolines while others caused a changed chemistry of environment to be less acidic by adjusting the pH [66].

The main concept of organic inhibitors is to build up a protective barrier film between the metal or alloy and its environment (Fig. 1-3). The basic mechanism is to change the active metallic surface status to a more passive one and reduce corrosion [2,67,68]. An appropriate and effective inhibitor is a substance which retards corrosion by different mechanisms when added in a small amount to the working media or as dissolvable pigments in organic coatings [3,7,21,27].

There are many physicochemical characteristics of the overall inhibitor structure containing functional groups (e.g. aromaticity, possible steric effects, electronic density of donors and/or acceptors) affected on the protective film formation and its stability on the metal surface. The adsorption ability of inhibitor molecules on the surface of metals is significantly affected by their molecular structure, the surface state and the surface excess charge of metal [69,70].
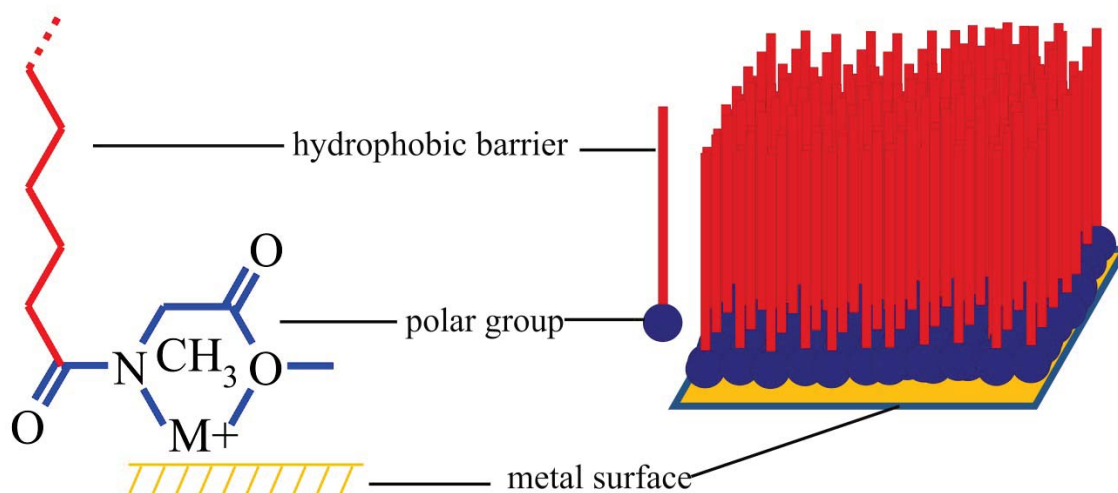
Fig. 1-3: Scheme of organic inhibitor mechanism shows polar group attach to metal surface and barrier film formed by hydrocarbon chain [26].

Additionally, other factors like elemental composition of basic metal, aggressiveness of the environment (pH-value), temperature, type and concentration of inhibitor, and exposure time govern the protection process [2,66]. In general, the presence of inhibitors causes shifting of corrosion potential E_{corr} to anodic or cathodic direction and decreasing exchange current density i_{corr} to lower value (Fig. 1-4).

Organic compounds including the present sarcosine fatty acid *N*-Acyl-derivatives are a matter of increasing interest because of their low cost and potential adsorption behavior to the metal surface [38,71,72]. The naturally occurring amino acid sarcosine derivatives investigated here [69], namely Cocoyl-(C), Lauroyl-(L), Myristoyl-(M), and Oleoylsarcosine-(O) are evaluated as potential inhibitors. The sarcosine candidates are of anionic nature and registered as mild amino acid based surfactants and known to show corrosion protection efficiencies as Na-salt [73], are environmentally friendly and possess aerobic and anaerobic biodegradability [74,75]. The derivatives of the sarcosine series used here only differ in the type and length of the attached fatty acid residue except Cocoylsarcosine (C) which contains a natural mixture of hydrocarbon chain length (C_8 - C_{18}). As it is well known, a longer carbon chain is more favorable for corrosion prevention and preferred to be a C3 chain or more [2,50-53].

Two organic compounds Oleyl-Imidazoline (OI) and Methyl-Imidazole (MI) are tested as synergists to improve the efficiency of selected inhibitors.

Herein low carbon steel grade CR4 (also denoted as 1.0330 or DC01) is used as basic metal. Protection against corrosion is tested by using selected organic compounds in 0.1 M NaCl and tab water. The corrosion experiments were electrochemically performed with a potentiostat and via impedance spectroscopy for short term. For more realistic and longer

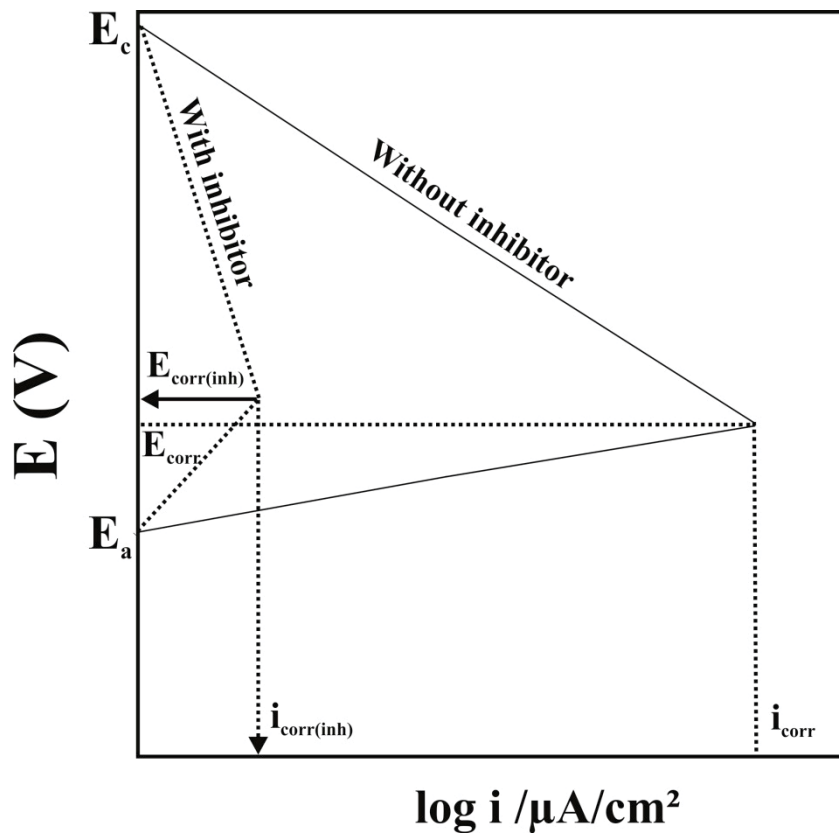duration the substances are evaluated via a homemade spray corrosion chamber and weight loss measurement.

Fig. 1-4: Scheme of anodic and cathodic polarization in absence and presence of an inhibitor during electrochemical system for steel in pickling acid [70].

Most organic inhibitors are dissolvable in water and they can be used directly by adding them into the test solution. Others including current compounds are not dissolvable in water. Therefore it is needed to find an experimental technique to use them in applications. In the current study, tested organic compounds are dissolved in toluene as best solvent in a certain concentration as discussed later.

The protective film formed directly when inhibitor molecules adsorbed on the metal surface during immersion of steel CR4 probes in appropriate inhibitor stock solutions prior the corrosion tests.

1.4 Optimization

The traditional procedures are used to implement most of experimental work in research and a high number of experiments is required which means a huge waste of materials, time, and cost [76,77]. Other point, the simple trial and error of usual experimental work which is

applied in electrochemical process cannot easily manage the complex analytics and problems [78]. Optimization replaces the usual experimental ways to none traditional techniques and gives a good solution to investigate the effect of several factors and their levels even if there is a complex interaction between studied variables [79]. Non-traditional experimental methods are done according to a schedule plan which is designed especially to ensure that all the possibilities of singular and interaction effects for investigated variables are included [80]. The statistical design of experiment (DOE) is a technique that can build an experiment model to involve all studied parameters in the process with less number of experiments that are required in any traditional way [81]. Besides reducing the number of required experiment, DOE develops the mathematical models to evaluate the singular and interaction effects of studied variables mathematically. Multivariate optimization methods avoid the fail that may occur by the use of the univariate procedure when the effect of one factor may be depend on the level of others. The first step in the multivariate optimization is screening the main effect of tested variables by fulfill the fractional factorial design that is used in statically optimization methods [82-84].

There are many mathematical techniques of DOE that are using univariate and multivariate methods and receive the independent variables as input then give the result as output like Box-Behnken Design (BBD) [81,85,86]. DOE can be classified depending on levels of studied variables. It can be a two level matrix when tested factors have lower and upper levels (-1, +1) and a three levels matrix if variables have lower, midpoint, and upper levels (-1, 0, +1). BBD is one of DOE technique requiring less numbers of experiments than other response surface design like central composite design (CCD) [85,87]. The three levels matrix for four variables depending on BBD is listed in Table 1-1. The main goal of applying DOE techniques is to optimize the effect of factors influencing on the process and predict the maximum response depending on studied levels by using a minimum number of experiments. To fulfill this, response surface methodology (RSM) is a combination of statistical and mathematical techniques supported by computer software was used in optimization and prediction process [88,89].

Response surface methodology (RSM) is one of the important optimization strategies that is attached to a complex experiment depending on three levels like Box-Behnken Design (BBD). It is approved as a useful tool by application in many studies [88-98]. RSM finds the best conditions of the process to obtain on optimum response theoretically, which is not included in the experiments [99]. The two main goals for RSM are to find the optimum response and understand how the response changes by a adjusting the design graphically.

In the case study here, the efficiency of inhibitor (**Y**) is the dependent response variable and it is a function of four independent variables which can be expressed as following Eq. [97]:

$$Y = f(A,B,C,D) + e$$ Eq. 1-1

Where: A, B, C, and D are independent variables, e is the experimental error.

Table 1-1: The layout of the 27 orthogonal arrays for coded and real values based on Box-Behnken design (BBD) conducted with coded value for four factors.

No.	A	B	C	D	No.	A	B	C	D
	Coded value					**Coded value**			
1	-1	-1	0	0	17	-1	0	-1	0
2	-1	1	0	0	18	-1	0	1	0
3	1	-1	0	0	19	1	0	-1	0
4	1	1	0	0	20	1	0	1	0
5	0	0	-1	-1	21	0	-1	0	-1
6	0	0	-1	1	22	0	-1	0	1
7	0	0	1	-1	23	0	1	0	-1
8	0	0	1	1	24	0	1	0	1
9	-1	0	0	-1	25	0	0	0	0
10	-1	0	0	1	26	0	0	0	0
11	1	0	0	-1	27	0	0	0	0
12	1	0	0	1					
13	0	-1	-1	0					
14	0	-1	1	0					
15	0	1	-1	0					
16	0	1	1	0					

Normally the response surface method starts with first-order model function when the response is a linear function of independent variables. For four independent variables, the first-order model can be expressed as [97]:

$$Y = \beta o + \beta 1 A + \beta 2 B + \beta 3 C + \beta 4 D + e$$ Eq. 1-2

Where β is the regression coefficient

When the response surface has a curvature then the second-order model that takes all possibility of effects for individual and interaction variables should be use and it can be expressed in Eq 1-3 [97].

$$\begin{aligned}
Y = {} & \beta o + \beta 1A + \beta 2B + \beta 3C + \beta 4D \\
& + \beta 11A^2 + \beta 22B^2 + \beta 33C^2 + \beta 44D^2 \\
& + \beta 12AB + \beta 13AC + \beta 14AD + \beta 23BC + \beta 24BD + \beta 34CD + e
\end{aligned}$$

Eq. 1-3

In this study, second order model for RSM was applied by using Minitab 17 to run the 27 experiments and determine the response effects by plotting these effects based on the proposed prediction model.

There are a specific numbers of experiments required in any classic experimental procedure and can be calculated by Eq 1-4.

$$S = l^k$$

Eq. 1-4

Where S is the number of experiment, l: number of levels, and k: number of variables.

In the present work, there are four independent variables that have three levels lower (-1), mid (0), and upper (+1) for each variable to be investigated. According to Eq. 1-4 the number of experiments required in a traditional way is equal to $(S = 3^4 = 81)$ while by applying BBD it reduces to just 27 experiments. The tested factors as (-1, 0, +1) levels are concentration of inhibitor (A), dip coating time of metal in inhibitor solution (B), temperature (C), and NaCl content (D).

Chapter two

Experimental work

2.1 Metal probes and preparation

Low carbon steel CR4 (also denoted as 1.0330 or DC01) [100] supplied by two different suppliers was used as basic metal in the present work. Steel sheets were laser cut in dimension $20 \times 20 \times 1$ mm and tested via three different evaluation systems (weight loss, electrochemical, and spray corrosion measurement). The chemical analysis of tested steel is determined by optical emission spectroscopy (variolab, Belec Spektrometrie Opto-Elektronik GmbH, Germany) and the result is summarized in Table 2-1. Blank 1 and 3 supplied by Fa. Janssen, CNC-Blechbearbeitungs GmbH, Germany and blank 2 by Nick-Stanztechnik, Germany.

Table 2-1: Analysis of used low carbon steel compared to the standard CR4 / DC01 [100].

Element	C	Si	Mn	P	S	Cu	Al	Cr	Mo	Ni	Co	W
CR4/ DC01	max. 0.120	n.a.	max. 0.600	max. 0.045	max. 0.045	n.a.	n.a.	n.a.	n.a.	n.a.	n.a.	n.a.
Blank 1	0.086	0.012	0.214	0.018	0.020	0.007	0.037	0.016	0.008	0.004	0.001	0.005
Blank 2	0.022	0.018	0.200	0.014	0.005	0.011	0.033	0.002	0.009	0.000	0.002	0.004
Blank 3	0.084	0.030	0.194	0.017	0.008	0.008	0.036	0.011	0.006	0.000	0.000	0.035

A proper preparation including the grinding is done according to DIN - ISO 9227:2006 [101] with silicon carbide P120 and P220 (Matador, waterproof 991A softflex grit) to remove any protective or oxidation films on the samples. In this step, at least 0.7 μm of metal on the probes' surface have to be eliminated [102] and this amount corresponds to mass loss of 3.125 to 3.750 mg. Afterwards samples were cleaned with isopropanol in an ultrasonic bath to remove oily residues and traces from grinding, then air dried and stored at 60 °C to avoid any further contamination if not used immediately. The final step of sample preparation is individually formation of the protective film on steel surface during immersion of coupons for 10 minutes in the toluene stock solutions that contain a certain concentration of selected organic substances (Fig. 2-1). After this step coupons were ready and immediately tested for corrosion.
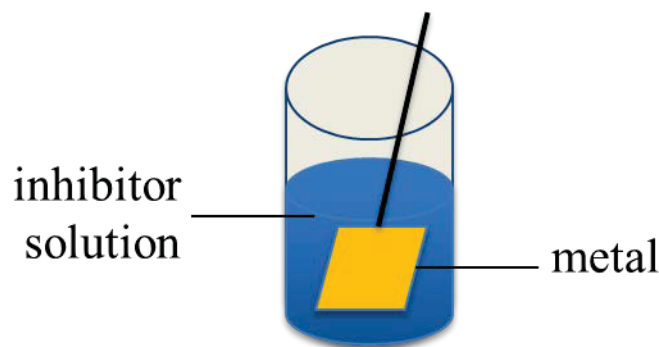
Fig. 2-1: Prepared steel CR4 immersed in stock containing of certain concentrations (25, 50, 75, 100) mmol/L of tested inhibitors.

Because samples were consumed during the measurement, there was the need to order a new amount of steel CR4 from the same suppliers to be used in experiments. The new amount ordered differed slightly from the previous ones. Details will be discussed on this later according to their use in experiments (compare Table 2-1).

2.2 Organic solvents and inhibitors

N-acyl sarcosine derivatives namely Cocoyl (C), Lauroyl (L), Myristoyl (M), and Oleoylsarcosine (O) are tested here as corrosion inhibitor. These derivatives are different in their molecular weight and fatty acid residues except compound C, because it contains a naturally mixture of different fatty acids (C_8 - C_{18}) (Fig. 2-2). The more polar amino acid part is linked to the unpolar hydrocarbon chain via an amidomethyl (-CONCH$_3$-) group at α-position (Figs. 1-3 and 2-2) [26,103-107]. The selected compounds have no negative effects to humans and they are certified for cosmetics like skin treatment and also they have a good stability at high temperature [74].

Two organic substances namely Oley-Imidazoline (OI) and Methy-limidazole (MI) are evaluated to work in combination with candidate inhibitors with synergistic effect (Fig. 2-2). OI compound contains a fatty acid residue and is used as single composition and as synergist to improve the efficiency of Cocoylsarcosine (C) (Fig. 2-2). The synergist OI consists of three components: first part is a five membered ring with two nitrogen atoms, second one is a tail of a long hydrocarbon chain and last portion is a pendant short hydrocarbon chain of -OH as an active functional group [108]. The last portion of OI is response to anchoring to the basic metal surface additionally to the main amine of the ring part. MI substance is composed of a five membered ring containing two nitrogen atoms and attached by a CH$_3$ at on N

(Fig. 2-2). The candidate compounds C, L, M, and O are used as single molecule compositions in four different concentrations 25, 50, 75, and 100 mmol/L.
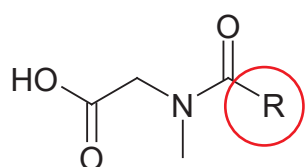
Sarcosine basic structure

C8 = 3.59%   **C14** = 21.76%

C10 = 4.85%   **C16** = 11.12%

C12 = 48.05%   **C18** = 10.64%

Cocoylsarcosine – **C**
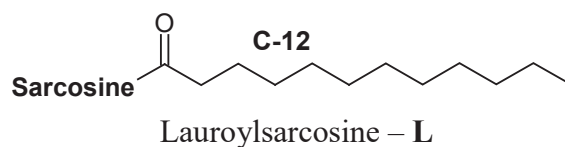
Lauroylsarcosine – **L**
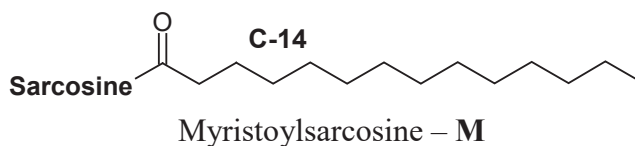
Myristoylsarcosine – **M**
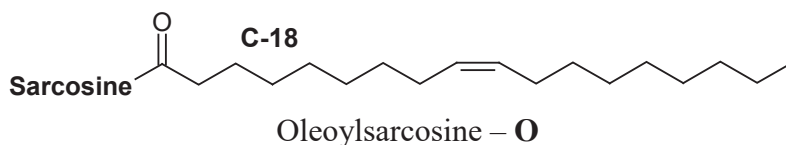
Oleoylsarcosine – **O**
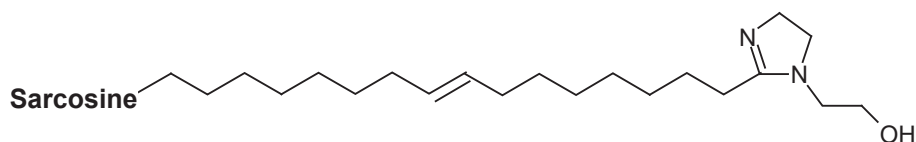
Oleyl-Imidazoline – **OI**
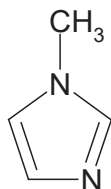
Methyl-Imidazole – **MI**

Fig. 2-2: Structure of tested sarcosine series C, L, M, O and synergists OI, MI. In the basic structure of the sarcosine amino acid the residue R (encircled red) represents one of the fatty residue derived and isolated from coconut.

Because the tested organic compounds are not dissolvable in water, it was needed to find an organic solvent that shows no additional effects on the corrosion protection process. Several organic substances summarized in Table 2-2 are evaluated like inhibitors in a single 100 % composition individually to detect their effect on the corrosion compared to blank material. The step after choosing a proper organic solvent to dissolve the selected inhibitors is to find the technique that allows applying the tested inhibitor in the protection process.
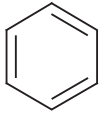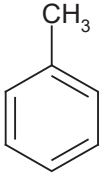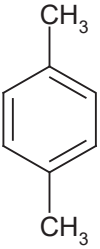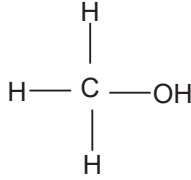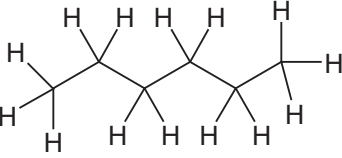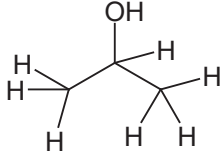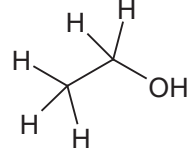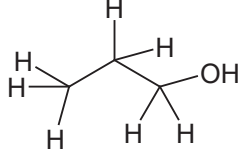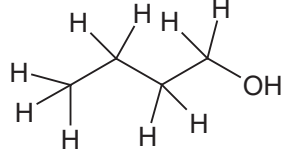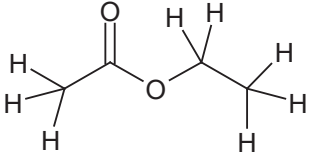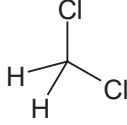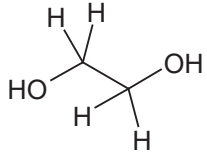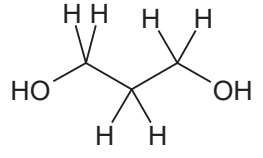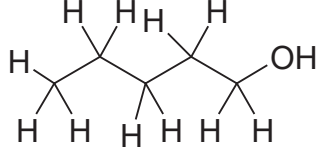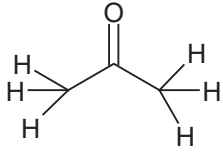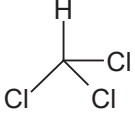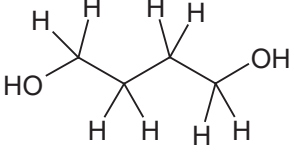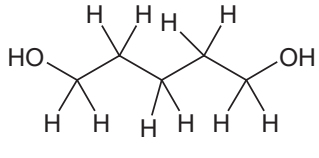
Immersion procedure of steel CR4 coupons in stock containing a certain concentration of selected inhibitors was used to allow the organic molecules adsorb on the steel surface and form a protective film. Different immersion times (1, 2.5, 5, 10, and 30 min) were used to test the dip coating time effects on the protection. After immersion step the probes were ready to be used immediately in the corrosion test. Toluene ($\geq$ 99,5 %, Carl Roth GmbH + Co. KG, Germany) as the best result of tested solvents was used to dissolve the present organic inhibitors (see details in results chapter).

2.3 Weight loss measurements

Selected organic compounds to protect steel CR4 in 0.1 M NaCl are tested via gravimetric measurement. The surface of steel probes was properly mechanically abraded with 120 and 220 grades of emery papers respectively (WS FLEX 18c water proof, HERMES, Germany) then washed with distilled water two times and rinsed carefully with isopropanol in ultrasonic bath to remove the grinding residues and dried at ambient conditions. A digital balance (KERN 770, error $\pm$ 0.01 mg) was used to weigh the samples before corrosion test. Steel probes prepared are immersed for 10 minutes in Toluene stock that contains a certain concentrations of inhibitors to adsorb the organic molecules by metal surface. The coated samples with studied inhibitors were immersed in 1 L of 0.1 M NaCl. After 24 h the steel probes were taken off and washed twice with distilled water then chemically treated for 10 seconds in 0.5 M HCl to evolve the corrosion products and washed directly with distilled water then rinsed with isopropanol and dried. The final step was weighing to check for any weight difference caused by mass loss [108-110].

Table 2-2: Structure of candidate solvents tested like corrosion inhibitors to protect steel CR4 in 0.1 M NaCl.

Benzene - C_6H_6	Toluene - C_7H_8	p-Xylene - C_8H_{10}
Methanol - CH_3OH	n-Hexane - C_6H_{14}	Isopropanol - C_3H_7OH
Ethanol - C_2H_5OH	1-Propanol - C_3H_7OH	1-Butanol - C_4H_9OH
Ethyl acetate – $C_2H_5COOCH_3$	Dichloromethane - CH_2Cl_2	Ethylenglycol - $C_2H_6O_2$
1,3-Propanediol - $C_3H_8O_2$	Pentanol - $C_5H_{11}OH$	Acetone – H_3CCOCH_3
Trichlormethane - $CHCl_3$	1,4-Butanediol - $C_4H_{10}O_2$	1,5-Pentanediol - $C_5H_{12}O_2$

2.4 Electrochemical measurements

Potentiodynamic polarization curves carried out to evaluate the candidate substances as inhibitor to protect steel CR4 against corrosion in 0.1 M NaCl. Laboratory - Galvanostate Wenking LPG03 system (Bank Electronic - Intelligent Controls GmbH, Germany) supported with TestPoint - based software CPC was used to analysis the results of polarization measurement. A single compartment consisting of a double-walled glass vessel (0.8 L) with three electrode configuration was used for polarization evaluation. The electrode system configured from: reference electrode (RE), Ag/AgCl, working electrode (WE) with 1 cm^2 surface area of steel CR4, and a platinum auxiliary electrode (AE). A whole electrode system including WE immersed in 0.8 L of 0.1 M aerated and stirred aqueous NaCl for 30 min at free potential to reach a steady state of open circuit potential (OCP). Afterwards the polarization was implemented at ± 200 mV according to OCP that recorded in holding time with a scan rate speed of 0.5 mV/s. A stable pH value 6.0 ± 0.5 was continuously checked during the measurement with a pH meter (Education line, EL20 / EL2, Toledo Group, Switzerland). A test series consists of at least three independent measurements for each sample type and inhibitor combination.

Electrochemical impedance spectroscopy (EIS) was also performed with a Frequency Response Analyzer PSM 1700 (Newtons4th Ltd, UK) to confirm the results that obtained in polarization measurement. The same cell, holding time, surface area, and solution test that are used in potentiodynamic test was used in EIS with two electrodes setup system (steel CR4 as WE and platinum as RE). EIS test was applied in a frequency sweep range from 100 kHz to 0.1 Hz with an AC amplitude of 4 mV. Fig. 2-3 shows the scheme of electrochemical technique used in the current work.

Fig. 2-3: Sketch explains outline of electrochemical techniques (potentiodynamic polarization curves and electrochemical impedance spectroscopy (EIS).
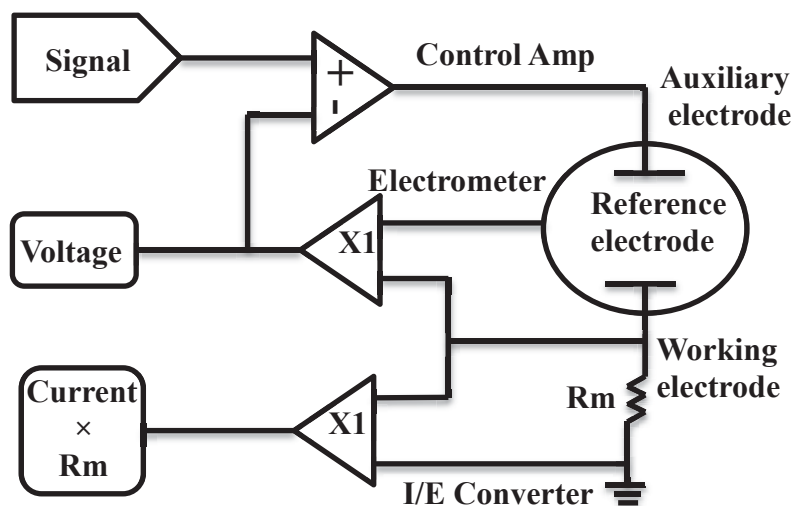
2.5 Spray corrosion tests

A chamber with dimensions $50 \times 40 \times 50$ cm was made from polymethyl methacrylate (PMMA) to evaluate candidate compounds in more realistic and longer duration test via spray corrosion measurement. The atmospheric conditions are provided during adjustable nozzle (Nozzle Model 970 S8, Düsen-Schlick GmbH, Germany) by mixed and sprayed the tab water that supplied by reservoir and condensed compressed air. The air stream with 1.4 bars is humidified by passing through distilled water heated to 60 °C before emission into the nozzle. A special plastic plate contains a magnetic and completely enclosed via shrinking tubes are designed and used to attach the steel probes and place inside the chamber. Same preparation steps that implemented in electrochemical evaluation are used here with additionally processes: After coating the samples with tested compounds during immersion process the probes are dried shortly at ambient conditions and three edges of the coated coupons were covered by transparent paint to avoid edge effect of rust formation during the corrosion test. The lower edge of each probe is equipped with a 2 mm stripe of waterproof paper sheet (Zweckform L4775^{TM}, AVERY Zweckform, Canada) to avoid any accumulation of water at the bottom. The experimental conditions of set up for the spray corrosion evaluation are summarized in Table 2-3. Afterwards the probes were placed inside the chamber and the spray corrosion test was immediately started. The test is stopped for ~ 10 min for scanning and documentation of samples then for the estimation of the corrosion rate at a five certain times (2, 4, 8, 14, and 24 h).

Table 2-3: Experimental conditions for the spray chamber test [26].

Parameter	Value
Dip coating time of probe in inhibitor	10 min.
Run time of the test	24 h
pH - value (tab water)	6.5
Temperature of distilled water inside humidifier	60 °C
Air pressure	1.4 bar

Each experimental series was done minimum two times to obtain at least ten single samples from two individual runs. The documentation was carried out by scanning the complete samples series at once using a conventional scanner (HP Scanjet G4010) with 1200 dpi resolution. Each image that scanned was evaluated with the Java-based image editing and image processing program ImageJ [111], which is especially used for measuring structures on

digitalized images in medicine or biology. Here ImageJ is used in particle mode to quantify corroded areas if present on the probes' surface. The evaluated section of the metal surface is a square of 20 mm x 20 mm excluding painted edges. The area size analysis was performed via the implementation of a macro (see appendix I), splitting firstly the color values of each image into the color channels (blue, green and red). Best results to detect corrosion areas over the grey metal background were found in the blue channel giving the greatest contrast. Furthermore, a threshold adjustment to color gradations from 0 to 85, out of 255, was done. After that, only certain color values are approved for rust over metal and ImageJ is able to recognize and evaluate the corroded areas. Additionally, the macro includes a restriction in particle size analysis smaller than 3×3 pixels to exclude artefacts, which result from contaminants or discolorations on the steel (dust, granular structure, crystallinity etc.). In sum, this procedure provides the corroded area and the number of corrosion spots on top of the probes. The final data processing was done with Orgin Pro 8.1 [112]. Fig. 2-4 shows a sketch outlining parts of the spray corrosion chamber test.

1- chamber, 2- nozzle, 3- samples, 4- reservoir, (tab water),
5- humidifier, 6- heater, 7- compressed air supply
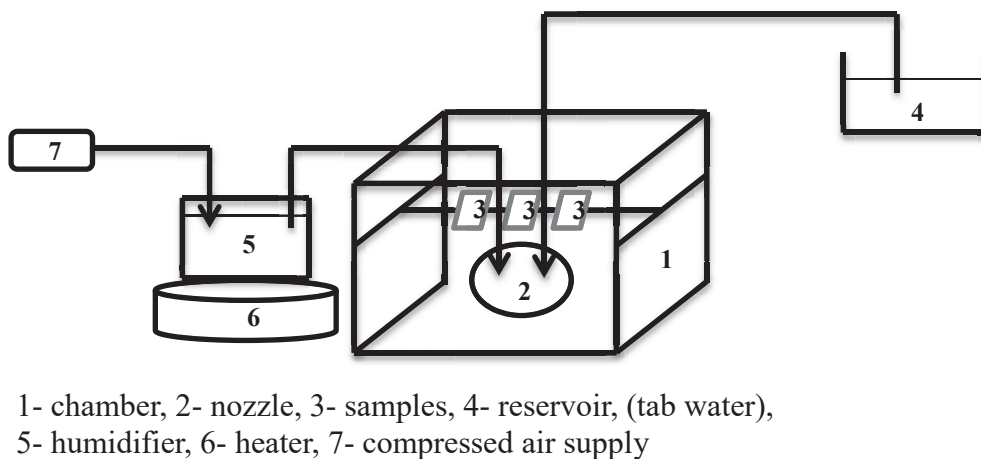
Fig. 2-4: Sketch shows the main parts of spray corrosion chamber test that are used to evaluate efficiency of investigated organic substances to protect steel CR4 against corrosion in normal water.

2.6 Design of experiment (DOE)

In the current investigation, BBD is used to find the optimum influence of four independent variables with their three levels that effect on the protection of steel CR4 in salt water. The studied factors are concentration of inhibitor O (A), dip coating time of steel in anticorrosive stock solution (B), temperament (C), and NaCl concentration in the testing solution (D). Each independent variable studied has three levels low, middle, and upper and they are designed as coded value (-1,0,+1). The dependent variable (objective function) is efficiency of inhibitor

to decrease the current density according to tested variables and their levels. The evaluation was with inhibitor O which is the best tested inhibitor that has highest efficiency according to results in the present study.

The proposed independent variables with their levels are conducted in coded values are summarized in Table 2-4.

Table 2-4: Independent variables proposed with their real and coded three levels that are used in current investigation to implement Box-Behnken Design (BBD).

No.	Variable code	Variable name	Coded and real levels		
			-1	0	+1
1	A	Inhibitor concentration (mmol/L)	25	50	75
2	B	Dip coating time (min)	1	10	30
3	C	Temperature (°C)	25	40	55
4	D	NaCl concentration (M)	0.05	0.1	0.2

The 27 orthogonal array of Box-Behnken Design (BBD) depending on a three level matrix conducted with a combination of real levels are summarizes in Table 2-5. The real number of experiments required in this investigation is 25 and experiments 26 and 27 were repeated of experiment 25 to complete the full matrix (compare Table 2-5).

In this work, to find all possible effects on the process the second-order model for response surface methodology (RSM) was used. The response surface methodology supporting with Minitab17 program used to implement the 27 experiments and determine the response effects with a plot of these effects based on the proposed prediction model.

Table 2-5: The layout of the 27 orthogonal arrays for coded and real values based on Box-Behnken design (BBD) conducted with real value.

Coded value						**Coded value**			
No.	A	B	C	D	No.	A	B	C	D
1	25	1	40	0.1	17	25	10	25	0.1
2	25	30	40	0.1	18	25	10	55	0.1
3	75	1	40	0.1	19	75	10	25	0.1
4	75	30	40	0.1	20	75	10	55	0.1
5	50	10	25	0.05	21	50	1	40	0.05
6	50	10	25	0.2	22	50	1	40	0.2
7	50	10	55	0.05	23	50	30	40	0.05
8	50	10	55	0.2	24	50	30	40	0.2
9	25	10	40	0.05	25	50	10	40	0.1
10	25	10	40	0.2	26	50	10	40	0.1
11	75	10	40	0.05	27	50	10	40	0.1
12	75	10	40	0.2					
13	50	1	25	0.1					
14	50	1	55	0.1					
15	50	30	25	0.1					
16	50	30	55	0.1					

Chapter three

Results and discussion

3.1 Corrosion behavior of steel CR4 supplied by two different producers

Three variance of steel CR4 supplied by two different companies that are slightly differing in chemical elements are tested via polarization and spray corrosion measurements to investigate the corrosion behaviour of them. In polarization evaluation 0.1 M NaCl was used as test solution while in spray corrosion test normal water that mixed and sprayed with compressed air was used to simulate the atmospheric environment. Results like current density (i_{corr}), corrosion potential (E_{corr}), and relative corrosion area (A) that are obtained in these two evaluation systems for tested steel CR4 variances are summarized in Table 3-1.

Table 3-1: Current density i_{corr} and corrosion potential E_{corr} obtained in potentiodynamic polarization measurements and relative corrosion area recorded in spray corrosion measurements for the present three variances of steel CR4.

Steel CR4	Current density (i_{corr}) µA/cm^2	Corrosion potential (E_{corr}) mV	Relative corrosion area (A) %
blank 1	85.16	-325	91.66
blank 2	61.93	-324	70.81
blank 3	73.91	-344	97.68

From results that are listed in Table 3-1, different corrosion behavior for steel variances that are slightly differing in element content was detected. Fig. 3-1 A shows the anodic and cathodic polarization curves of the present three variances of steel CR4 and inset chart B represents the current density recorded for them during polarization test. The polarization curves for blank 1 shows different corrosion behaviour especially for anodic part (Fig. 3-1 A black line) with highest current density (Fig. 3-1 inset chart B). Other blanks (2 and 3) show more or less same polarization behaviour (Fig. 3-1 A red and blue line) but somehow different in current density (Fig. 3-1 inset chart B).
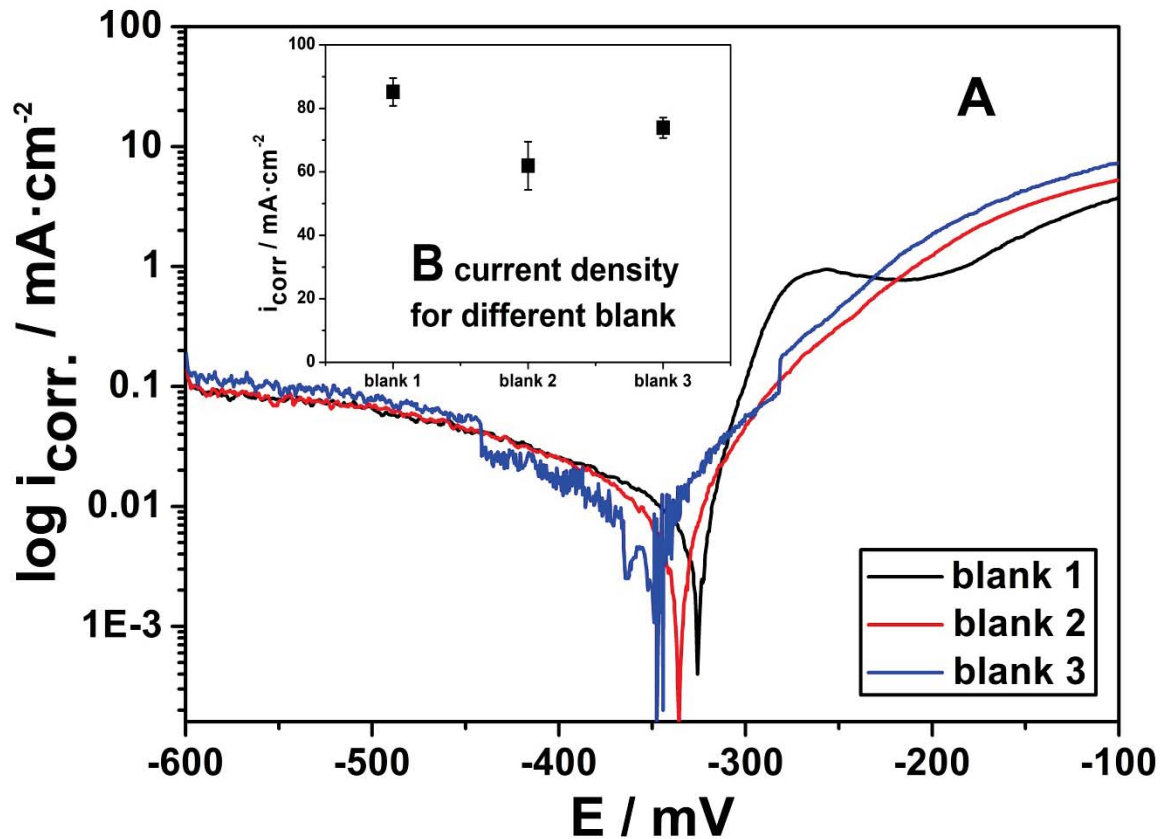
Fig. 3-1: Anodic and cathodic polarization curves and current density recorded for the present three variances of steel CR4 during polarization measurement. Blank 1 displayed in black, blank 2 in red and blank 3 in blue. Inset chart **B** for current density recorded through polarization test.

These three variances were also tested during more realistic system and longer duration via corrosion spray measurement. Fig. 3-2 shows the corrosion process on steel CR4 surface according to time. In the beginning a lot of small size corrosion dots appear with small corroded area and after 8 h most of surface for blank 1 and 3 was covered with corrosion products till complete coverage after 24 h (first and third row in Fig. 3-2). The average of relative corrosion area for ten samples result by two independent measurements for three variances steel CR4 used is summarized in Fig. 3-3 (blank 1 in black, blank 2 in red, and blank 3 in blue). Blank 2 has better corrosion resistance compared to blank 1 and 3 and this higher resistance because of the slight differences in element percentage (compare Table 2-1 and Fig. 3-3). After 2 h there are a lot of small light corrosion dots corresponding to small relative corrosion area was detected on the surface of blank 2 while corrosion spots was less and bigger size with larger corrosion area for other blank 1 and 2 (Fig. 3-2). Corroded surface of blank 2 was increased with time but it is still less than blank 1 and 2 (compare Table 3-1, Figs. 3-2 second row and 3-3 red color).
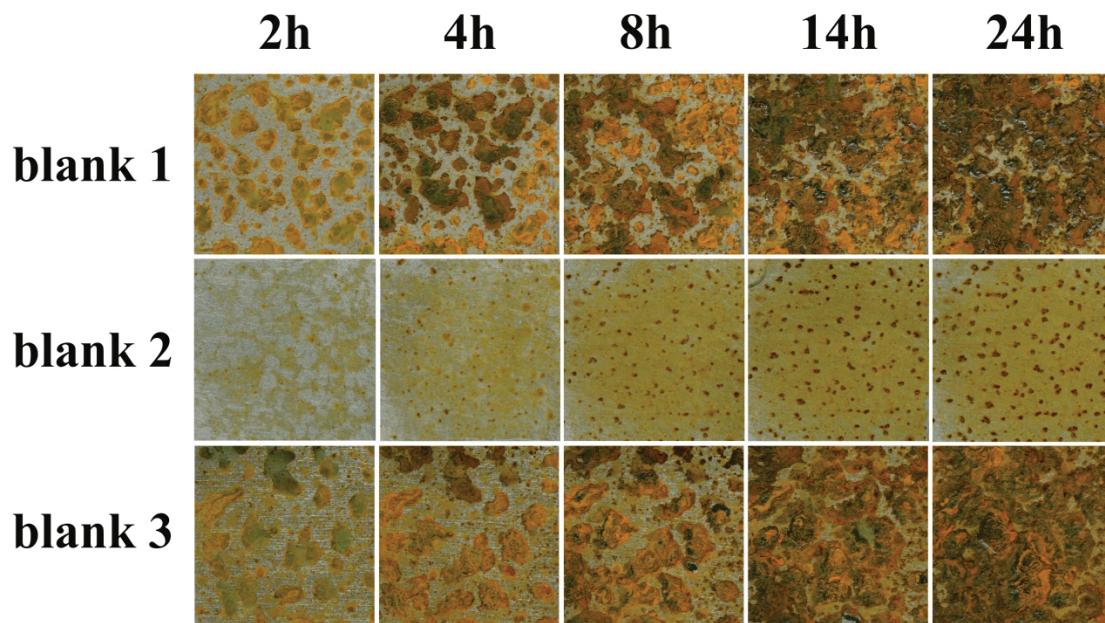
Fig. 3-2: Corrosion process for three variances of steel CR4 at specific times (2, 4, 8, 14, and 24 h). Images represent one series of ten samples tested by two independent measurements.
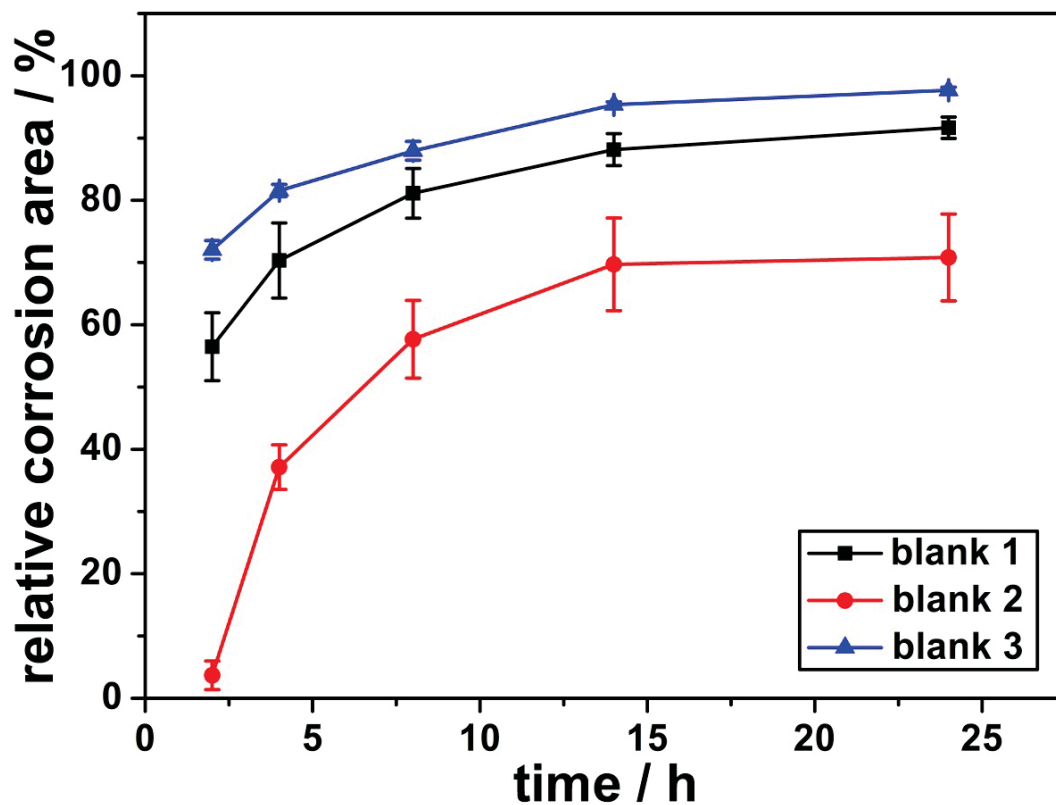
Fig. 3-3: Average of relative corrosion area for ten samples tested by two independent measurements for three variances of steel CR4 during specific times (2, 4, 8, 14, and 24 h). Blank 1 is displayed in black, blank 2 in red and blank 3 in blue. The data points are connected for better readability.

3.2 Open circuit potential measurement (OCP)

Polarization measurements were carried out to evaluate different media like boric, phosphate, NaCl, distilled water, and tab water to record open circuit potential (OCP) and find the most stable system. Steel CR4 used in this evaluation was blank 2 (compare Table 2-1). Phosphate and boric were having highest potential around -150 mV and -200 mV respectively (Fig. 3-4 A green and magenta lines respectively). Tab water was having unstable potential (Fig. 3-4 A red line). Distilled water and 0.1 M NaCl were having lower potential around -560 mV and -420 mV respectively (Fig. 3-4 A blue and black lines respectively). The selected test solution to evaluate studied inhibitors was 0.1 M NaCl because it has a low and stable potential. This will not affect the process during over potential and NaCl provides a good conductivity for the solution test.

OCP for candidate organic compounds was recorded for 2 h and results of potential vs time are shown in Fig. 3-4 B. The stable values of OCP were recorded after half hour. For steel CR4 blank, OCP was around -420 mV and -390 mV for coated steel CR4 with inhibitor O (Fig. 3-4 B black and green lines respectively). For coated steel CR4 with inhibitor C, L, and M, OCP was around -424 mV, -470 mV, and -412 mV respectively (Fig. 3-4 B red line, blue line, and magenta line respectively).

Uncoated and coated steel CR4 with sarcosine O and M with different grinding grades (220 and 1200) were tested during polarization measurement to detect the effect of grinding on corrosion and protection process. For coated steel CR4 with inhibitor O and M, OCP recorded refers to there is no big effect of grinding grades on the potential because the surface is already completely covered with inhibitor molecules in both grades (Fig. 3-4 C). OCP recorded for blank grinded with 220 grades was different and higher than with 1200 grades (Fig. 3-4 C black and magenta color respectively).

Depending on the result obtained, the best tested conditions to use in electrochemical measurements are 0.1 M NaCl as test solution, 30 min of holding time at free potential for OCP and steady state, and 220 grades for grinding.
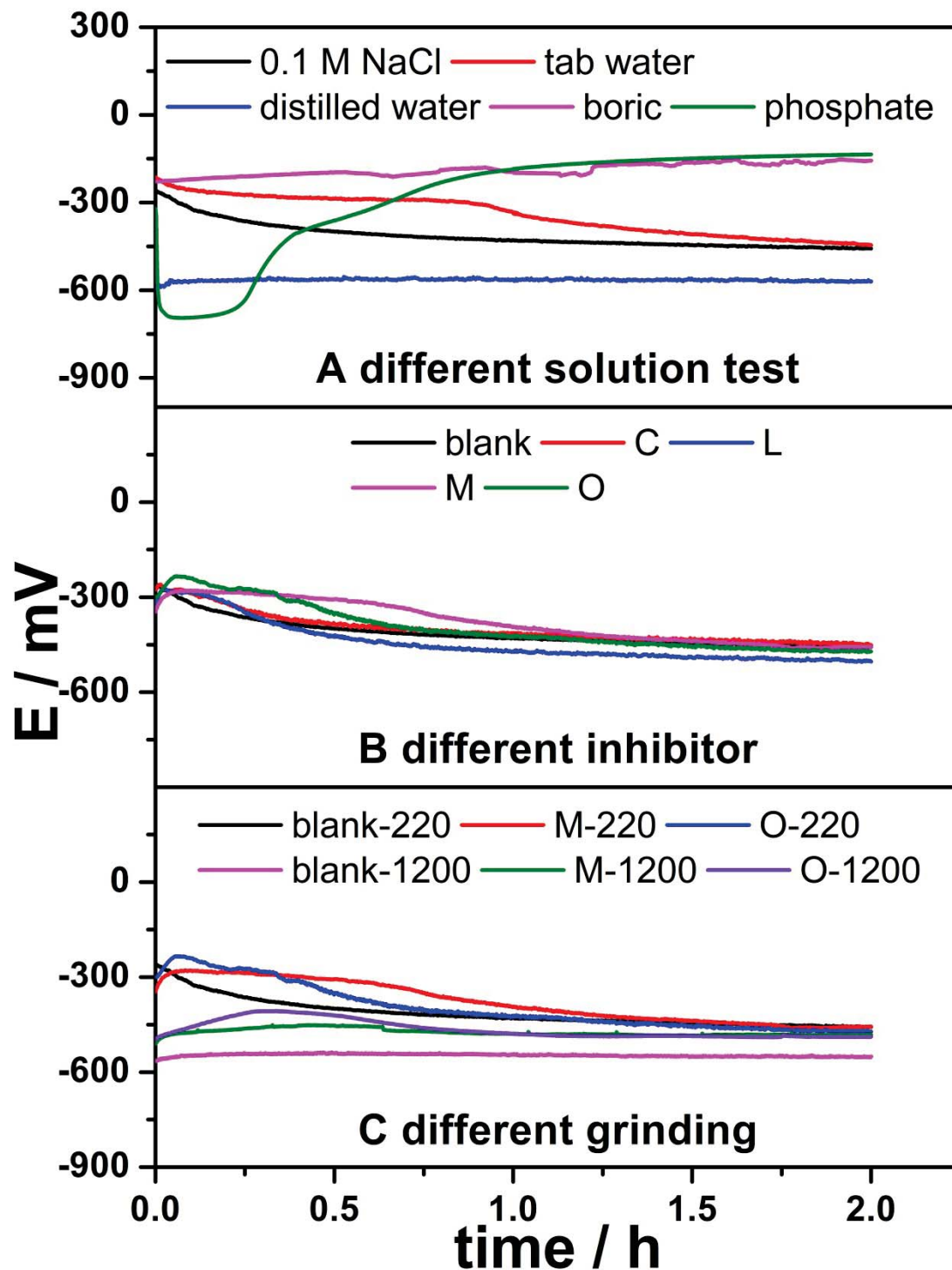
Fig. 3-4: OCP recorded within 2 h for steel CR4 at different conditions. Chart **A** for blank metal in different solution tests (0.1 M NaCl in black, tab water in red, distilled water in blue, boric buffer in magenta, and phosphate buffer in green). Chart **B** is for coated steel CR4 with tested inhibitors C, L, M, and O compared to blank metal in 0.1 M NaCl (blank in black, C in red, L in blue, M in magenta, and O in green). Chart **C** is for different grinding grades (blank grinded with 220 and 1200 are display in black and magenta respectively, M grinded 220 and 1200 in red and green respectively, and O grinded with 220 and 1200 in blue and violet respectively).

3.3 Evaluation of suitable solvents

Several organic solvents are tested via potentiodynamic polarization curves like inhibitors to detect the best one that has a negligible or lowest effect on the corrosion protection process of steel CR4 in 0.1 M NaCl to dissolve candidate inhibitors. Steel CR4 used in this evaluation was blank 2 (compare Table 2-1).

OCP measurements for steel CR4 as a blank metal and with different organic solvents are recorded for 30 min and shown in Fig. 3-5 A. Toluene has more or less same OCP for blank metal with potential around -424 mV (compare Table 3-2 and Fig. 3-5 B black and blue color).

The anodic and cathodic polarization curves that recorded during potentiodynamic polarization curves of uncoated and coated steel CR4 with studied organic solvents as inhibitors are shown in Fig. 3-6 A. Tested substances showed E_{corr} shifts in different ways. Most of them shift E_{corr} to negative and positive direction while other did not make any shift like toluene, dichloromethane and 1,3-propanediol (compare Table 3-2 and Fig. 3-6 A). The electrochemical parameters obtained by potentiodynamic polarization curves like corrosion potential E_{corr}, corrosion current density i_{corr}, Tafel slope β_a and β_c, corrosion rate **CR** according to Faraday's law [17], surface coverage $\boldsymbol{\Theta}$ obtained by (**IE /100**)[67], and inhibition efficiency **IE (%)** which is calculated by Eq. 3-1 [113] are summarized in Table 3-2. The values of Tafel slope for anodic and cathodic polarization listed in Table 3-2 indicate to there is almost no change of the corrosion behavior in present tested organic substances.

$$IE(\%) = \frac{i_{corr} - i_{inh}}{i_{corr}} \cdot 100 \qquad \qquad \text{Eq. 3-1}$$

Where i_{corr} and $i_{inh.}$ is the corrosion current density in absence and presence substances respectively.

efficiency up to 46 % followed by 1,4 butandiol with efficiency up to 37 % (compare Table 3-2 and Fig. 3-7 grey and dark yellow color respectively). Lowest effect was for benzene, toluene, and p-xylene with efficiency up to 2 %, 3 %, and 4 % respectively (compare Table 3-2 and Fig. 3-7 red, blue, and magenta color respectively). The rest of tested solvents have efficiencies between 14 % to 28 % which is considered high effect on the corrosion process (compare Table 3-2 and Fig. 3-7). correlation relation between efficiency and number of C atom of tested solvents was detected. Higher effect of tested solvents to decreasing in i_{corr} was found with more number of C atoms in -OH and -2OH groups in their structure (compare Tables 2-2 and 3-2, Fig. 3-7).
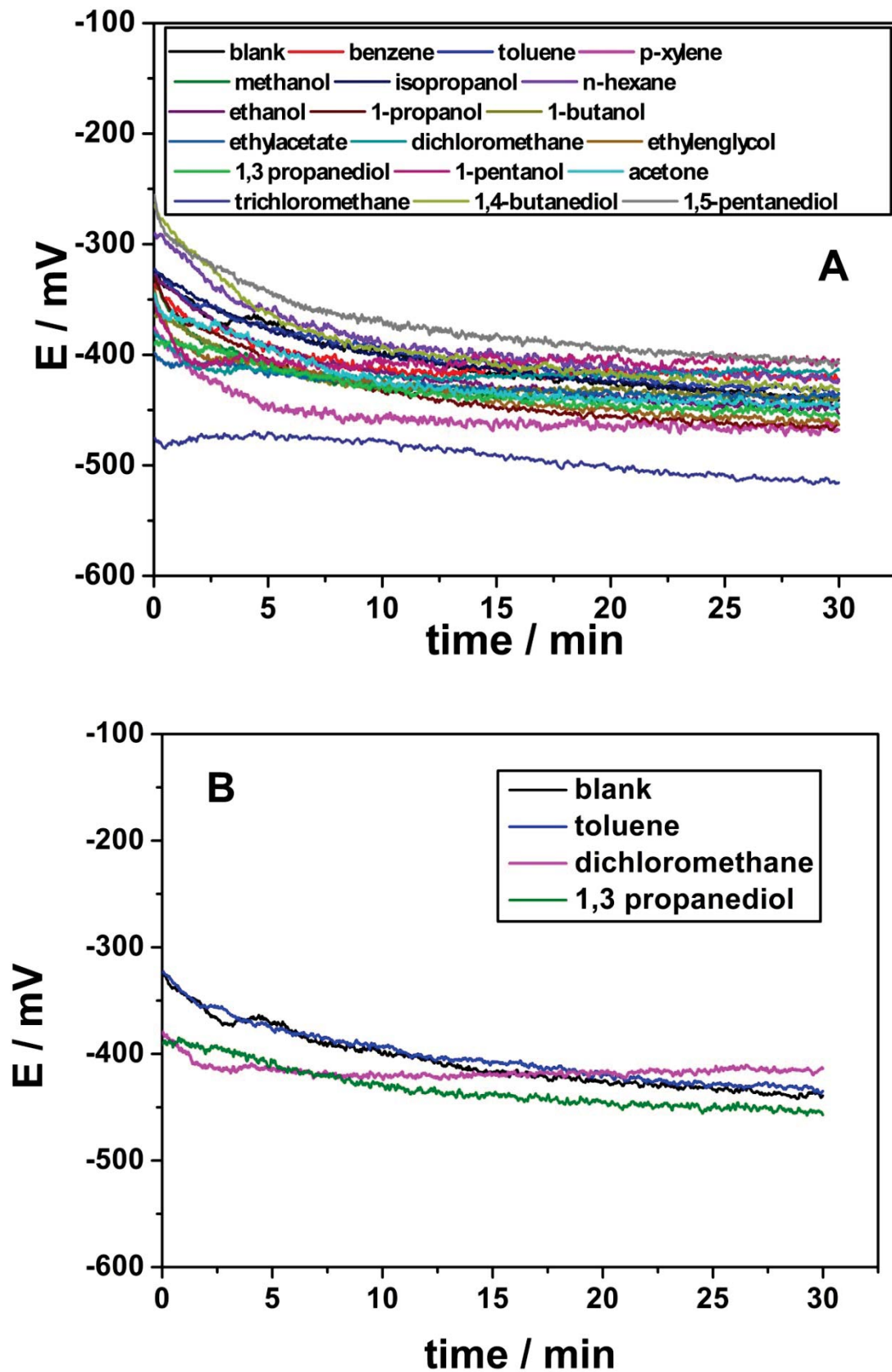
Fig. 3-5: OCP recorded for 30 min for coated steel CR4 with tested solvents as inhibitor compared to blank metal during potentiodynamic polarization measurement in 0.1 M NaCl. Chart **A** for all tested solvents and chart **B** for three best solvents.
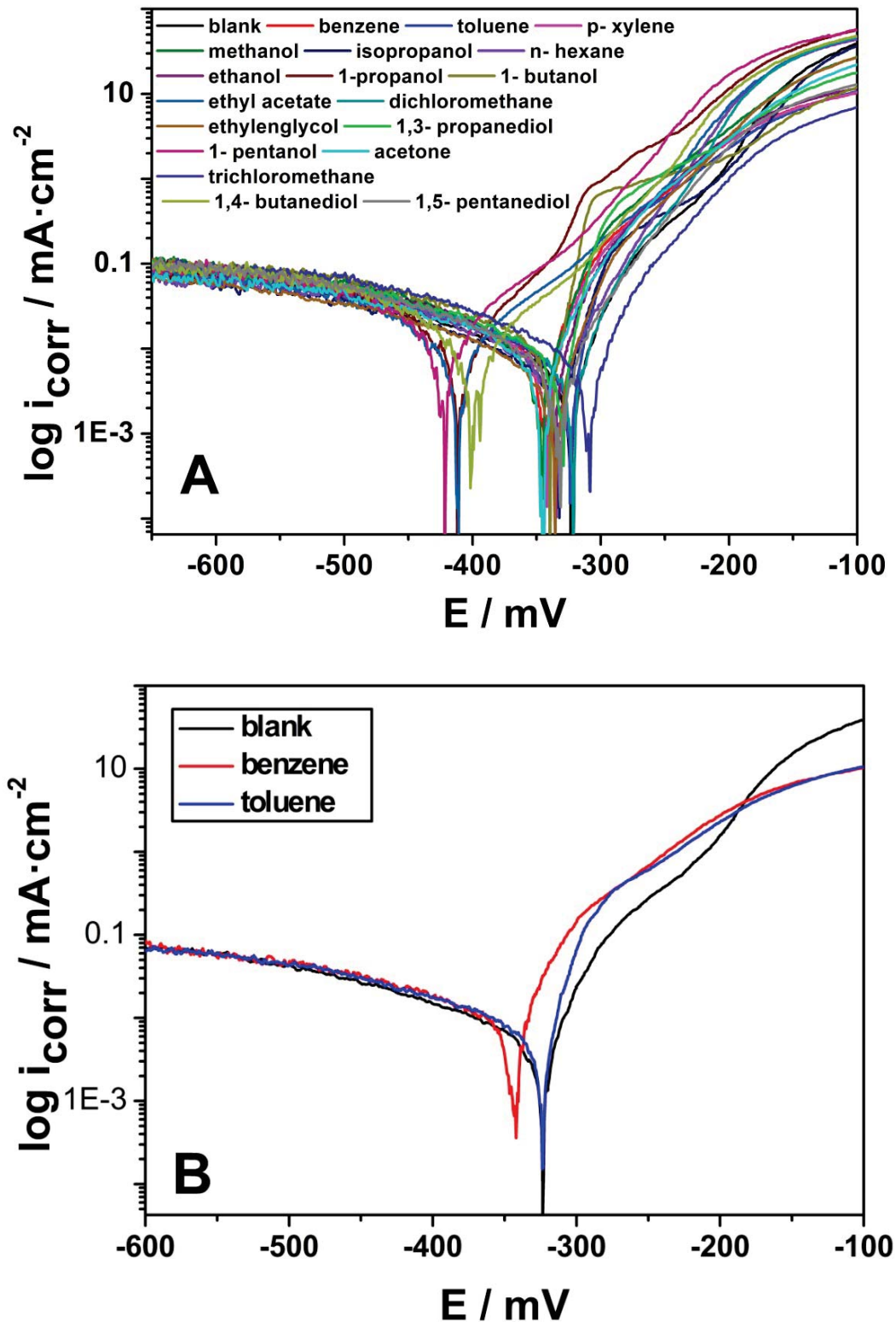
Fig. 3-6: Anodic and cathodic polarization curves for coated steel CR4 with different tested solvents like inhibitor compared to blank metal in 0.1 M NaCl through potentiodynamic curves evaluation. Chart **A** with the series of full solvents chart **B** only with toluene, dichloromethane, and 1,3 propandiol.

The current density i_{corr} of uncoated and coated steel CR4 with tested solvents as inhibitors is presented in Fig. 3-7. The highest effect to decrease i_{corr} was for 1,5 pentanediol with A

Toluene and benzene have least effect on corrosion process compared to blank. Benzene caused shift in E_{corr} to more negative value with potential -341 mV (compare Table 3-2 and Fig. 3-6 B red color) while toluene did not cause any change and E_{corr} stay in same range with blank around -323 mV (compare Table 3-2 and Fig. 3-6 B blue color). The best compound to work as solvent having negligible effects on the process from the current survey is toluene.

Table 3-2: Parameters obtained in potentiodynamic polarization curves for uncoated and coated steel CR4 with tested organic solvents. The corrosion rate (**CR**) is given by millimetre per year (mm/y) depending on current density (i_{corr}), β_a and β_c are the anodic and cathodic Tafel slope, E_{corr} represents the corrosion potential, surface coverage Θ, and **IE (%)** is the corrosion reduction efficiency of the chosen solvents like inhibitors compared to the blank material.

Inhibitor	$i_{corr.}$ ($\mu A/cm^2$)	CR (mmy)	β_a	β_c	$E_{corr.}$ (mV)	Surface coverage (Θ)	IE (%)
Blank	61.96	1.339	0.0016	-0.0029	-324	-	-
Benzene	60.49	1.277	0.0091	-0.0020	-341	0.0237	2.4
Toluene	59.94	1.254	0.0103	-0.0025	-323	0.0326	3.3
p-Xylene	59.07	1.218	0.0099	-0.0027	-343	0.0466	4.7
Methanol	54.46	1.035	0.0113	-0.0030	-346	0.1210	12.1
Isopropanol	53.37	0.994	0.0186	-0.0035	-332	0.1386	13.8
n-Hexane	53.27	0.991	0.0171	-0.0029	-334	0.1402	14.0
Ethanol	50.985	0.908	0.0097	-0.0023	-334	0.1771	17.7
1-Propanol	50.38	0.886	0.0122	-0.0023	-410	0.1870	18.7
1-Butanol	50.16	0.878	0.0098	-0.0021	-337	0.1904	19.0
Ethyl acetate	49.84	0.867	0.0137	-0.0024	-412	0.1956	19.5
Dichloromethane	47.9	0.801	0.0173	-0.0023	-320	0.2269	22.7
Ethylenglycol	47.77	0.797	0.0130	-0.0027	-335	0.2290	22.9
1,3-Propanediol	46.05	0.740	0.0094	-0.0022	-328	0.2567	25.7
1-Pentanol	45.11	0.710	0.0083	-0.0029	-420	0.2719	27.2
Acetone	44.77	0.7000	0.0113	-0.0023	-345	0.2774	27.7
Trichlormethane	44.74	0.699	0.0101	-0.0027	-307	0.2779	27.8
1,4-Butanediol	38.93	0.529	0.0118	-0.0025	-400	0.3716	37.1
1,5-Pentanediol	33.09	0.382	0.0115	-0.0028	-332	0.4659	46.6
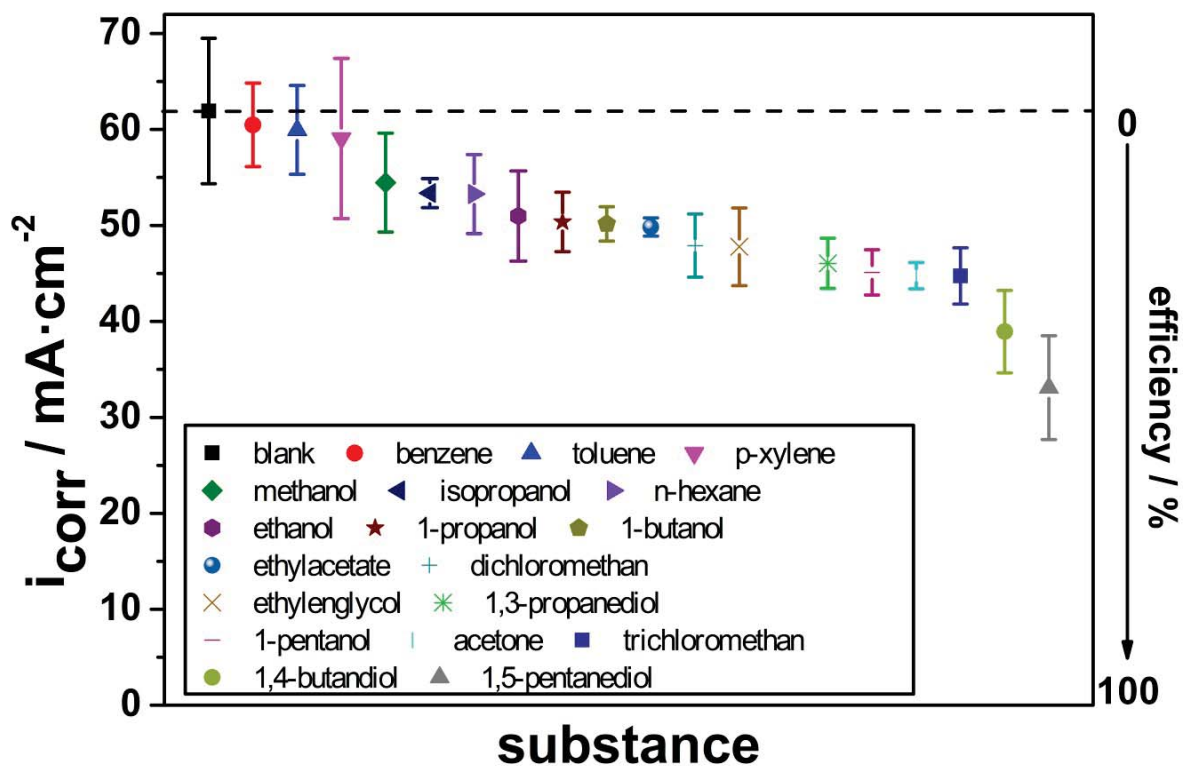
Fig. 3-7: Current density recorded and efficiency calculated by polarization measurement for steel CR4 coated with tested solvents as inhibitor compared to blank metal in 0.1 M NaCl. Blank efficiency (0) is display as black dotted line.

The probes tested in polarization evaluation with solvents are scanned with 1200 dpi resolution by using (Scanner HP Scanjet G4010) to reveal the differences in the surface of samples after the measurement (Fig. 3-8).
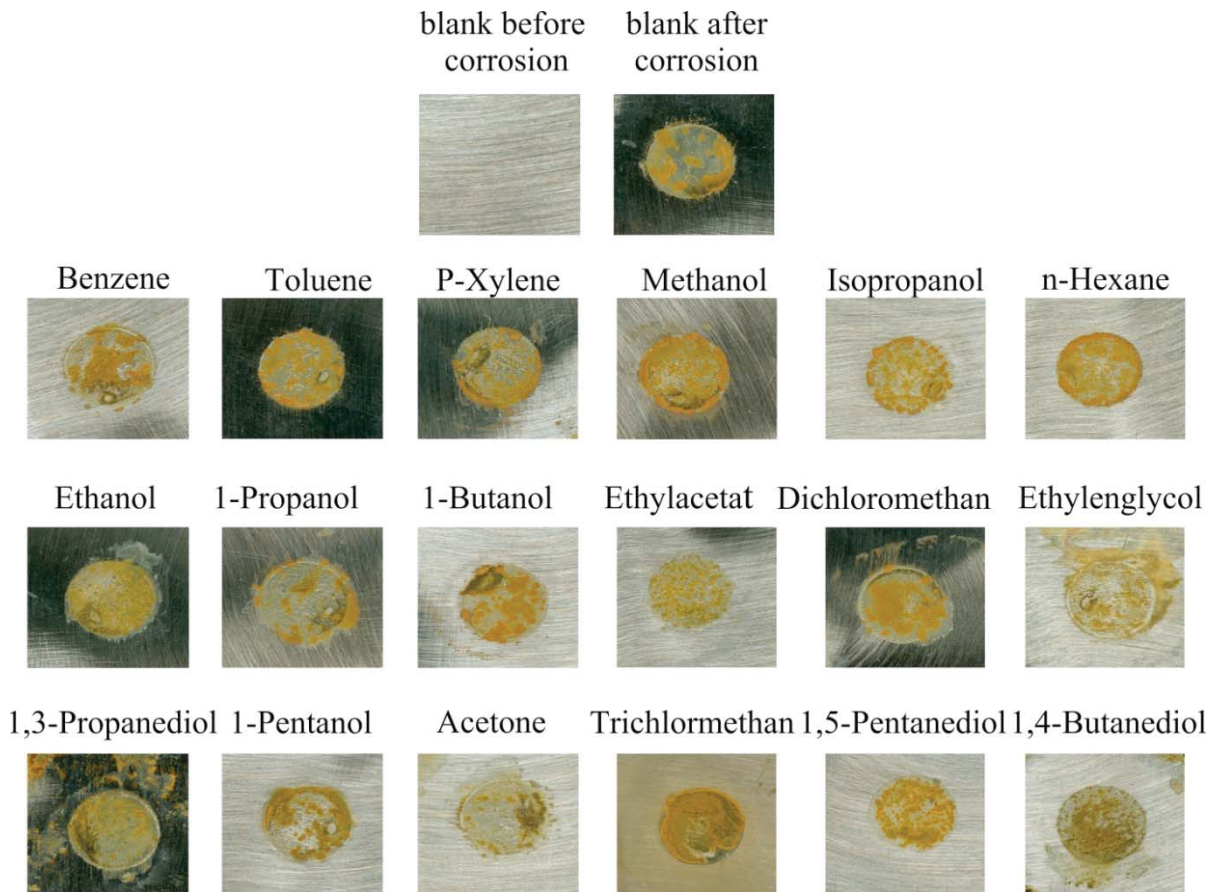
Fig. 3-8: Images scanned with 1200 dpi for coupons tested with different solvents as inhibitors compared to blank steel CR4 before and after corrosion test in 0.1 M NaCl during potentiodynamic polarization curve measurements.

3.4 Weight loss measurements

Steel CR4 in absent and present tested inhibitors with different concentrations are evaluated by weight loss measurement for 24 h in 0.1 M NaCl. Steel CR4 used in this evaluation was blank 2 (compare Table 2-1). The parameters of gravimetric test like weight loss ΔW, corrosion rate (**CR**) (Eq. 3-2), surface coverage θ (obtained by **IE**/100), and efficiency **IE (%)** (Eq. 3-3) [67,109,110,114] are summarized in Table 3-3.

$$CR = \Delta W / A \cdot t \qquad \text{Eq. 3-2}$$

$$IE(\%) = \frac{\Delta W - \Delta W_{inh}}{\Delta W} \cdot 100 \qquad \text{Eq. 3-3}$$

Where ΔW and ΔW_{inh} are the weight loss of steel CR4 without and with inhibitor respectively, **A** is the total area of sample, and **t** is the relevant immersion time of the coupon in the 0.1 M NaCl test solution.

Table 3-3: Results of weight loss ΔW, corrosion rate **CR**, surface coverage θ, and inhibition efficiency **IE** of steel CR4 combinations with different concentrations C_{inh} of tested inhibitors by immersion for 24 h in 0.1 M NaCl at room temperature during gravimetric measurement.

	C_{inh} (mmol·L^{-1})	ΔW (mg)	CR (mg cm^{-2} h^{-1})×10^{-5}	θ	IE (%)
Blank	0	0.00570	1.900	-	-
Inhibitor					
C	25	0.00340	1.133	0.4035	40.3
	50	0.00325	1.083	0.4298	42.9
	75	0.00323	1.077	0.4328	43.2
	100	0.00313	1.041	0.4517	45.1
OI	25	0.00385	1.283	0.3245	32.4
	50	0.00337	1.122	0.4094	40.9
	75	0.00330	1.100	0.4210	42.1
	100	0.00325	1.083	0.4298	42.9
L	25	0.00345	1.150	0.3947	39.4
	50	0.00315	1.105	0.4473	44.7
	75	0.00283	0.944	0.5029	50.2
	100	0.00267	0.891	0.5307	53.0
M	25	0.00184	0.613	0.6771	67.7
	50	0.00178	0.595	0.6867	68.6
	75	0.00173	0.577	0.6959	69.5
	100	0.00142	0.473	0.7508	75.0
O	25	0.00124	0.413	0.7824	78.2
	50	0.00114	0.380	0.8000	80.0
	75	0.00098	0.327	0.8280	82.8
	100	0.00080	0.266	0.8596	85.9
C+OI	25	0.00150	0.500	0.7368	73.6
	50	0.00124	0.413	0.7824	78.2
	75	0.00103	0.343	0.8192	81.9
	100	0.00098	0.328	0.8273	82.7

It is obvious from results in Table 3-3 that the efficiency enhanced when inhibitor concentration increased. The best tested concentration that gave optimum efficiency for all studied inhibitors was 100 mmol/L (compare Table 3-3 and Fig. 3-9). Inhibitor O gives the best protection of steel CR4 in all tested concentrations and the maximum efficiency was up to 86 % with 100 mmol/L (Fig. 3-9 green color). The second single combination M has an good efficiency up to 67 % with tested concentrations and highest efficiency was up to 75 % at 100 mmol/L (compare Table 3-3 and Fig. 3-9 dark yellow color). Sarcosine L has

acceptable efficiency up to 50 % at 75 and 100 mmol/L concentration and less than 50 % at 25 and 50 mmol/L concentration (compare Table 3-3 and Fig. 3-9 magenta color). The rest single compounds C and OI, have insignificant effect with all tested concentration with efficiencies less than 50 % (compare Table 3-3 and Fig. 3-9).

Synergistic effects of compound OI to improve the efficiency of substance C when they are working together as combination (C+OI) was very clear from results obtained. Efficiency of C and OI as single compound increased from less than 50 % up to 83 % with 100 mmol/L (compare Table 3-3 and Fig. 3-9 violet).

The increase in efficiency with higher concentrations is herein obvious by the raise of the surface coverage θ (Table 3-3). The reason for this improved merit is the adsorption of organic molecules via steel surface promoted with increasing of inhibitor concentration which causes a decrease of the contact area between metal surface and environment [109].
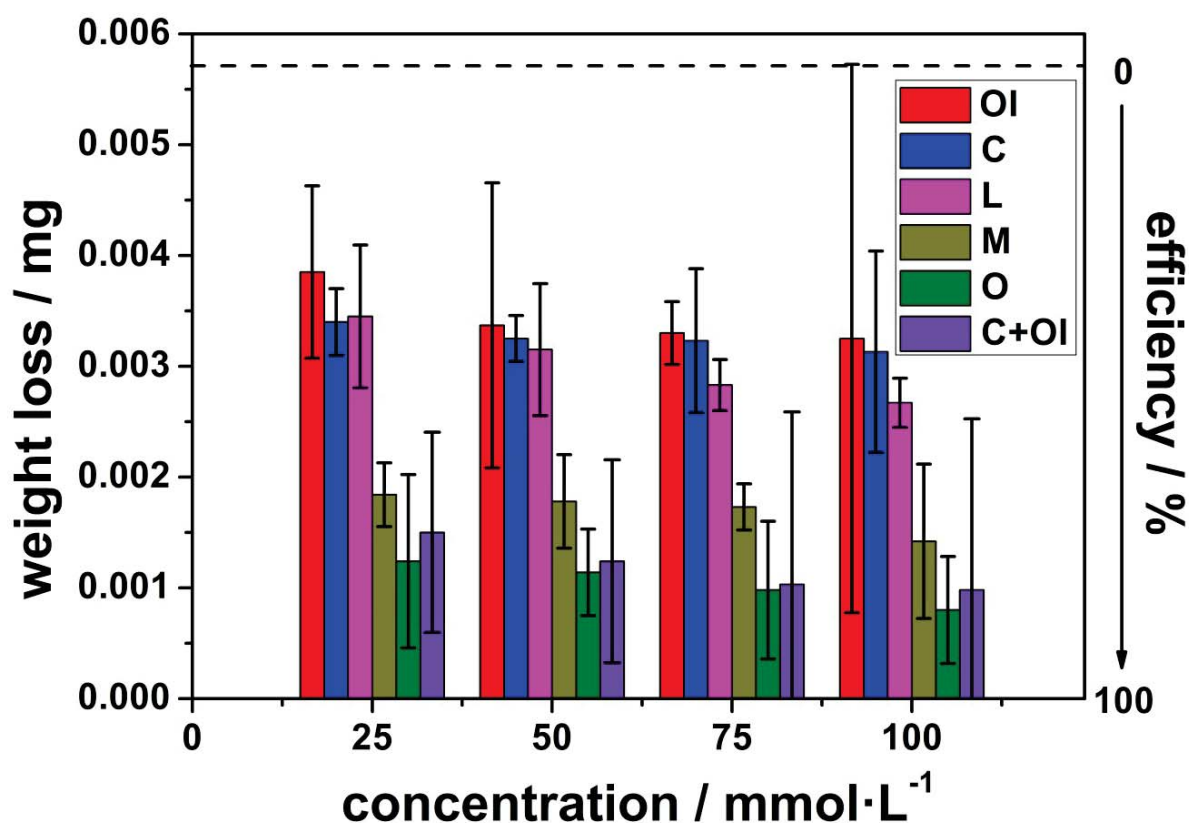
Fig. 3-9: Weight loss and calculated efficiency of tested synergist OI and inhibitors C, L, M, O and combination C+OI compared to blank steel CR4 for 24 h immersed in 0.1 M NaCl during gravimetric measurement. Blank is displayed in black dotted line, synergist OI in red, inhibitors C in blue, L in magenta, M in dark yellow, O in green, and combination C+OI in violet.

 Steel CR4 samples were directly examined by optical microscope with 50 μm magnification (KEYENCE VH-S30K, Deutschland GmbH, Germany) to monitor the change on the surface

after 24 h of immersion during weight loss test (Fig. 3-10). It is obvious that there are a lot of corrosion products on the surface for steel CR4 coated with OI, C, and L even with high concentration (Fig. 3-10 first to third column). For inhibitor M, there is less of corrosion products on the surface and the protection enhanced with higher concentration (Fig. 3-10 fourth column). Steel CR4 coated with inhibitor O has no corrosion detectable on the surface with all tested concentrations (Fig. 3-10 fifth column). Again as expected for synergist effect of OI when it work as one combination with C there is a great improvement in the protection when the corrosion goes less and less than C and OI as a single compound (Fig. 3-10 sixth column).
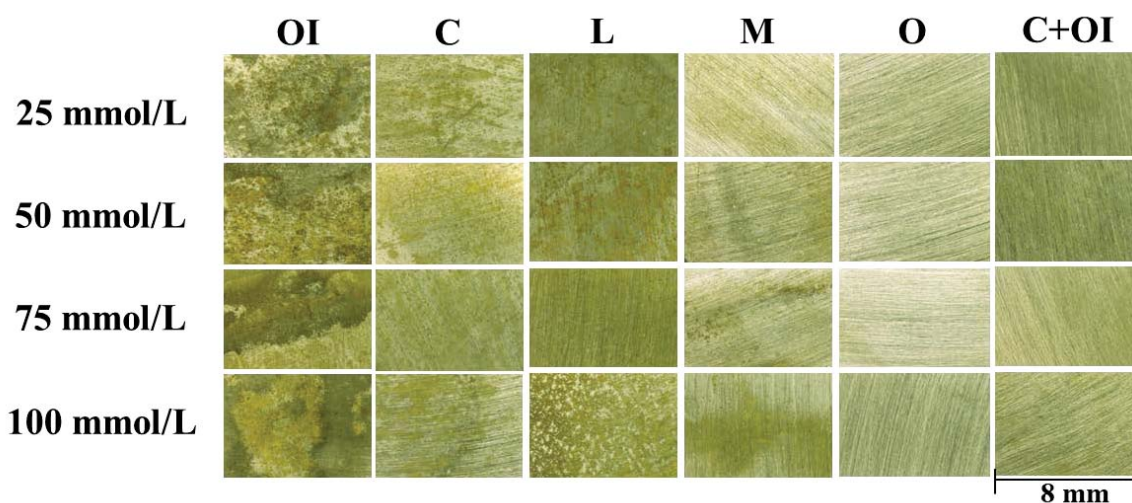
Fig. 3-10: Optical microscope images after 24 h of immersion coated steel CR4 with tested inhibitors at different concentrations (25, 50, 75, and 100 mmol/L) in 0.1 M NaCl during weight loss measurements with 50 μm magnification.

To test the efficiency of current inhibitor for longer duration, weight loss measurement was done for uncoated and coated steel CR4 with substances L, M, and O at 50 mmol/L concentration for 96 h in 0.1 M NaCl (Fig. 3-11). Inhibitor O is still having effect to decrease corrosion with efficiency more than 50 % after 96 h (Fig. 3-11). Compound M has efficiency around 30 % and L just 3 % (Fig. 3-11). These results indicate that adsorbed inhibitor on the steel surface are washed out into the test solution during the time. Therefore the investigated inhibitors can be applied only for a terminated respective short time protection.
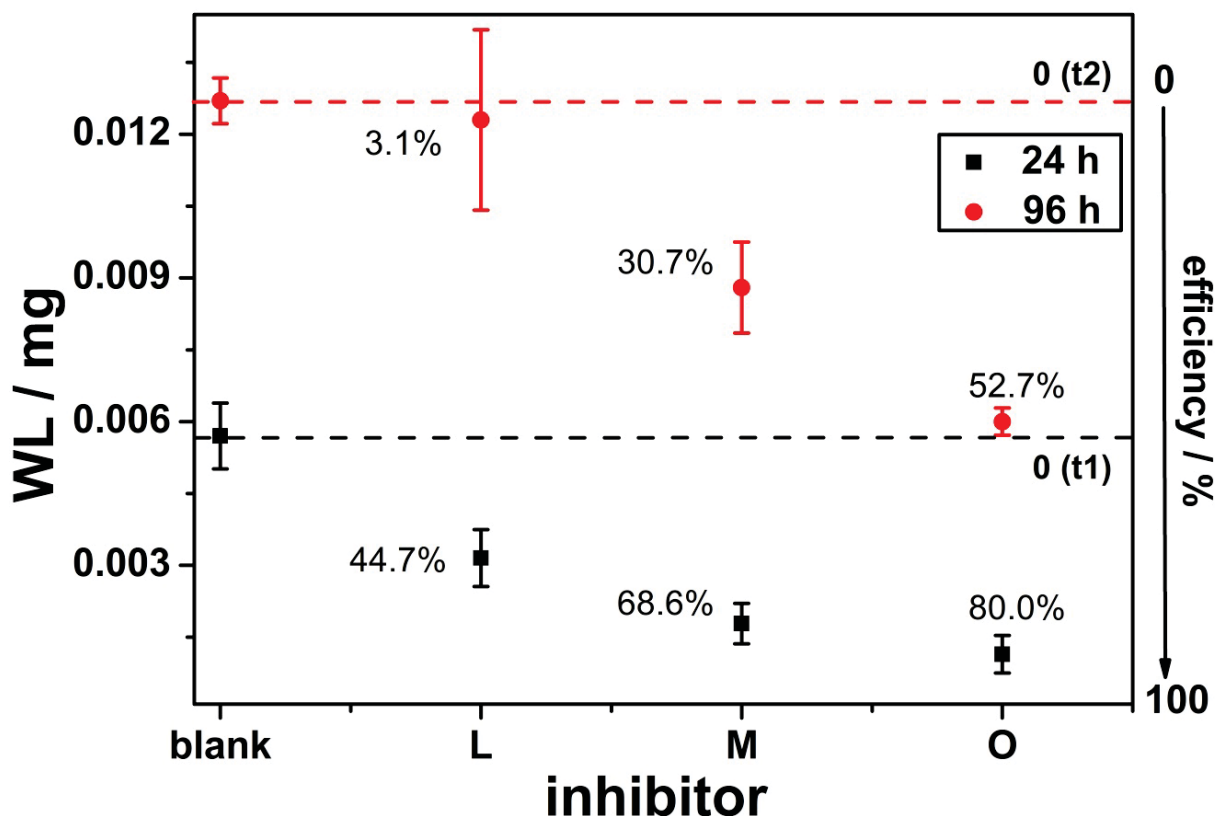
Fig. 3-11: Weight loss and calculated efficiency obtained by gravimetric measurement of tested inhibitors L, M, and O with 50 mmol/L concentration compared to blank steel CR4 for immersion time 24 h and 96 h in 0.1 M NaCl. Blank efficiency 0 (t1) is display in black for 24 h and 0 (t2) in red for 96 h.

3.5 Electrochemical measurements

3.5.1 Potentiodynamic polarization measurements

Candidate substances were tested at different concentrations (25, 50, 75, and 100 mmol/L) via polarization measurement to protect steel CR4 against corrosion in 0.1 M NaCl. Steel CR4 used in this evaluation was blank 2 (compare Table 2-1).

Before starting the evaluation, polarization tests were combined with different holding time to check the stability of the protective film formed on steel CR4 surface by compounds C, L, M, and O with 50 mmol/L concentration compared to blank metal. Complete holder system included uncoated and coated steel CR4 with tested inhibitors as working electrode was immersed in 0.1 M NaCl for 0, 0.5, 1, 2, 4, 8, 12, and 24 h at free potential then applied ± 200 mV according to OCP recorded and measured the current density i_{corr} for each time. Fig. 3-12 shows the anodic and cathodic polarization curves for uncoated and coated steel CR4 with tested substances at different holding time (0, 0.5, 1, 2, 4, 8, 12, and 24 h).
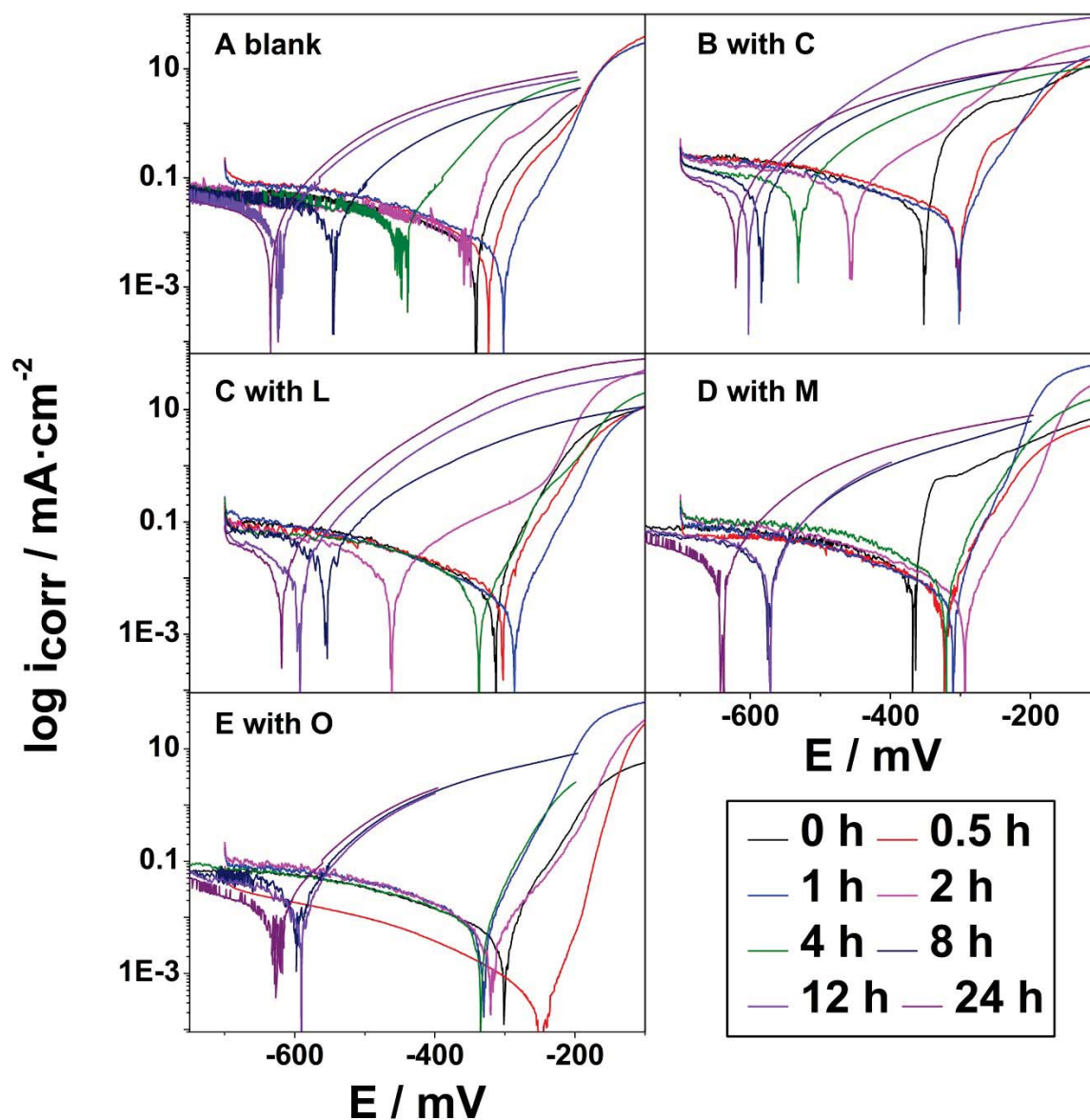
Fig. 3-12: Anodic and cathodic polarization curves for steel CR4 coated with 50 mmol/L concentration of tested inhibitors C, L, M, and O after different holding time in 0.1 M NaCl. Chart **A** for blank, **B** for sarcosine C, **C** for L, **D** for M, and **E** for O. Holding time 0 h is displayed in black, 0.5 h in red, 1 h in blue, 2 h in magenta, 4 h in green, 8 h in navy , 12 h in violet, and 24 h in purple, each as solid line.

Corrosion potential E_{corr} was shifted slightly to positive direction at 0.5 h and 1 h of holding time compared to 0 h (Fig. 3-12 A red and blue color respectively compared to black color). Increased holding time from 2 h to 24 h shifted E_{corr} to more negative value compared to 0 h of holding time (Fig. 3-12 A). Similar behavior was found for steel CR4 with and without inhibitors C, L, M, and O to shift E_{corr} to positive direction at 0.5 h and 1 h of holding time while shifting to more negative value with increased immersion time 2, 4, 8, 12, and 24 h (Fig. 3-12 A, B, C, D, and E).

Current density i_{corr} was recorded for each holding time and summarized in Table 3-4 and Fig. 3-13.

Table 3-4: Current density i_{corr} for uncoated and coated steel CR4 with tested inhibitors C, L, M, and O at different immersion time 0, 0.5, 1, 2, 4, 8, 12, and 24 h in 0.1 M NaCl during polarization measurement.

i_{corr} µA.cm^{-1}	Holding time in 0.1 M NaCl before polarization start[h]							
	0	**0.5**	**1**	**2**	**4**	**8**	**12**	**24**
Blank	44.1	60.7	64.8	56.9	34.1	30.7	26.2	21.8
C	39.8	40.5	44.1	38.8	30.6	28.9	22.5	21.7
L	32.7	37.9	38.5	40.4	43.9	35.4	24.5	22.4
M	20.8	22.6	24.6	25.9	26.8	25.3	24.8	20.1
O	5.8	5.8	5.9	6.2	14.8	22.6	22.8	20.2

Current density i_{corr} for steel CR4 blank and coated with compound C raised when holding time increased from 0 h to 0.5 h and 1 h then starting to decreased with increase immersion time from 2 h to 24 h (compare Table 3-4 and Fig. 3-13 black and blue color). For steel CR4 coated with inhibitors L, M, and O the current density i_{corr} was increased till 4 h then decreased with holding time increased from 8 h to 24 h (compare Table 3-4 and Fig. 3-13 magenta, dark yellow and green color). The protective film formed by inhibitor O has a good stability till 4 h of holding time in 0.1 M NaCl and after 8 h to 24 h the current density i_{corr} value increased to be similar to blank (compare Table 3-4 and Fig. 3-13 green color). Inhibitor M has good efficiency to reduce i_{corr} till 2 h of holding time; afterwards i_{corr} increased to be like blank (compare Table 3-4 and Fig. 3-13 dark yellow color). Sarcosine C effected to decrease i_{corr} in good value till 1 h of holding time and after this time the efficiency with decreasing current was less and less till it shows similar behavior like blank (compare Table 3-4 and Fig. 3-13 blue color). Inhibitor L has low efficiency to decrease i_{corr} at 0, 0.5, and 1 h of holding time then the current raised to higher value than in blank at 4 h and 8 h and decreased again to be like blank at 12 h and 24 h of holding time (compare Table 3-4 and Fig. 3-13 magenta color). The explanation for the decrease of the current density i_{corr} after 2 h of immersion blank steel CR4 in 0.1 M NaCl as the sample was already corroded and oxide film respective to the rust was formed on the surface and this film is working as a protective film then decreased i_{corr}. Steel CR4 coated with tested inhibitors was corroded after a certain holding time when the protective film washed out and dissolved into test solution. Afterwards the oxide film was formed and decreased i_{corr} to value very close to blank. This evaluation approved that compounds M and O are powerful to form a protective

film for up to 4 h (= "short time"), when in direct contact with the test solution. After 4 h the inhibitor probably starts slightly to dissolve into the working solution and the probes act more and more as the blank material. For the following polarization evaluations, 0.5 h was used for holding samples in the test solution at free potential OCP until steady state.
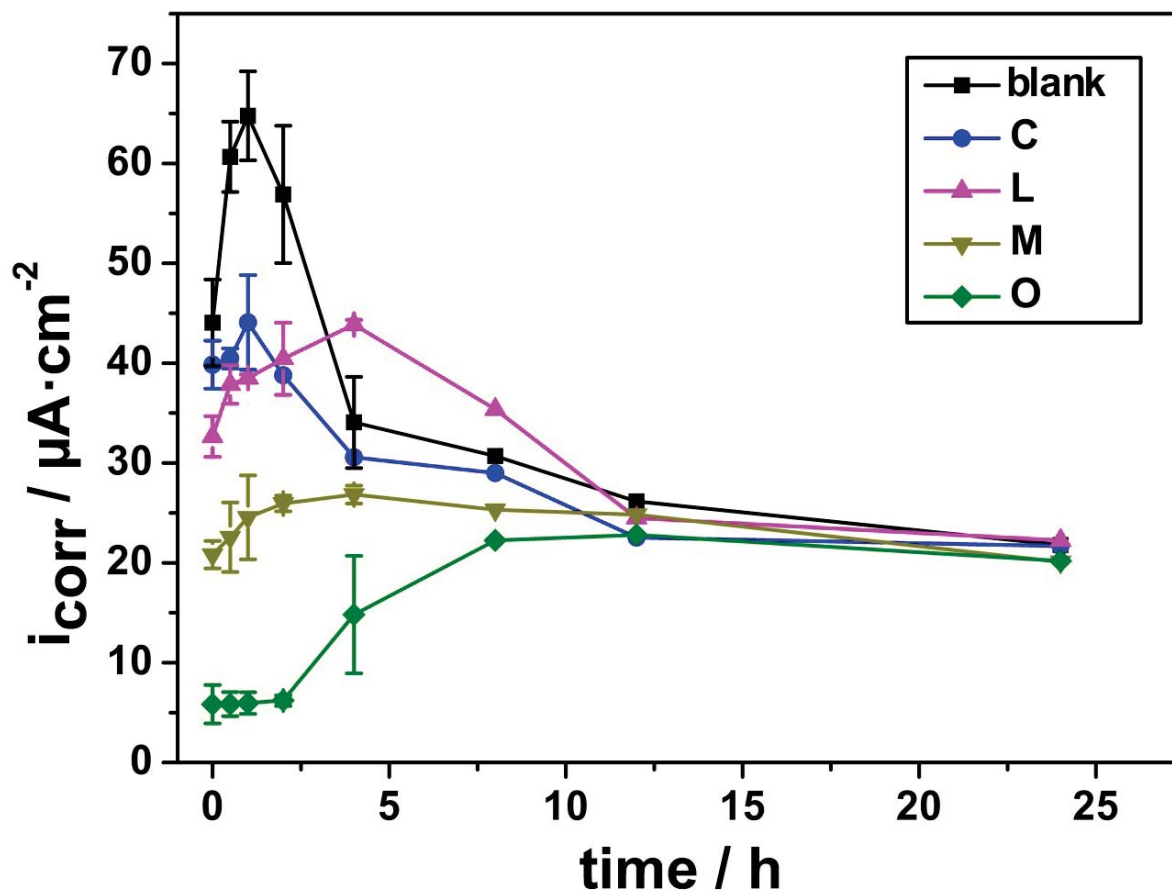
Fig. 3-13: Current density i_{corr} for 50 mmol/L concentration of tested inhibitors C, L, M, and O at different holding time in 0.1 M NaCl compared to blank metal. Blank material is displayed in black, C in blue, L in magenta, M in dark yellow, and O in green, each as solid line.

Preliminary tests for selected single inhibitors and combination of them with studied synergists are done with 50 mmol/L concentration via polarization measurement to detect their significant effect. Table 3-5 and Fig. 3-14 summarize the exchange current density and calculated efficiency obtained during polarization measurement. Inhibitor O has the highest effect to reduce i_{corr} with efficiency up to 95 % followed by inhibitor M with efficiency up to 70 % when they are tested as single inhibitor (compare Table 3-5 and Fig. 3-14 green and dark yellow color respectively). Sarcosine L and C as single inhibitors have efficiency up to 46 % and 35 % (compare Table 3-5 and Fig. 3-14 magenta and blue color respectively).

Table 3-5: Exchange current density i_{corr} and calculated efficiency **IE** (%) for single tested inhibitor C, L, M, and O and for combination of synergists OI and MI with studied inhibitor at 50 mmol/L concentration during polarization measurement in 0.1 M NaCl.

Compound	i_{corr} / μAmp.cm^{-2}				Eff. / %			
	C	L	M	O	C	L	M	O
Inhibitor	40.34	33.56	18.58	2.91	34.8	45.8	70.0	95.3
OI	8.52	24.68	17.08	13.41	86.2	60.1	72.4	78.3
MI	35.7	33.78	43.70	20.58	42.3	45.4	29.4	66.7

Synergist OI has a good effect to improve the efficiency of sarcosine C from 35 % to 86 % and small effect to enhance efficiency up to 60 % and 72 % of inhibitor L and M respectively while it has negative effect with inhibitor O when it decreased the efficiency of O from 95 % down to 78 % (compare Table 3-5 and Fig. 3-14). The second tested synergist MI has very small effect to increase the efficiency of sarcosine C from 35 % up to 42 % (compare Table 3-5 and Fig. 3-14). Synergist MI has a big negative effect on inhibitor M and O when it decreases the efficiency from 70 % down to 29 % and from 95 % down to 67 % respectively (compare Table 3-5 and Fig. 3-14 dark yellow and green color respectively). MI caused a very slight decrease in efficiency of inhibitor L (compare Table 3-5 and Fig. 3-14 magenta color).

The current results obtained indicate that there is a strong point and worthwhile to continuous the investigation of synergist OI and how it effects especially on inhibitor C at different concentrations, different dip coating times, and longer duration time of testing during spray corrosion measurement. Because synergist MI showed negative effects on L, M, and O and just a slight improvement for C it was not worthwhile to continue further investigations.
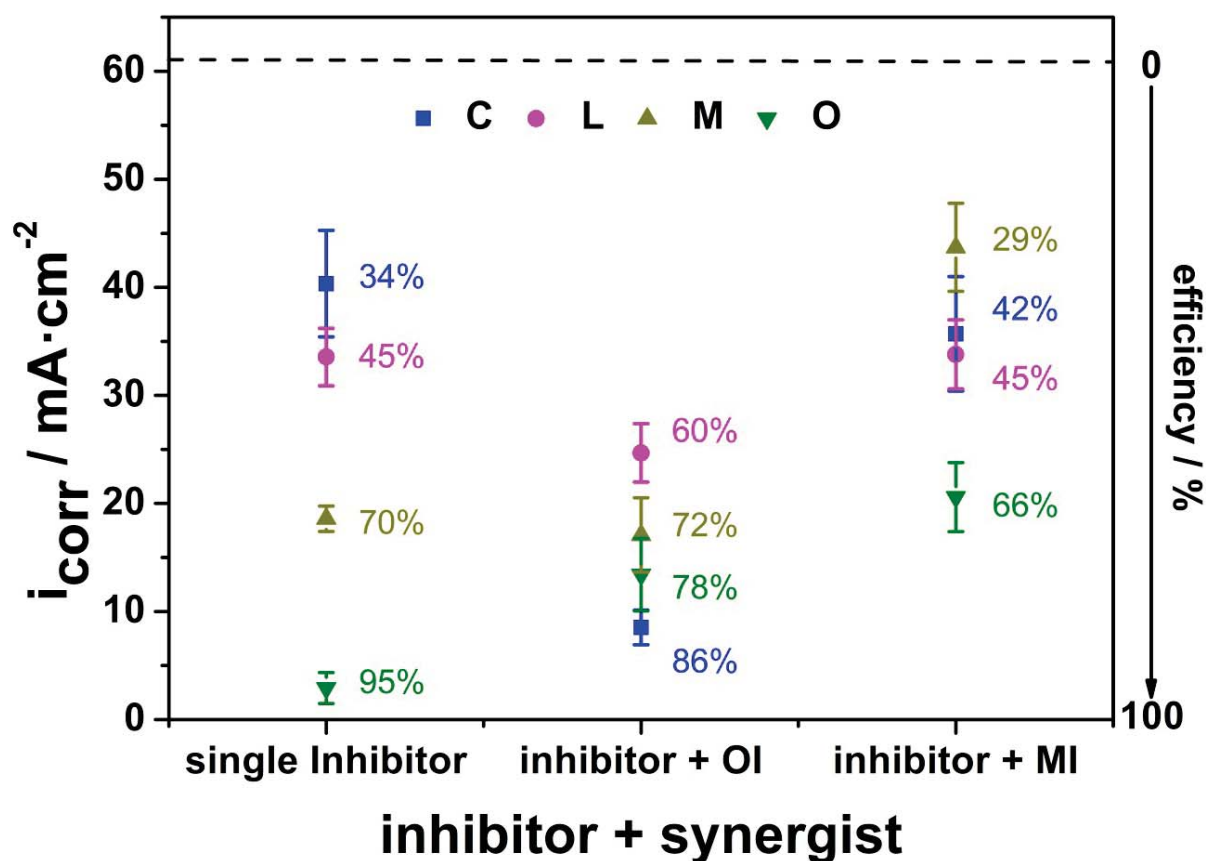
Fig. 3-14: Exchange current density i_{corr} and calculated efficiency IE (%) for single tested inhibitor C, L, M, and O and for combination with synergists OI and MI at concentration 50 mmol/L during polarization measurement in 0.1 M NaCl.

Polarization measurement was continued to investigate the influence of selected substances (C, OI, L, M, O and combination of C+OI) with four different concentrations on the protection of steel CR4 in 0.1 M NaCl. Anodic and cathodic polarization curves for studied substances with different concentrations (25, 50, 75, and 100 mmol/L) compared to blank metal are shown in Fig. 3-15.

The electrochemical parameters obtained in the current evaluation like exchange current density i_{corr} resp. i_{inh}, corrosion rate CR, anodic and cathodic Tafel slope β_a and β_c, corrosion potential E_{corr}, surface coverage θ and inhibition efficiency IE (%) are given in Table 3-6.
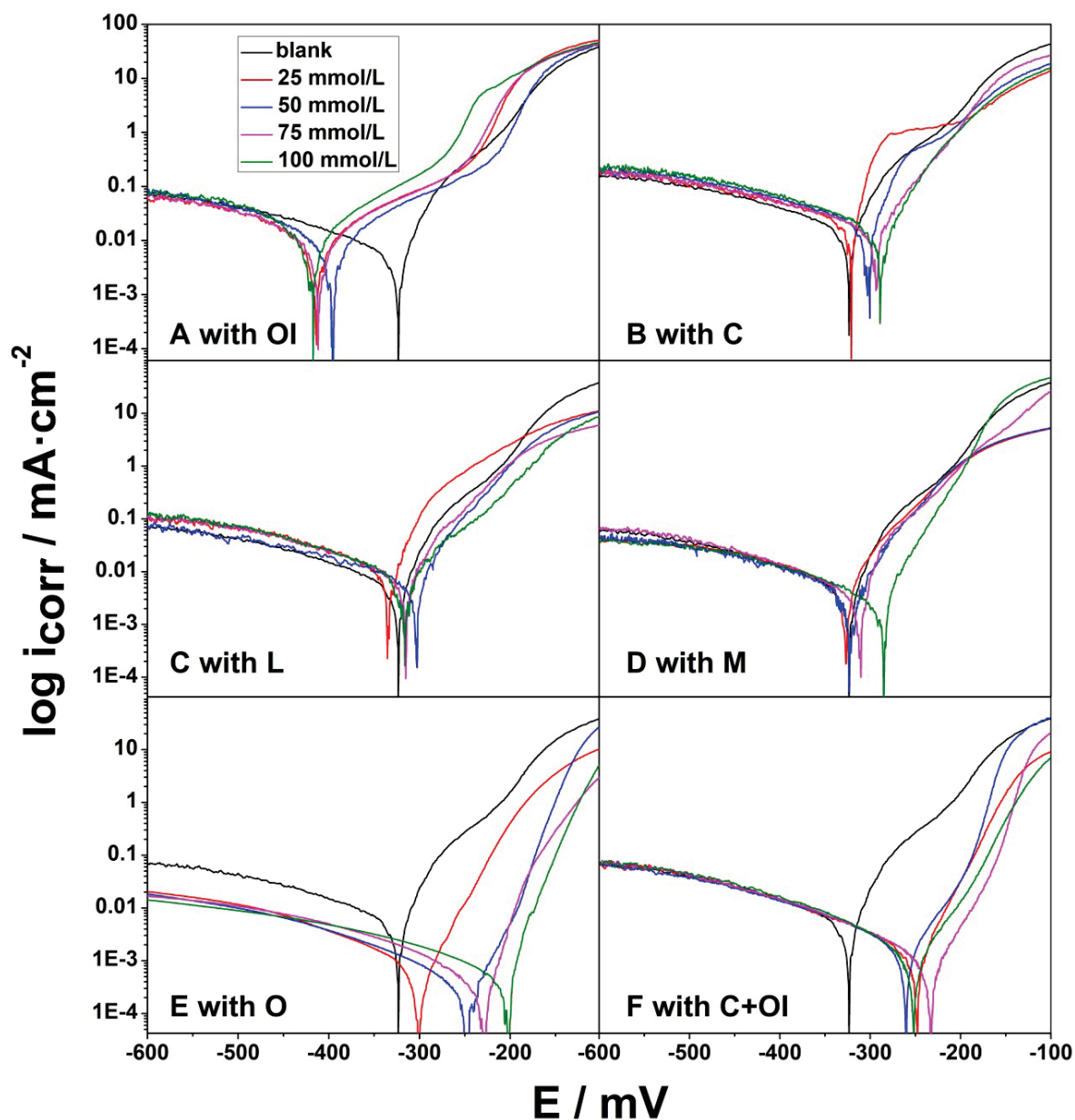
Fig. 3-15: Anodic and cathodic polarization curves in the absence and presence of selected inhibitors (chart **A** for OI, **B** for C, **C** for L, **D** for M, **E** for O, and **F** for C+OI) at different concentrations. Blank material is displayed in black, 25 mmol/L in red, 50 mmol/L in blue, 75 mmol/L in magenta, and 100 mmol/L in green, each as solid line. The legend in chart **A** is the same for chart **B, C, D, E** and **F**.

It is clear from the data in Table 3-6 that the protection of steel CR4 is improved with increased concentration of inhibitor. Increasing in concentration of tested sarcosine C, M, and O lead to shifted E_{corr} to more positive direction compared to blank (compare Table 3-6 and Fig. 3-15 B, D, and E). The result recorded for inhibitor L indicates to the shifting of E_{corr} a negative direction with concentration 25 and 50 mmol/L while it moved in positive direction with 75 and 100 mmol/L (compare Table 3-6 and Fig. 3-15 C).

Table 3-6: Electrochemical parameters obtained by polarization evaluation for present steel CR4 in 0.1 M NaCl. The corrosion rate **CR** is given by millimeter per year (mm/y) depending on current density i_{corr} resp. i_{inh}, β_a and β_c are the anodic and cathodic Tafel slope, E_{corr} represents the corrosion potential, θ is the surface coverage of metal surface with inhibitor, and **IE** in % is the corrosion reduction efficiency of chosen compounds at different concentrations directly compared to the blank material.

	C_{inh} (mmol/L)	i_{corr} resp. i_{inh} (μA/cm^2)	**CR** (mm/y)	β_a	β_c	E_{corr} (mV)	θ	**IE** (%)
Blank	0	61.93	1.339	0.0168	-0.0029	-324	-	-
Inhibitor								
	25	45.55	0.988	0.0207	-0.0034	-413	0.265	26.5
	50	41.76	0.906	0.02784	-0.0036	-395	0.326	32.6
OI	75	36.73	0.797	0.02365	-0.0039	-411	0.407	40.7
	100	33.88	0.735	0.03059	-0.0030	-417	0.453	45.3
	25	49.89	1.082	0.031	-0.0035	-321	0.195	19.5
	50	40.34	0.875	0.0303	-0.0034	-300	0.349	34.9
C	75	34.59	0.750	0.0218	-0.0043	-293	0.442	44.2
	100	32.78	0.711	0.0222	-0.0040	-288	0.471	47.1
	25	43.76	0.946	0.0110	-0.0035	-335	0.293	29.3
	50	33.56	0.727	0.0191	-0.0038	-345	0.458	45.8
L	75	30.56	0.661	0.0170	-0.0039	-315	0.506	50.6
	100	30.19	0.653	0.0171	-0.0047	-316	0.512	51.2
	25	22.86	0.494	0.0158	-0.0020	-325	0.630	63.0
	50	18.58	0.401	0.0173	-0.0029	-306	0.700	70.0
M	75	16.54	0.357	0.0161	-0.0039	-305	0.733	73.3
	100	10.84	0.234	0.0286	-0.0030	-271	0.825	82.5
	25	8.26	0.178	0.0252	-0.0038	-294	0.866	86.6
	50	2.91	0.062	0.0454	-0.0042	-242	0.953	95.3
O	75	2.37	0.051	0.0218	-0.0036	-234	0.961	96.1
	100	1.73	0.037	0.0405	-0.0031	-211	0.972	97.2
	25	15.77	0.342	0.0296	-0.0042	-249	0.745	74.5
	50	8.52	0.184	0.02928	-0.0034	-260	0.862	86.2
C+OI	75	5.86	0.126	0.03608	-0.0040	-232	0.905	90.5
	100	5.31	0.115	0.0259	-0.0036	-253	0.914	91.4

Synergist OI caused shift in E_{corr} to more negative direction compared to blank at all tested concentrations (compare Table 3-6 and Fig. 3-15 A). Combination of C+OI shifted E_{corr} to more positive direction compared to blank at all tested concentration (compare Table 3-6 and Fig. 3-15 F). Highest shifting in E_{corr} was with inhibitor O and combination C+OI (Fig. 3-

15 E and F). Inhibitor O has the maximum effect to decrease the current on both anodic and cathodic sides (Fig. 3-15 E). Combination C+OI slightly decreased the current on the cathodic polarization while it was much more on the anodic part (Fig. 3-15 F). Sarcosine C and L increased the current on the cathodic side with all tested concentrations while it decreased the current on the anodic polarization except at concentration 25 mmol/L (Fig. 3-15 B and C). Inhibitor M decreased the current in both anodic and cathodic curves with all tested concentrations and higher decrease was on the anodic part with concentration 100 mmol/L (Fig. 3-15 D). Synergist OI effected a slight reducing of the current on the cathodic part while it influenced to increase the current on the anodic reaction with all studied concentrations (Fig. 3-15 A).

The efficiency of tested inhibitors with different concentration was calculated from i_{corr} obtained in polarization evaluation and it is shown in Fig. 3-16. Inhibitor O has the best effect to decrease corrosion at all tested concentrations already starting with efficiency from 86 % and up to 97 % at 25 mmol/L and 100 mmol/L respectively (compare Table 3-6 and Fig. 3-16 green color). The second inhibitor that has a good effect was M with efficiency 83 % at highest concentration (compare Table 3-6 and Fig. 3-16 dark yellow color). For inhibitor L the efficiency was up to 50 % with concentrations 75 and 100 mmol/L and less than 50 % with 25 and 50 mmol/L (compare Table 3-6 and Fig. 3-16 magenta color). Both substances C and OI have insignificant efficiency below 50 % when they are working as individual inhibitor (compare Table 3-6 and Fig. 3-16 blue and red color respectively). Synergist OI improved the efficiency of C when they are working as combination C+OI and increased efficiency from up to 47 % to 91 % with highest concentration and from up to 19 % to 75 % with lowest concentration (compare Table 3-6 and Fig. 3-16 navy color). The optimum efficiency of protection was obtained at highest concentration 100 mmol/L for inhibitor O and combination C+OI with efficiency up to 97 % and 91 % respectively (compare Table 3-6 and Fig. 3-16 green and navy color respectively). The highest concentration of inhibitor M showed satisfied efficiency up to 82 % and only up to 51 % for inhibitor L (compare Table 3-6 and Fig. 3-16 dark yellow and magenta color respectively).

It can be concluded, with increasing sarcosine concentration the current in the anodic polarization is more suppressed than cathodic part. A significant and gradual shift in E_{corr} to more noble potentials is detected for increasing concentrations of inhibitor O (compare Table 3-6 and Fig. 3-15 E). Therefore with higher concentrations the cathodic region extents before anodic processes start giving a better protection [26,106,107].
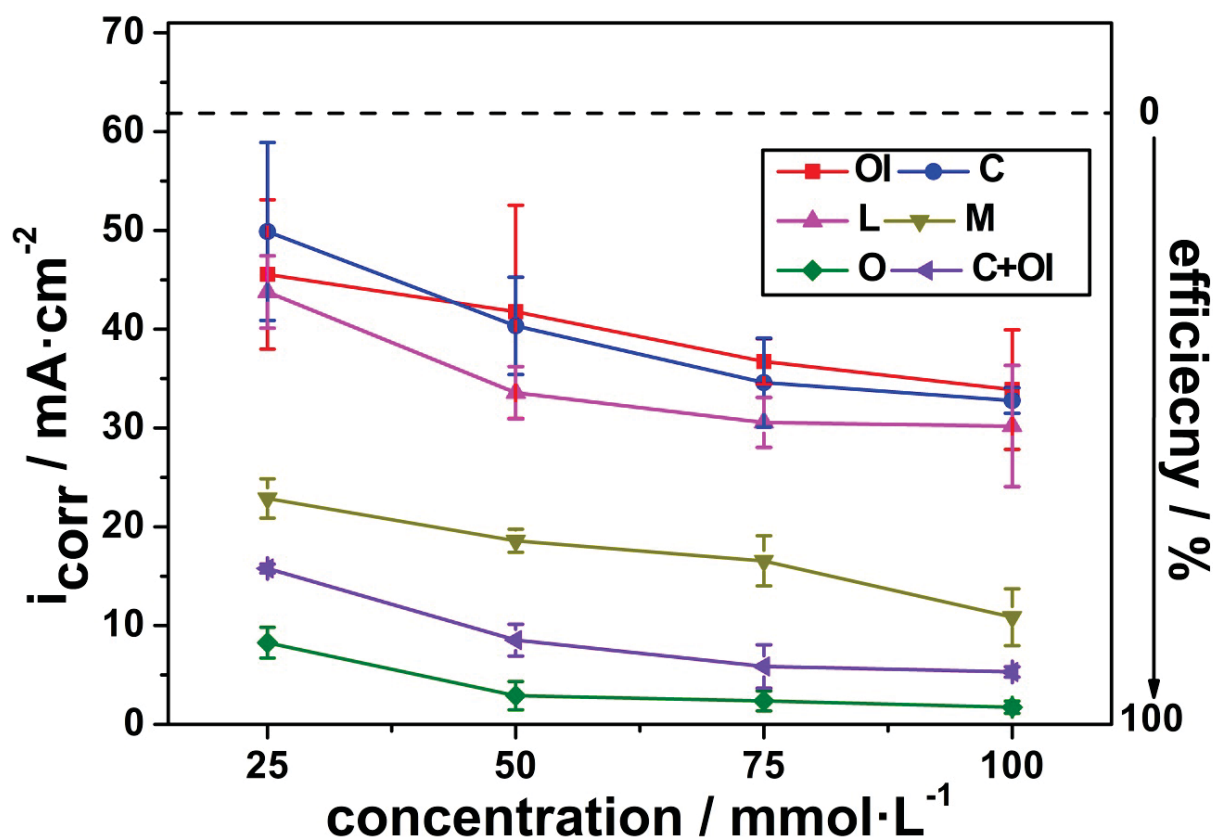
Fig. 3-16: Corrosion current density i_{corr} and calculated efficiency to protect steel CR4 coupons during polarization evaluation at different concentrations of tested inhibitors. The level for blank steel material is displayed as black dotted line (0 % efficiency, indicated on the right), inhibitor C in blue, OI in red, L in magenta, M in dark yellow, O in green, and combination C+OI in navy (each with solid line for better readability).

3.5.2 Electrochemical impedance spectroscopy measurements (EIS)

Electrochemical impedance spectroscopy (EIS) measurement was carried out to test candidate compounds (C, L, M, O, and combination C+OI) with different concentrations and synergist OI with 50 mmol/L concentration. Steel CR4 used in this evaluation was blank 2 (compare Table 2-1). Fig. 3-17 shows Randel's cell which is used as equivalent circuit to calculate the result obtained by EIS measurements [117].

EIS characteristics are presented in Nyquist plot (Fig. 3-18) and Bode plot (Fig. 3-19) for coated steel CR4 with L, M, O, and combination C+OI at different concentrations, and synergist OI individual with 50 mmol/L concentration. The intercept of impedance spectra at high frequency with real impedance (x-axis) represents the solution resistance R_s while the intercept with same axis of the spectra at low frequency is the sum of resistance of solution and charge transfer ($R_s + R_{ct}$) and the diameter of semicircle represent R_{ct}.
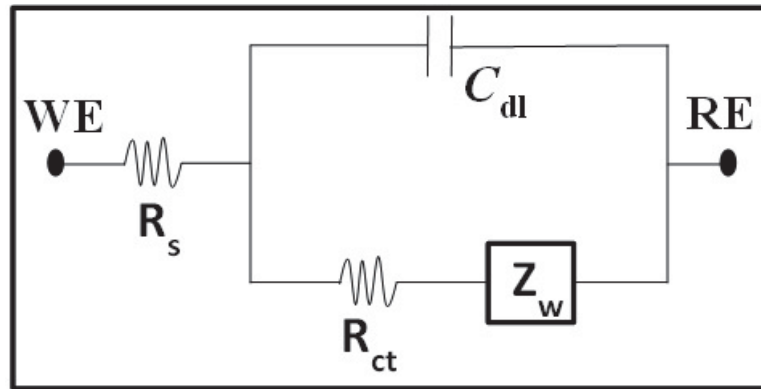
Fig. 3-17: Randle's cell used as equivalent circuit to calculated the result obtained by electrochemical impedance spectroscopy (EIS) tests.

The expansion in diameter of semicircles curves in Nyquist plot indicates to the charge transfer resistance R_{ct} increased with inhibitor concentration increasing (Fig. 3-18). The spectra of impedance show inhibitor O has an excellent effect to satisfying a good covering of steel CR4 surface with protective film followed by inhibitor M (Fig. 3-18 E and D respectively). Inhibitor L at all tested concentrations is controlled by diffusion processes (Fig. 3-18 C). For inhibitor C is a good increase in value of real impedance (x-axis) is satisfying but the imaginary (y-axis) was too low. Especially at concentrations of 25 and 50 mmol/L while at concentration 75 and 100 mmol/L the spectra show semi-circle curves with efficiency less than other studied compounds (Fig. 3-18 B). The deviation of semicircle curves in Nyquist plot (Fig. 3-18) explicit the interaction between steel surface and electrolyte correlated with kinetic and diffusion process and produce the polarization interface [113-117].

The capacitance of double layer C_{dl} can obtain from the intercept value of linear region extrapolation with absolute impedance axis Z (y-axis) in Bode plot (Fig. 3-19) [117].

The electrochemical parameters obtained by EIS measurement like resistance of solution R_s and charge transfer R_{ct}, double layer capacitance C_{dl}, surface coverage with inhibitor molecules $\boldsymbol{\Theta}$, and efficiency $IE\ (\%)$ of tested compounds calculated by (Eq. 3-4) are summarized in Table 3-7.

$$IE(\%) = \frac{R_{ct,inh} - R}{R_{ct,inh}} \times 100$$

Eq. 3-4

Where $R_{ct,inh.}$ and R is the resistance with and without inhibitor respectively.
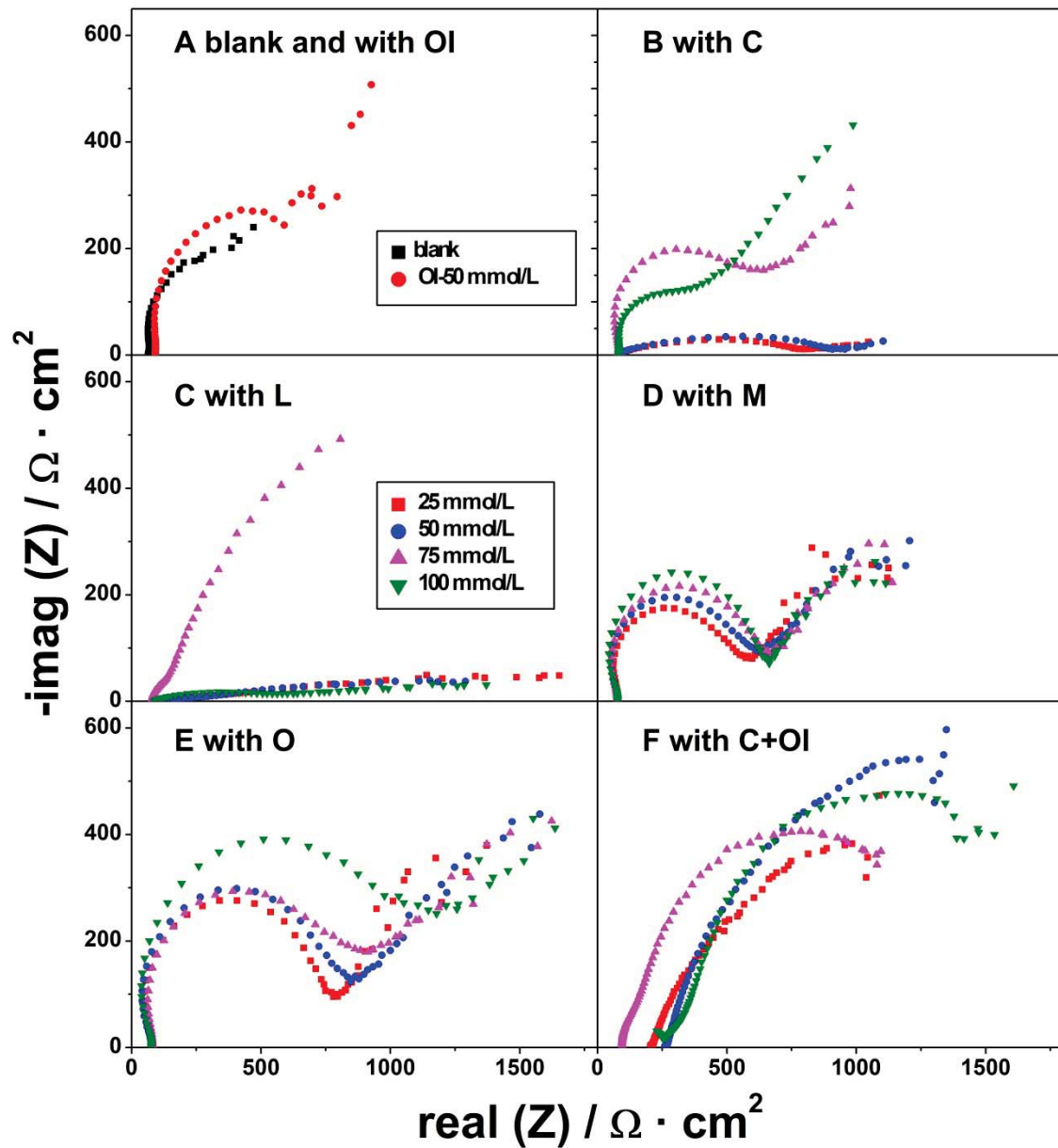
Fig. 3-18: EIS spectra of tested inhibitors at different concentrations (chart **A** for blank displays in black and OI at 50 mmol/L concentration in red, **B** for C, **C** for L , **D** for M, **E** for O, and **F** for combination C+OI). Color code refers to concentration (25 mmol/L in red, 50 mmol/L in blue, 75 mmol/L in magenta, and 100 mmol/L in green). The diameter of the semicircle corresponds to the charge transfer resistance R_{ct}. The non-semicircle shape for C at 25 and 50 mmol/L, OI, and L corresponds to diffusion controlled processes. The legend in chart **C** is the same for charts **B**, **C**, **D**, **E**, and **F**.
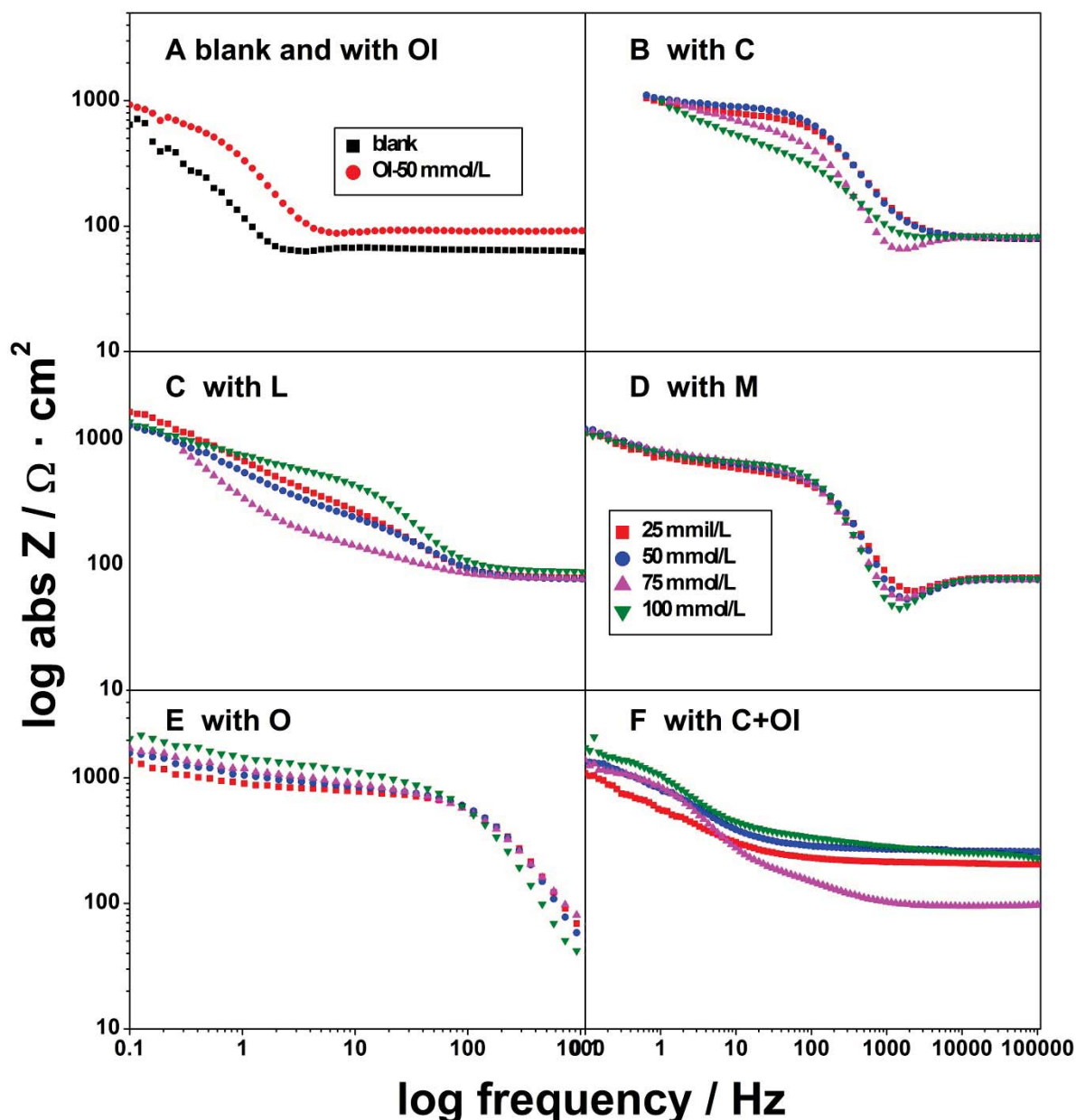
Fig. 3-19: Bode plot of tested inhibitors at different concentrations (chart **A** for blank in black and OI at 50 mmol/L concentration in red, **B** for C, **C** for L , **D** for M, **E** for O, **F** for combination C+OI). Color code refers to concentration (25 mmol/L in red, 50 mmol/L in blue, 75 mmol/L in magenta, and 100 mmol/L in green). The legend in chart **D** is the same for charts **B**, **C**, **D**, **E**, and **F**.

The semicircle is depressed at high frequency followed by inductive loop in the low frequency regions. These results indicate that the corrosion process in absence and presence of studied compounds is controlled by a charge transfer [103,118]. Bode plots shows the impedance increases with increasing inhibitor concentration (Fig. 3-19).

The result of EIS in Table 3-7 reveal to that the barrier film formed on the steel CR4 surface by inhibitor O increased R_{ct} with efficiency up to 84 % at highest tested concentration

(compare Table 3-7 and Fig. 3-18 E green color). The second best single inhibitor is M with inhibition efficiency up to 69 % (compare Table 3-7 and Fig. 3-18 D green color).

Table 3-7: Electrochemical parameters measured by EIS for steel CR4 in 0.1 M NaCl. The solution and charge transfer resistance R_s , R_{ct} is given by (Ω cm^2), double layer capacitance C_{dl}, surface coverage θ, and IE (%) is the corrosion reduction efficiency of the chosen substances compared to the blank material.

	C_{inh} (mmol/L)	R_s Ω cm^2	R_{ct} (Ω cm^2)	C_{dl} $\mu F/cm^2$	Θ	IE (%)
Blank	0	64.38	178.86	2.6425	-	-
Inhibitor						
OI	50	90.95	331.33	2.1919	0.4601	46.0
C	25	79.50	570.12	1.6087	0.6862	68.6
	50	80.34	687.26	1.5994	0.7397	73.9
	75	81.40	350.28	1.5242	0.4893	48.9
	100	82.17	301.33	1.8155	0.4064	40.6
L	25	78.92	315.05	2.0742	0.4322	43.2
	50	77.00	337.28	2.0769	0.4696	46.9
	75	77.31	381.21	2.5067	0.5308	53.0
	100	87.89	435.73	1.7435	0.5895	58.9
M	25	78.62	494.33	1.4984	0.6381	63.8
	50	76.22	541.67	1.4602	0.6697	66.9
	75	76.09	586.11	1.4548	0.6948	69.4
	100	77.47	586.43	1.3796	0.6950	69.5
O	25	74.94	674.46	1.3904	0.7348	73.4
	50	75.79	770.76	1.3455	0.7679	76.7
	75	79.42	833.97	1.4205	0.7855	78.5
	100	76.70	1101.76	1.3147	0.8376	83.7
C+OI	25	204.15	779.33	2.2667	0.7704	77.0
	50	267.67	977.13	2.1470	0.8169	81.6
	75	96.6	1077.27	2.1034	0.8176	81.7
	100	229.56	1158.68	2.0878	0.8456	84.5

Sarcosine C has an insignificant effect to decrease corrosion even at highest tested concentrations 75 and 100 mmol/L with efficiencies less than 50 % (compare Table 3-7 and Fig. 3-18 B magenta and green color respectively). The efficiency of sarcosine C at concentration 25 and 50 mmol/L is high because the calculation depends on real axis mathematically while the value of imaginary axis is too less (compare Table 3-7 and Fig. 3-18 B red and blue color respectively). Synergist OI at concentration 50 mmol/L gives a

surface protection with an efficiency around 46 % (compare Table 3-7 and Fig. 3-18 A red color).

The current results indicate to the investigated substances C and OI are an effective corrosion inhibitor when they are working as one combination (C+OI) in equivalent amounts for each one and at all tested concentrations with efficiencies up to 85 % at highest concentration of 100 mmol/L (compare Table 3-7 and Fig. 3-18 F green color).

The current results indicate to a good stability of barrier film formed on the steel surface by inhibitors O, M, and combination C+OI.

The mechanism of inhibitor acts via attachment on metal surfaces and can be explained by an adsorption isotherm. The data set obtained from EIS measurement in Table 3-7 for L, M, O and combination C+OI was used to determine the adsorption constant K. The correlation between θ and C_{inh} is presented by the Langmuir adsorption isotherm (Eq. 3-5) [68]. Adsorption constant can determined by intersect of C_{inh}/θ in Fig. 3-20 that shows the relation between C_{inh} and C_{inh}/θ.

$$C_{inh}/\theta = \frac{1}{K} + C_{inh} \qquad \text{Eq. 3-5}$$

Furthermore, the standard free energy adsorption ΔG_{ads} is an important parameter process during adsorption and it can be estimated by Eq. 3-6, where 55.5 present the water concentration in ml/L [119]. The results for K and ΔG_{ads} for C, L, M, O, and combination C+OI are listed in Table 3-8.

$$K = \frac{1}{55.5} \exp(-\frac{\Delta G_{ads}}{RT}) \qquad \text{Eq. 3-6}$$
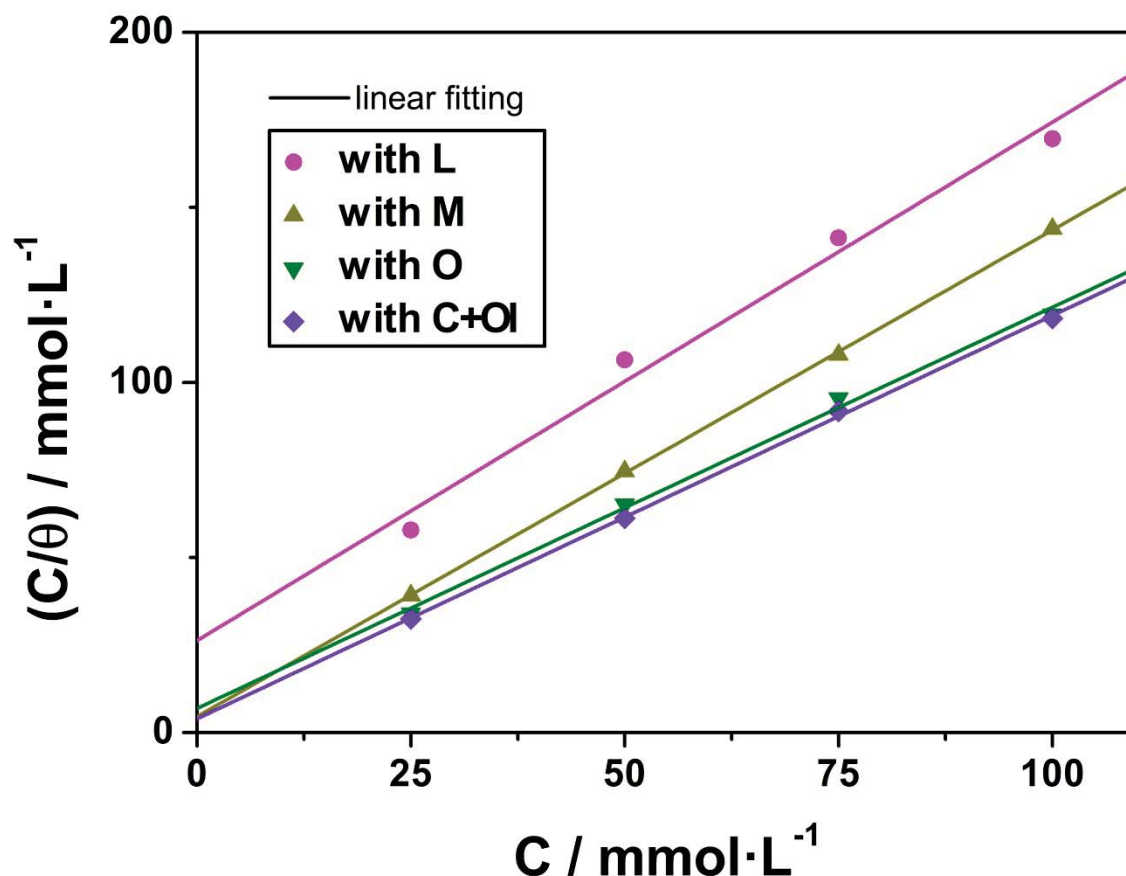
Fig. 3-20: Correlation between concentration C_{inh} and C_{inh}/θ obtained from EIS measurements for steel CR4. The single steel coupons are coated with L (magenta), M (dark yellow), O (green), and C+OI (navy) at different concentrations. Each solid line presents the fitting results and is displayed for better readability.

Table 3-8: Adsorption constant K and standard free energy ΔG_{ads}, for inhibitors L, M, O, and C+OI in 0.1 M NaCl determined from EIS measurements.

Inhibitor	R^2	K (L mmol^{-1})	ΔG_{ads} (KJ.mmol^{-1})
L	0.977	0.0381	-1.8557
M	0.999	0.2194	-6.1938
O	0.995	0.1452	-5.1704
C+OI	0.999	0.2550	-6.5660

The linear correlation between the inhibitor concentrations C_{inh} associated to C_{inh}/θ as best fit is clearly shown in Fig. 3-20. The regression coefficient R^2 for each tested inhibitor L, M, O, and C+OI is nearly equal to unity (1) indicating that the adsorption of studied inhibitors is followed by Langmuir (compare Table 3-8 and Fig. 3-20). The results of K and ΔG_{ads} in Table 3-8 demonstrate higher adsorption ability for inhibitor O and M which has highest molecular weight, longest hydrocarbon chain, and double bond in its structure compared to

other single compound L. Combination C+OI satisfied greatest value of **K** and ΔG_{ads} (compare Table 3-8).

As reported in refrences [67,80], negative ΔG_{ads} point out to more stable inhibition film formed on the steel surface and the spontaneity of the adsorption process. The values of ΔG_{ads} can give an indication of the interaction process when the organic molecules adsorbed on the metal surface by its value. When the value of ΔG_{ads} < -20 KJ/mol then the adsorption of inhibitor molecules are ingredient with physisorption that have an electrostatic interaction between charged of organic molecules and metal surface [120]. While the adsorption is controlled by chemisorption when ΔG_{ads} value is higher than -20 KJ/mol till -40 KJ/mol [121]. The adsorption process for the present organic substances can be assigned to physisorption depending on the obtained values of ΔG_{ads}, which are in the current investigation less than -20 KJ/mol (compare Table 3-8).

3.5.3 Dip coating time dependency

Different dip coating times **t** of coupons in a stock containing 50 mmol/L of present compounds were investigated by polarization measurement to detect the influence of exposure time on protection of steel CR4 in 0.1 M NaCl. Steel CR4 used in this evaluation was blank 2 (compare Table 2-1).

Table 3-9 summarizes the electrochemical parameters like i_{corr}, **CR**, anodic and cathodic Tafel slope β_a and β_c, E_{corr}, surface coverage θ, and inhibition efficiency **IE** (%) for different dip coating times.

Tafel slope values β_a and β_c that are listed in Table 3-9 indicates to that there is no change in anodic and cathodic polarization behavior with increased dip coating time. Fig. 3-21 shows the anodic and cathodic polarization curves for 50 mmol/L concentration of tested compounds C, OI, L, M, O, and combination C+OI with different dip coating time (1, 2.5, 5, 10, and 30 min) compared to blank metal.

The polarization curves in Fig. 3-21 refer to the increasing dip coating time of samples in stock inhibitor shifted E_{corr} to more positive direction for inhibitor O and combination C+OI while it was slightly shifted in both positive and negative direction for inhibitors M and C (compare Table 3-9 and Fig. 3-21 E, F, D, and B respectively). Compounds L and OI are shifted for E_{corr} to more negative direction compared to blank except with compound OI at 2.5 min (compare Table 3-9 and Fig. 3-21 C and A respectively).

Table 3-9: Results obtained by polarization for uncoated and coated CR4 steel with 50 mmol/L concentration of tested compounds in 0.1 M NaCl at different immersion times. The coating time t is given in minutes, corrosion rate **CR** in (mm/y) depending on current density i_{corr}, β_a and β_c are the anodic and cathodic Tafel slope, E_{corr} is corrosion potential, θ is the surface coverage, and **IE** (%) is efficiency of the chosen sarcosine with 50 mmol/L concentration.

	T (min)	i_{corr} resp. i_{inh} ($\mu A/cm^2$)	CR (mm/y)	β_a	β_c	E_{corr} (mV)	θ	IE (%)
Blank	0	61.93	1.339	0.0168	-0.0029	-324	-	-
Inhibitor								
OI	1	46.06	0.996	0.0205	-0.0028	-395	0.256	25.6
	2.5	43.31	0.936	0.0225	-0.0037	-280	0.300	30.0
	5	41.52	0.898	0.0174	-0.0036	-406	0.329	32.9
	10	35.67	0.771	0.0278	-0.0036	-395	0.424	42.4
	30	47.74	1.032	0.0195	-0.0042	-331	0.229	22.9
C	1	58.62	1.268	0.0181	-0.0029	-307	0.053	5.3
	2.5	51.66	1.117	0.0156	-0.0041	-307	0.165	16.5
	5	36.85	0.797	0.0145	-0.0042	-304	0.404	40.4
	10	36.68	0.793	0.0303	-0.0034	-300	0.407	40.7
	30	47.21	1.021	0.0110	-0.0035	-319	0.237	23.7
L	1	39.05	0.844	0.0166	-0.0032	-327	0.369	36.9
	2.5	36.42	0.787	0.0219	-0.0039	-327	0.411	41.1
	5	36.42	0.787	0.0166	-0.0034	-333	0.412	41.2
	10	33.56	0.727	0.0191	-0.0038	-345	0.457	45.7
	30	34.23	0.740	0.0147	-0.0039	-325	0.447	44.7
M	1	27.98	0.605	0.0168	-0.0033	-320	0.548	54.8
	2.5	23.04	0.498	0.0153	-0.0040	-332	0.628	62.8
	5	20.24	0.437	0.0166	-0.0033	-326	0.673	67.3
	10	18.58	0.401	0.0286	-0.0030	-306	0.700	70.0
	30	20.56	0.444	0.0279	-0.0042	-327	0.668	66.8
O	1	14.64	0.316	0.0215	-0.0032	-292	0.763	76.3
	2.5	8.87	0.191	0.0213	-0.0039	-308	0.857	85.7
	5	2.73	0.059	0.0238	-0.0038	-305	0.956	95.6
	10	2.91	0.062	0.0218	-0.0036	-242	0.953	95.3
	30	2.99	0.064	0.0253	-0.0041	-307	0.952	95.2
C+OI	1	17.64	0.381	0.0199	-0.0055	-289	0.715	71.5
	2.5	13.32	0.288	0.0137	-0.0055	-280	0.784	78.5
	5	8.95	0.193	0.0144	-0.0053	-289	0.855	85.5
	10	8.52	0.184	0.0166	-0.0041	-260	0.862	86.2
	30	9.06	0.195	0.0123	-0.0047	-267	0.853	85.4
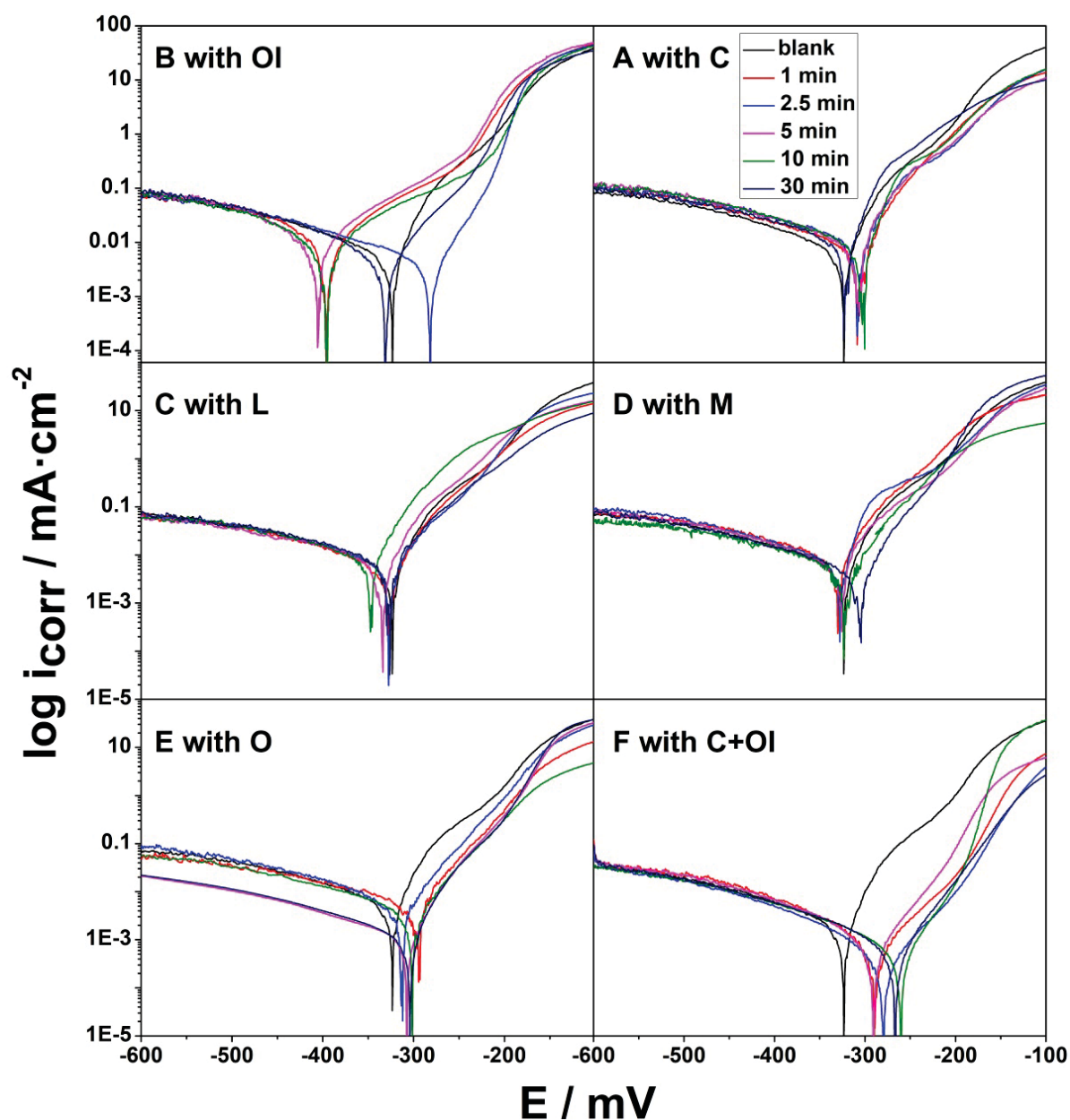
Fig. 3-21: Anodic and cathodic polarization curves for 50 mmol/L of tested sarcosine (C, L, M, and O), synergist OI, and combination C+OI at different coating times (chart **A** for OI, **B** for C, **C** for L, **D** for M, **E** for O, and **F** for C+OI). Blank material is displayed in black, red 1, blue 2.5, magenta 5, green 10, and navy 30 min, each as solid line. The legend in chart **B** is the same for chart **A**, **C**, **D**, **E**, and **F**.

Fig. 3-22 shows the current density and calculated efficiency obtained by polarization evaluation for different dip coating times of samples with tested compounds to protect steel CR4 against corrosion in 0.1 M NaCl. Efficiency for all tested compounds was enhanced with longer dip coating time resulted from more molecules adsorbing on the steel surface with increase of immersion time (compare Table 3-8 and Fig. 3-22). The best region that gave a highest efficiency of protection is that located between 5 min and 10 min with small differences in value but results are still within the error bar (compare Table 3-9 and Fig. 3-22

light gray rectangle). Three highest dip coating times (5, 10, and 30 min) have maximum effect to decrease current density with efficiency up to 95 % for inhibitor O, 86 % for combination C+OI, and 67 % for inhibitor M (compare Table 3-9 and Fig. 3-22 green, navy, and dark yellow colors respectively).
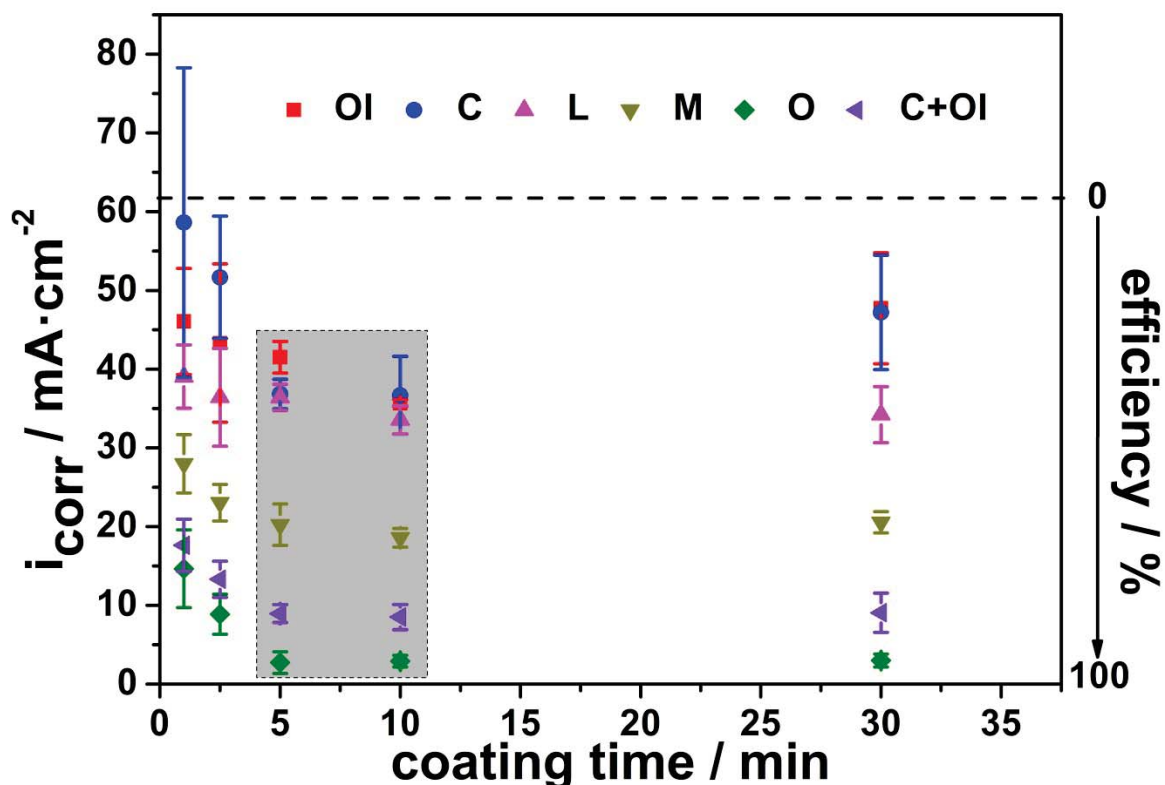
Fig. 3-22: Current density obtained by potentiodynamic measurement correlated to the calculated efficiency for synergist OI (red), sarcosine C (blue), L (magenta), M (dark yellow), O (green), and combination C+OI (navy) for different coating times to protect steel CR4 against corrosion in 0.1 M NaCl. Blank material used as reference is displayed with dotted black line on top as 0 % efficiency (indication on the right). The light gray rectangle refers to the most suitable dip coating time including 5 and 10 minutes.

Other tested compounds C, OI, and L have efficiencies less than 50 % at all investigated dip coating times (compare Table 3-9 and Fig. 3-22). After 10 min of coating time the efficiency was less somehow than with 10 min but it is still in the range of the error bar (compare Table 3-9 and Fig. 3-22). Depending on results obtained in dip coating time dependency the best immersion time is 10 min which gave a saturated surface of steel with inhibitor molecules.

3.6 Spray corrosion measurement technique

Spray corrosion measurement was carried out to evaluate selected compounds OI, C, L, M, O, and combination C+OI with 50 mmol/L concentration to protect steel CR4 in longer time and more realistic system. The evaluation is done for 24 h according to the experimental procedure fore mentioned at section 2.5 spray corrosion chamber.

Corrosion can be analyzed and monitored by several values but the most important one is the observation of corroded area on the surface. The determination of this area is done after a certain steps like scanning samples, documentation of images, and digitalization of each individual sample by java program ImageJ [112]. Relative corrosion area term that obtained from corroded surface area divided by the entire observed surface area of sample was used to indicate the corroded area in percentage. Effective inhibitors result in none or less corroded area and ineffective ones vice versa. Fig. 3-23 shows steel CR4 samples digitalized by scanner with 1200 dpi resolution after a certain time (2, 4, 8, 14, and 24 h) of corrosion. This figure displays the corrosion progress of one representative measurement for blank (first row) and investigated compounds in the order of OI, C, L, M, O, C+OI (rows 2-7). For steel blank, corrosion spots are already detectable after 2 h and some of them are merging together and grow bigger and get darker with time (Fig. 3-23). Most of blank surface was covered with corrosion products after 24 h (compare Table 3-10 and Fig. 3-23).

The relative corrosion area and calculated efficiency by Eq. 3-7 represent the result for a series consisting of ten single steel CR4 coupons that are obtained by two independent experimental runs in five ones each and summarized in Table 3-10.

$$Eff.\ \% = ((A_1 - A_2)\ /\ A_1) \times 100 \qquad\qquad \text{Eq. 3-7}$$

Where Eff. % is the calculated efficiency, A_1, A_2 are the relative corrosion areas in absence and presence of selected compounds.

In Table 3-10, two steel CR4 variations with slightly different chemical composition shows different values of corrosion area. Efficiency of tested compounds is calculated compared to different the two types of blank; L, M, and O for blank 2 and C, OI, and combination C+OI for blank 3 (compare Table 2-1).

Fig. 3-24 summarizes the average value of relative corrosion area for ten independent measurements and the resulting corrosion progress for each series.
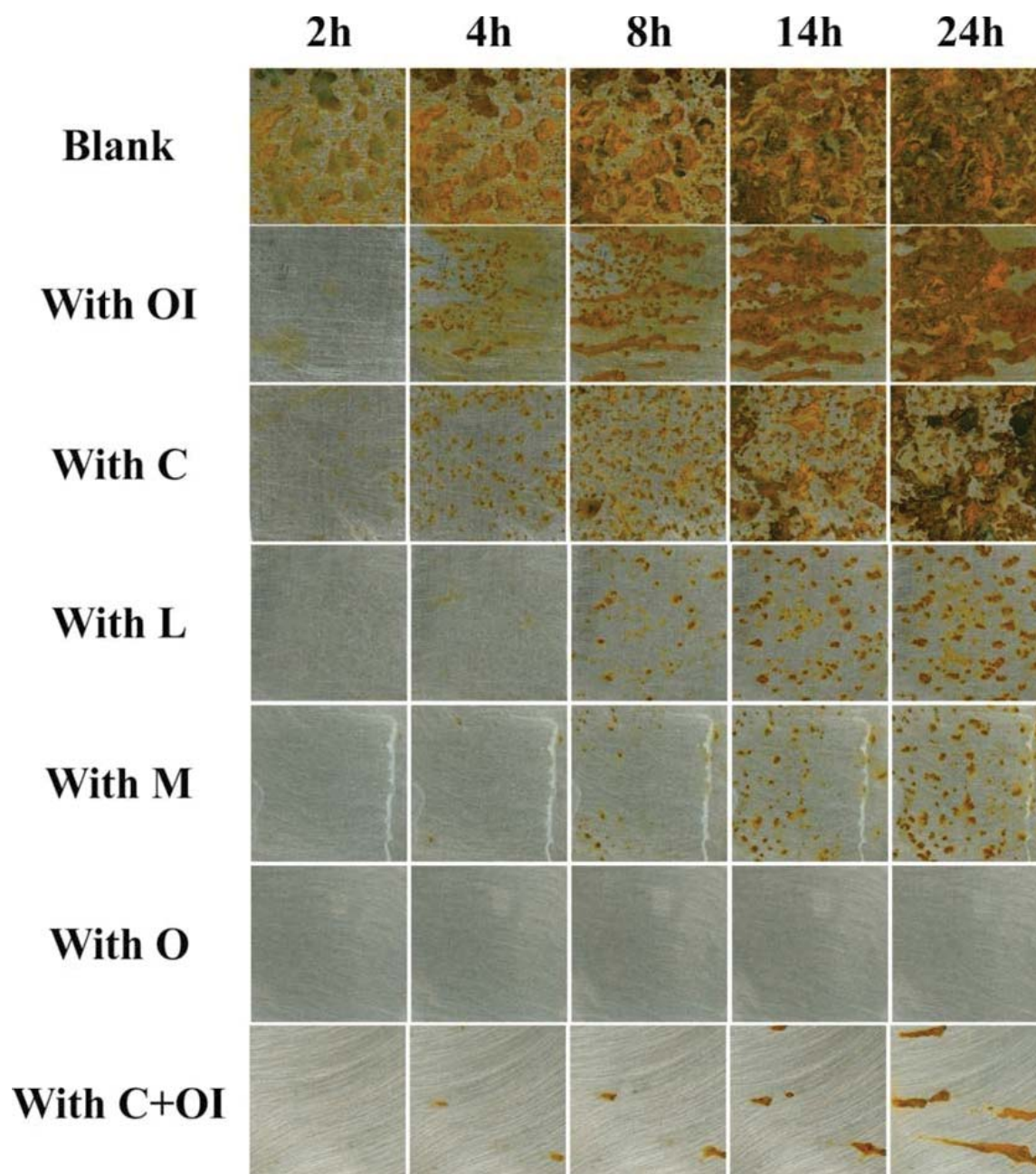
Fig. 3-23: Overview of the corrosion process of steel CR4 in the absence (blank) and presence of 50 mmol/L tested compounds sarcosine C, L, M, and O, synergist OI, and combination (C + OI) is given per selected time. Each treatment shows one exemplary run out of ten independent ones with characteristic corrosion patterns.

It is clear from Table 3-10, Figs. 3-23 and 3-24 that the corrosion behavior is different depended on tested compounds and exposure time. The data points in Fig. 3-24 are connected for better readability. Figs. 3-23 (sixth row) and 3-24 (green color) shows excellent protection efficiency for inhibitor O because there is no corrosion detectable on the surface even after 24 h with efficiency up to 99 % (compare Table 3-10). Inhibitors L and M have a very good efficiency to reduce corrosion area till 14 h with efficiency up to 90 % but this decreased after 24 h to 72 % and 79 % for L and M respectively (compare Table 3-10, Figs. 3-23 fourth

and fifth rows) and 3-24 magenta and dark yellow color respectively). Protection efficiency was up to 74 % after 2 h and 58 % after 4 h for inhibitor C then it decreased to 17 % after 24 h (compare Table 3-10 and Fig. 3-24 blue color). Compound OI has an efficiency up to 73 % after 2 h then decreased to 35 % after 4 h and 13 % after 24 h (compare Table 3-10 and Fig. 3-24 red color). Synergist OI improved the effect of inhibitor C and reduced corrosion with efficiency up to 80 % after 24 h when they are working in combination C+OI (compare Table 3-10, Figs. 3-23 seventh row and 3-24 navy color).

A good point that has to be clarified is images in Fig. 3-23 are an individual sample of a series while the result in Table 3-10 and Fig. 3-24 represent the average of ten samples. For this reason the information in Table 3-10 and Fig. 3-24 are sometimes different to the corrosion patterns in Fig. 3-23.

It is worth to mention that steel variances which are used in current study were differing very slightly in chemical composition and this small difference caused a different corrosion behavior of these variances. Because of this point the efficiency of combination C+OI could be somehow less than for inhibitor O.

Table 3-10: Corrosion reduction efficiency (see equation 3-7) for the spray corrosion chamber calculated for each sarcosine compared to the blank material at given times via corroded areas.

time (h)	Blank 2	L	Efficiency L (%)	M	Efficiency M (%)	O	Efficiency O (%)
2	3.69	0.03	99.5	0.24	93.5	0.16	95.3
4	37.12	0.55	98.5	0.48	98.7	0.36	99.1
8	57.67	2.98	94.8	4.03	93.0	0.39	99.3
14	69.69	7.33	89.5	6.90	90.1	0.39	99.5
24	70.81	20.22	71.5	14.87	79.0	0.32	99.6
time (h)	Blank 3	C	Efficiency C (%)	OI	Efficiency OI (%)	C+OI	Efficiency C+OI (%)
2	72.03	18.76	74.0	19.79	73.0	0.25	99.7
4	81.54	34.28	58.0	52.79	35.3	1.27	98.4
8	87.94	51.90	41.0	64.05	27.2	2.66	97.0
14	95.34	68.38	28.3	77.10	19.1	9.04	91.0
24	97.68	81.56	16.5	84.63	13.4	19.67	80.0
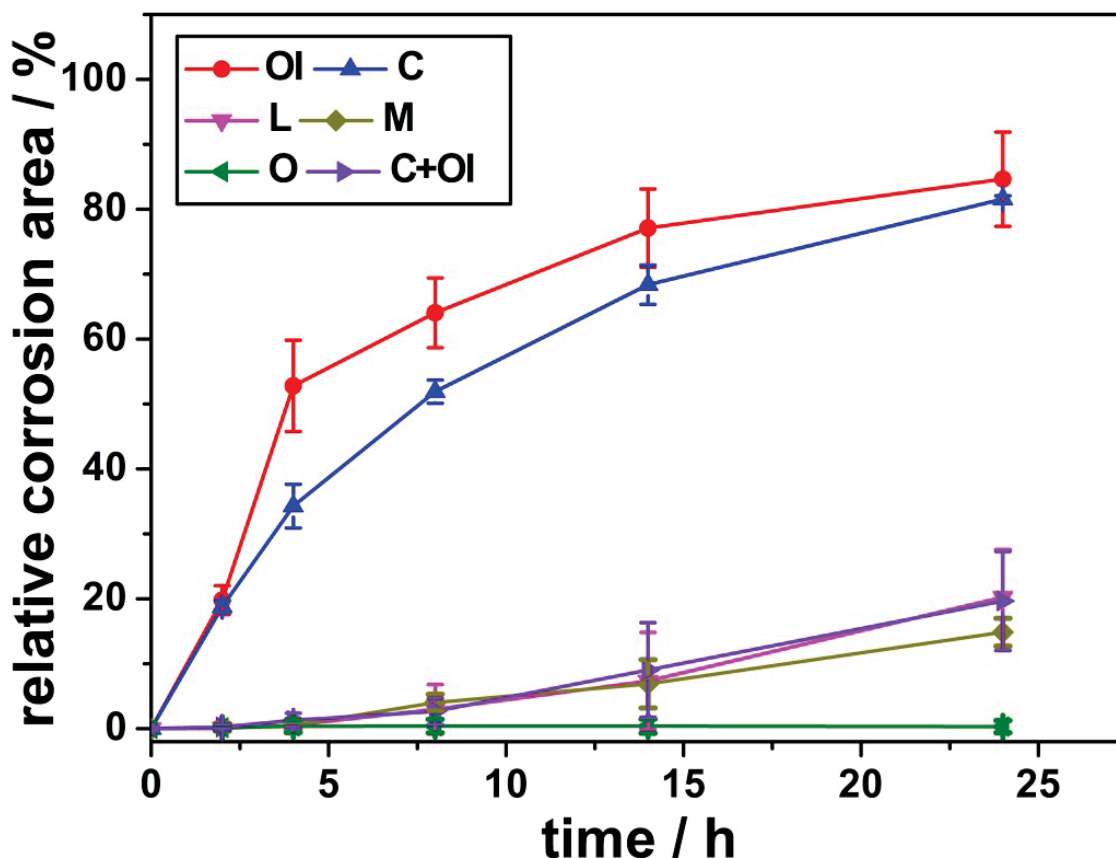
Fig. 3-24: Relative corrosion area evaluated with ImageJ and averaged for steel CR4 with 50 mmol/L of candidate organic substances during a 24 h run. Every series comprises ten individual metal probes resulting in the presented mean value for each time. Sarcosine C displays in blue, L in magenta, M in dark yellow, and O in green, synergist OI in red, and combination (C + OI) in navy each as solid line (data points are connected with solid lines for better readability).

The number of corrosion spots is another parameter that can exhibit the corrosion progress through the metallic surface. The relative number of corrosion spots per cm^{-2} was used here and it is representing a sum of individual corrosion spots on the respective corrosion area (2 cm x 2 cm = relative corrosion area) and not a whole surface area (see section 2.5). Fig. 3-25 illustrates the relation between the relative number of corrosion spots and relative corrosion area at the specific exposure times (square = 2, circle = 4, tringle up = 8, tringle down = 14, and diamond = 24 h).
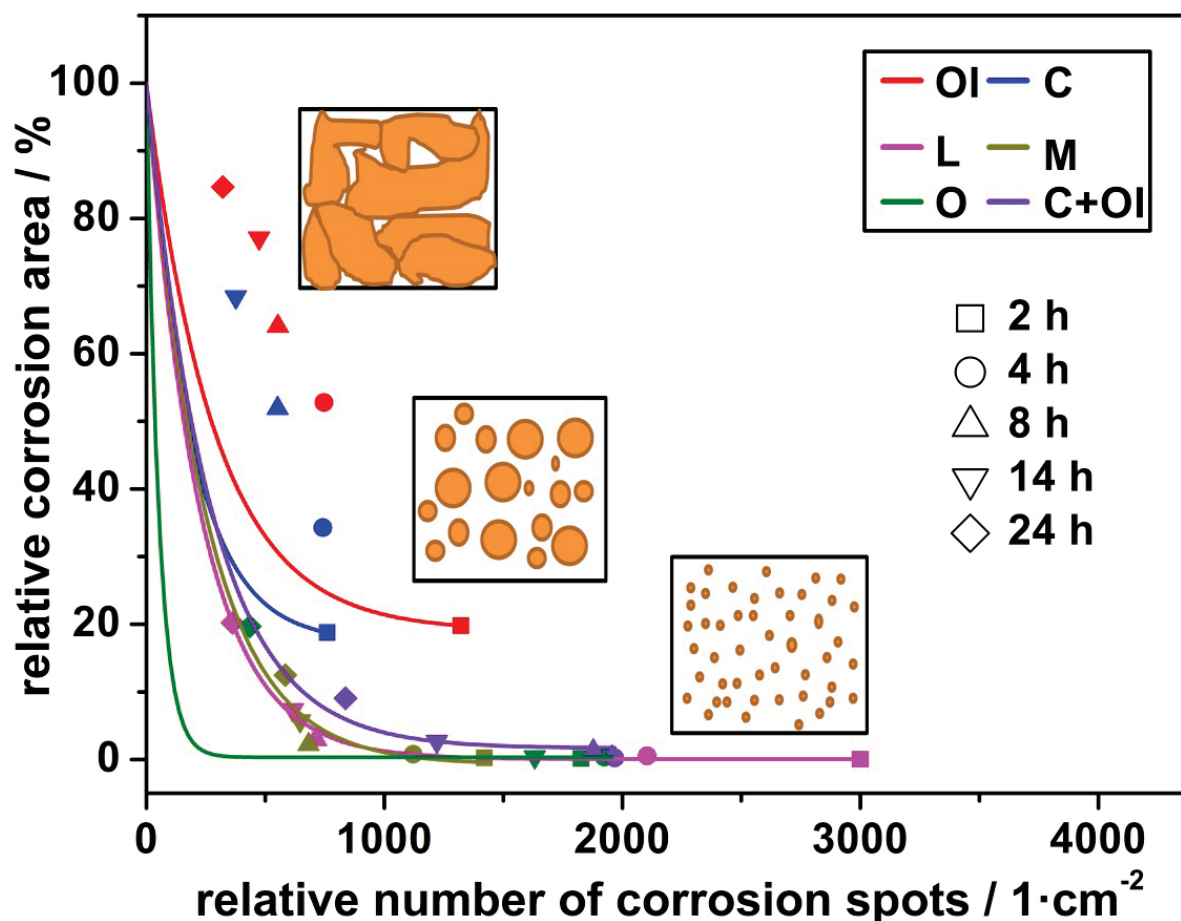
Fig. 3-25: Exponential decays for the relative number of corrosion spots related to the relative corrosion area for steel CR4 with selected inhibitors according to specific exposure times. Sarcosine inhibitor C in blue, L in magenta, M in dark yellow, O in green, synergist OI in red, and combination C+OI in navy. The different exposure times are indicated by square = 2 h, circle = 4 h, triangles up = 8 h, triangle down = 14 h, and diamond = 24 h. The sketches display the corrosion development according to the following relation: A lot of small corrosion dots with less corroded area progress to a few big corrosion spots with a larger corroded area.

An exponential decay is used in Fig. 3-25 to display the corrosion progress in presence of tested compounds (OI in red, C in blue, L in magenta, M in dark yellow, O in green and C+OI in navy). All lines are connected to zero number of spots and 100 % of corrosion area. It is obvious that in the beginning at the first exposure time there are many small dots of corrosion corresponding to small corrosion area (see the inset sketch picture in Fig. 3-25). The bigger corrosion spots in less number appear at larger corrosion area with increasing of the exposure time (see the inset picture, data points, and lines in Fig. 3-25).

To describe the corrosion progress more clearly the linear relation of exposure times and root of corrosion area was used (Fig. 3-26). The numbers in Fig. 3-24 refers to calculated value of the slope for tested compounds corresponding to the color code for lines (OI in red, C in blue, L in magenta, M in dark yellow, O in green, and combination C+OI in navy). The lower slope value exhibiting a flat line indicates that the inhibitor has a good efficiency to reduce

corrosion and less effective ones show higher slope values. Inhibitor O has the highest efficiency to decrease corrosion as mentioned before according to the current results therefore it shows the smallest slope value around 0.01 ± 0.004 (Fig. 3-26 green line). Other good inhibitors are M, L, and combination C+OI with slopes 0.15 ± 0.009, 0.16 ± 0.009, and 0.17 ± 0.005 respectively (Fig. 3-26 dark yellow, magenta, and violet lines respectively). Compounds C and OI have a higher slope value 1.48 ± 0.171 and 1.78 ± 0.096 respectively which indicates them insignificant to inhibit corrosion (Fig. 3-26 blue and red lines respectively).

As mentioned before for substances L, M, and O are tested in spray corrosion measurement with steel CR4 differ slightly than which are used with C, OI, and combination C+OI. This reason is why the combination C+OI may has slightly higher slope than inhibitors L and M in Fig. 3-26.
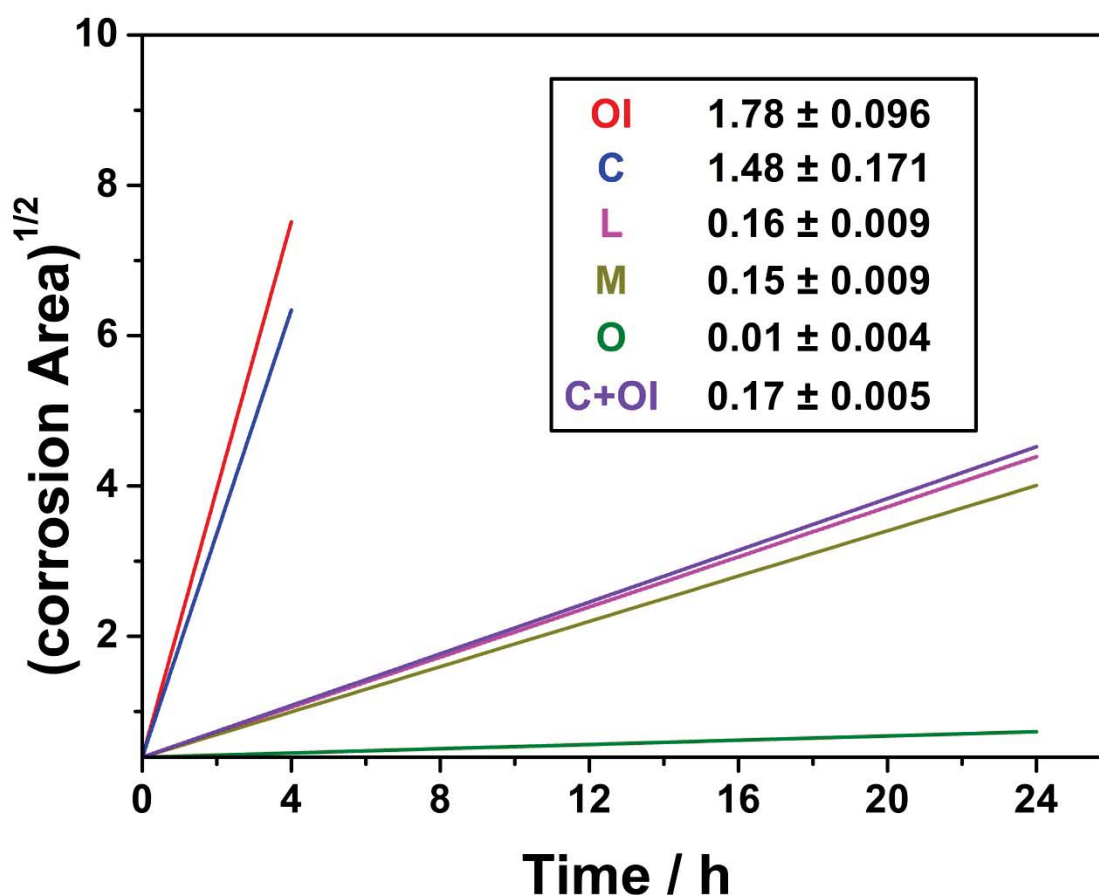
Fig. 3-26: Linear approximation displaying the root of the relative corrosion area to the exposure time for steel CR4 for present compounds. The course of the linear performance for synergist OI is displayed in red, sarcosine C in blue, L in magenta, M in dark yellow, O in green, and combination (C + OI) in violet. The numbers in the legend show the calculated results of the slope values, indicating good inhibitors with small values and less efficient ones with larger values.

There efficiencies (***IE %***) obtained by weight loss, potentiodynamic polarization, electrochemical impedance spectroscopy, and spray corrosion measurement are different because of the different evaluation methods used may not accurately comparable when each technique is differ than other even immersion time used is not the same in all evaluation methods.

3.7 Analysis and optimization of factors influencing corrosion protection

Box-Behnken Design (BBD) and its tools are used to optimize the effect of four different independent variables with their three levels on protection of steel CR4 in salt water. Response surface methodology (RSM) was used to predict the optimum efficiency obtained from tested levels for studied factors. Steel CR4 used in this investigation was blank 3 (compare Table 2-1). Experiments are done with potentiodynamic polarization. The result of analysis and optimization step can be summarized as following:

- Main effect of individual variables
- Response table and graph
- Normal probability plot
- Response surface plot
- Predict best level combination
- Experimental confirmation

3.7.1 Main effect of individual variables

The first step in any experiment is to know how each factor effects on the process and which one has a significant effect and which one not. Main effect plot shows the effect of tested variables individually when the mean response changes across the levels of the factor (Fig. 3-27). Concentration of inhibitor O (A) caused slightly increased from 92 % to 94 % when it changed from lower to upper level (Fig. 3-27 A). Both dip coating time (B) and NaCl concentration (D) have a small effect on the efficiency when they are changed across lower to upper level (Fig. 3-27 B and D respectively). Temperature (C) has a big effect on the process and changed the efficiency in high value when its levels crossed from lower to upper level (Fig. 3-27 C). Only inhibitor concentration (A) satisfied highest efficiency at upper level (+1)

compared to lower and middle level (-1,0) while other factors (B, C, and D) are giving highest efficiency at lower level (-1) compared to other levels (Fig. 3-27 B, C, and D respectively).
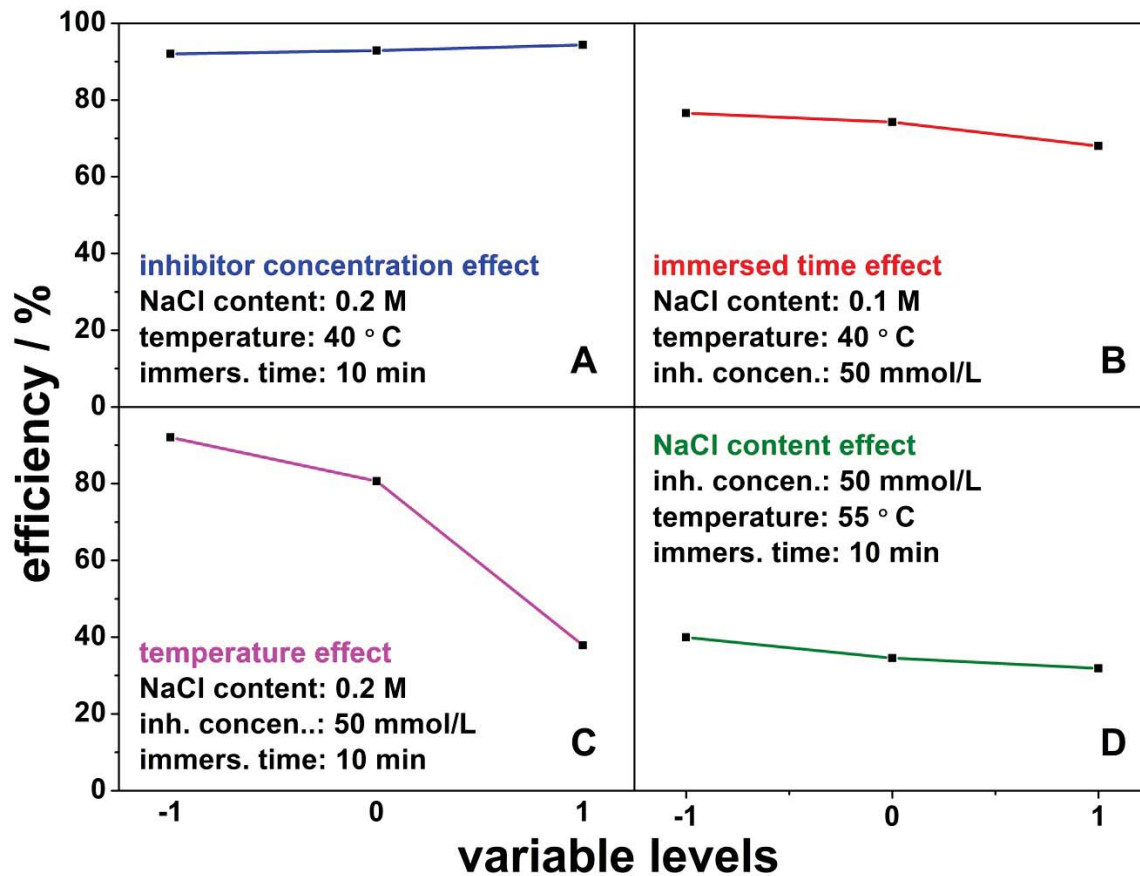
Fig. 3-27: Main effect of studied variables with their three levels (-1, 0, +1) on efficiency of protection steel CR4 in salt water by using Oleylsarcosine (O) during polarization measurement.

3.7.2 Response table and graph

The analysis of factors and interaction influence starts by screening the effect in a complete fractional factorial which is called the response table. All possibilities of effects on the response function (efficiency) depending on tested variables and their interaction are taken into account and listed in response table for three levels of four independent variables in 27 runs for BBD (Table 3-11). Sum value for each individual factors and interaction listed in Table 3-11 estimated by ($\ell H - \ell L$) where ℓH and ℓL represent higher value and lower value of effect in three tested levels for each variable. Each number in efficiency that is listed in response table represents the average of two independent experiments for reproducibility.

Table 3-11: The complete response table for three levels of four independent variables, the efficiency is the output of 27 runs based on Box-Behnken design (BBD).

No	IE (%)	A -1	A 0	A +1	B -1	B 0	B +1	C -1	C 0	C +1	D -1	D 0	D +1
1	85.20	85.20			85.20				85.20			85.20	
2	77.99	77.99					77.99		77.99			77.99	
3	66.77			66.77	66.77				66.77			66.77	
4	69.87			69.87			69.87		69.87			69.87	
5	89.11		89.11			89.11		89.11			89.11		
6	92.06		92.06			92.06		92.06					92.06
7	39.94		39.94			39.94				39.94	39.94		
8	37.86		37.86			37.86				37.86			37.86
9	70.05	70.05				70.05			70.05		70.05		
10	52.40	52.40				52.40			52.40				52.40
11	85.57			85.57		85.57			85.57		85.57		
12	74.59			74.59		74.59			74.59				74.59
13	92.86		92.86		92.86			92.86				92.86	
14	50.15		50.15		50.15					50.15		50.15	
15	91.96		91.96				91.96	91.96				01.96	
16	41.80		41.80				41.80			41.80		41.80	
17	91.98	91.98				91.98		91.35				91.98	
18	54.26	54.26				54.26				54.26		54.26	
19	94.35			94.35		94.35		94.35				94.35	
20	46.03			46.03		46.03				46.03		46.03	
21	86.46		86.46		86.46				86.46		86.46		
22	80.63		80.63		80.63				80.63				80.63
23	76.51		76.51				76.51		76.51		76.51		
24	73.55		73.55				73.55		73.55				73.55
25	74.23		74.23			74.23			74.23			74.23	
26	74.23		74.23			74.23			74.23			74.23	
27	74.23		74.23			74.23			74.23			74.23	
Value	27	6	15	6	6	15		6	15	6	6	15	6
Av.	72.02	71.98	71.70	72.86	77.01	70.06		92.05	74.82	45.01	74.61	72.39	68.52
Effect = High-Low		1.158			6.952			47.046			6.091		

No	IE (%)	AB -1	AB 0	AB +1	AC -1	AC 0	AC +1	AD -1	AD 0	AD +1	BC -1	BC 0	BC +1
1	85.20			85.20		85.20			85.20			85.20	
2	77.99	77.99				77.99			77.99			77.99	
3	66.77	66.77				66.77			66.77			66.77	
4	69.87			69.87		69.87			69.87			69.87	
5	89.11		89.11			89.11			89.11			89.11	
6	92.06		92.06			92.06			92.06			92.06	
7	39.94		39.94			39.94			39.94			39.94	
8	37.86		37.86			37.86			37.86			37.86	
9	70.05		70.05			70.05				70.05		70.05	
10	52.40		52.40			52.40		52.40				52.40	
11	85.57		85.57			85.57		85.57				85.57	
12	74.59		74.59			74.59				74.59		74.59	
13	92.86		92.86			92.86			92.86				92.86
14	50.15		50.15			50.15			50.15		50.15		
15	91.96		91.96			91.96			91.96		91.96		
16	41.80		41.80			41.80			41.80				41.80
17	91.98		91.98				91.98		91.98			91.98	
18	54.26		54.26		54.26				54.26			54.26	
19	94.35		94.35		94.35				94.35			94.35	
20	46.03		46.03				46.03		46.03			46.03	
21	86.46		86.46			86.46			86.46			86.46	
22	80.63		80.63			80.63			80.63			80.63	
23	76.51		76.51			76.51			76.51			76.51	
24	73.55		73.55			73.55			73.55			73.55	
25	74.23		74.23			74.23			74.23			74.23	
26	74.23		74.23			74.23			74.23			74.23	
27	74.23		74.23			74.23			74.23			74.23	
Value	27	2	23	2	2	23	2	2	23	2	2	23	2
Av.	72.02	72.38	71.51	77.54	74.31	72.09	69.01	68.99	72.26	72.32	71.06	72.52	67.33
Effect = High-Low		6.021			5.300			3.335			5.186		

No	IE (%)	BD -1	BD 0	BD +1	CD -1	CD 0	CD +1	ABC -1	ABC 0	ABC +1	ABD -1	ABD 0	ABD +1
1	85.20		85.20			85.20			85.20			85.20	
2	77.99		77.99			77.99			77.99			77.99	
3	66.77		66.77			66.77			66.77			66.77	
4	69.87		69.87			69.87			69.87			69.87	
5	89.11		89.11				89.11		89.11			89.11	
6	92.06		92.06		92.06				92.06			92.06	
7	39.94		39.94		39.94				39.94			39.94	
8	37.86		37.86				37.86		37.86			37.86	
9	70.05		70.05			70.05			70.05			70.05	
10	52.40		52.40			52.40			52.40			52.40	
11	85.57		85.57			85.57			85.57			85.57	
12	74.59		74.59			74.59			74.59			74.59	
13	92.86		92.86			92.86			92.86			92.86	
14	50.15		50.15			50.15			50.15			50.15	
15	91.96		91.96			91.96			91.96			91.96	
16	41.80		41.80			41.80			41.80			41.80	
17	91.98		91.98			91.98			91.98			91.98	
18	54.26		54.26			54.26			54.26			54.26	
19	94.35		94.35			94.35			94.35			94.35	
20	46.03		46.03			46.03			46.03			46.03	
21	86.46			86.46		86.46			86.46			86.46	
22	80.63	80.63				80.63			80.63			80.63	
23	76.51	76.51				76.51			76.51			76.51	
24	73.55			73.55		73.55			73.55			73.55	
25	74.23		74.23			74.23			74.23			74.23	
26	74.23		74.23			74.23			74.23			74.23	
27	74.23		74.23			74.23			74.23			74.23	
Value	27	2	23	2	2	23	2	0	27	0	0	27	0
Av.	72.02	78.57	70.76	80.01	66.00	73.29	63.49		72.02			72.02	
Effect = High-Low			9.244			9.805			-			-	

68

No	IE (%)	ACD			CBD			ABCD		
		-1	0	+1	-1	0	+1	-1	0	+1
1	85.20		85.20			85.20			85.20	
2	77.99		77.99			77.99			77.99	
3	66.77		66.77			66.77			66.77	
4	69.87		69.87			69.87			69.87	
5	89.11		89.11			89.11			89.11	
6	92.06		92.06			92.06			92.06	
7	39.94		39.94			39.94			39.94	
8	37.86		37.86			37.86			37.86	
9	70.05		70.05			70.05			70.05	
10	52.40		52.40			52.40			52.40	
11	85.57		85.57			85.57			85.57	
12	74.59		74.59			74.59			74.59	
13	92.86		92.86			92.86			92.86	
14	50.15		50.15			50.15			50.15	
15	91.96		91.96			91.96			91.96	
16	41.80		41.80			41.80			41.80	
17	91.98		91.98			91.98			91.98	
18	54.26		54.26			54.26			54.26	
19	94.35		94.35			94.35			94.35	
20	46.03		46.03			46.03			46.03	
21	86.46		86.46			86.46			86.46	
22	80.63		80.63			80.63			80.63	
23	76.51		76.51			76.51			76.51	
24	73.55		73.55			73.55			73.55	
25	74.23		74.23			74.23			74.23	
26	74.23		74.23			74.23			74.23	
27	74.23		74.23			74.23			74.23	
Value	27	0	27	0	0	27	0	0	27	0
Av.	72.02		72.02			72.02			72.02	
Effect = High-Low			-			-			-	

The absolute estimated effect of variables and their interactions in response table used to plot the response graph of Fig. 3-28, that can give a fast and easy screening for all possibilities of influences. From response graph it is obvious that the temperature (C) has highest effect on corrosion protection $E_f / C = 47$ (Fig. 3-26 magenta line). The second greatest effect was sharing between the interaction of variables BD and CD with estimated effect $E_f = 9$ for each one (Fig. 3-26 dark yellow and dark cyan lines respectively). Dip coating time (B) takes place 3 in ranking with E_f around 7 (Fig. 3-28 blue line). On rank 4 is the NaCl concentration (D) and its interaction of inhibitor concentration and dip coating time (AB) with $E_f = 6$ for each one (Fig. 3-28 green and dark blue lines respectively). Interaction of AC and BC rank 5 with $E_f = 5$ for each one (Fig, 3-28 violet and bordeaux lines respectively). Rank 6 is the interaction of inhibitor concentration and NaCl content (AD) with $E_f = 3$ (Fig. 3-28 purple line). The last place of effect was for inhibitor concentration (A) with $E_f = 1$ (Fig. 3-28 red line). Interaction of more than two variables has no effect on the corrosion protection when the estimated effect was equal to the mean efficiency of the process (compare Table 3-11 and Fig. 3-28).
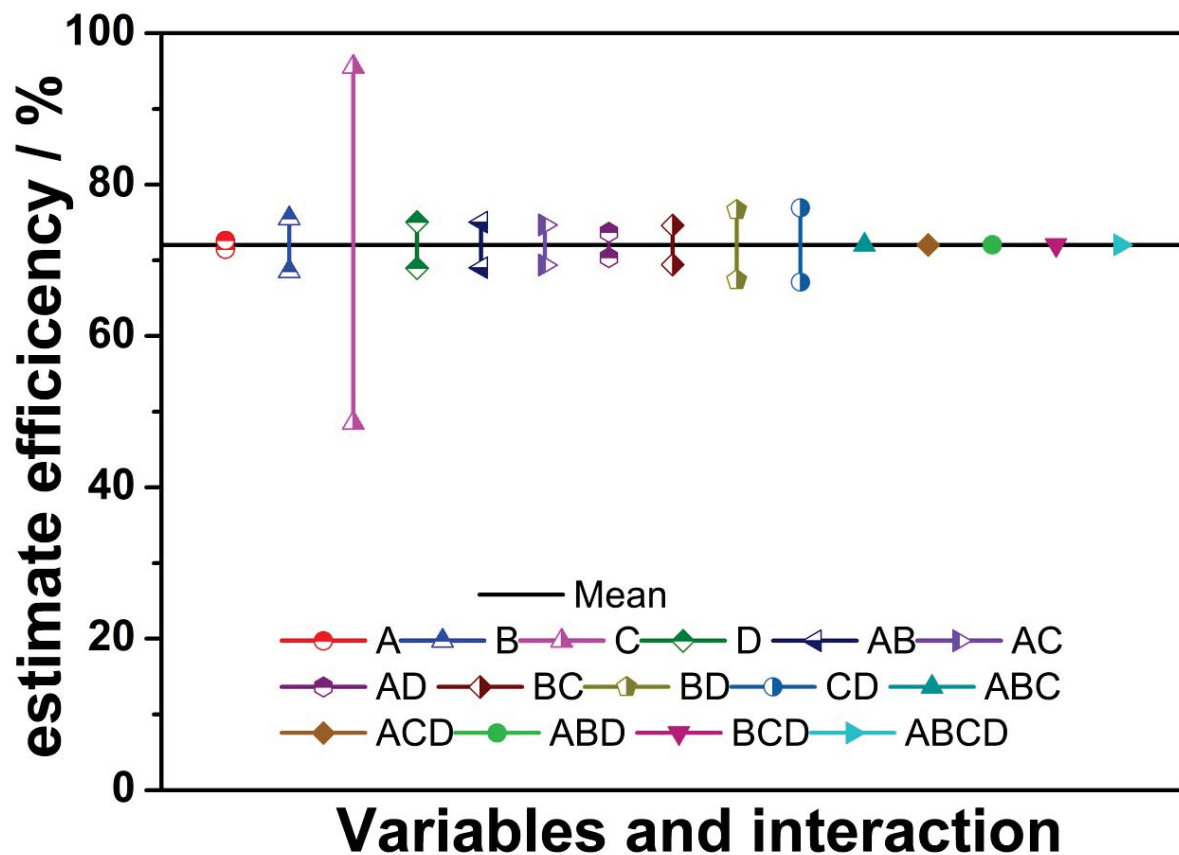

Fig. 3-28: Response graph of estimated effect for tested variables and their interactions on efficiency of protection steel CR4 in salt water. The estimated effect used here depends on the response table (Table 3-11).

3.7.3 Normal probability distribution

As shown in response graph there are some variables and interactions with larger effect on the corrosion protection than others and response plot cannot give more information about them. To realize if these effects are real or just take placed by chance during the process, normal probability distribution was used. The required calculations for normal probability plot are obtained from response table and listed after arranged the estimated effects from higher to lower in Table 3-12.

Table 3-12: Normal probability calculations (i = rank of the effect)

Variable and interaction	Estimated effect	Rank (i)	Probability (Pi)=100(i-0.5)/10
C	47.046	1	5
CD	9.805	2	15
BD	9.244	3	25
B	6.952	4	35
D	6.0916	5	45
AB	6.021	6	55
AC	5.3	7	65
BC	5.186	8	75
AD	3.335	9	85
A	1.158	10	95
Mean of estimated effect	10.014		

In normal probability distribution the effect is considered significant or insignificant on the response of process (efficiency of corrosion protection) depending on the location of the estimated data respect to the mean line (Fig. 3-29). Any factor or interaction of variables in Fig. 3-29 is located far away from the mean line, meaning it has a significant effect and these are closed to the mean refers to insignificant influence (color diamond, red for highest, green for good, and blue for insignificant effect). Temperature (C) and inhibitor concentration (A) have the largest effect as they are located far away from the mean line (Fig. 3-29 red diamonds). Interactions of immersed time and Nacl content (BD), temperature and NaCl concentration (CD) takes placed close to the mean line then they have insignificant influence on the response of the process (Fig. 3-29 blue diamonds). Other variables dip coating time (B), and NaCl concentration (D) and interactions of, inhibitor concentration and NaCl

concentration (AD), dip coating time and temperature (BC), inhibitor concentration and temperature (AC), and inhibitor concentration and immersed time (AB) have a good effect on the response of the process as they are not located near to the mean line (Fig. 3-29 green diamonds).

It is intelligible from normal distribution that inhibitor concentration (A) has a large effect on the response while it was insignificant according to response plot (compare Fig. 3-28 red line and 3-29 red diamonds). Also the interactions of dip coating time and NaCl concentration (BD); temperature and NaCl concenetration (CD) have insignificant effect in normal probability distribution (Fig. 3-29 blue diamonds) while in response plot they showed good effects and have higher ranking (Fig. 3-28 dark yellow and dark cyan lines respectively). This point is approved that the normal probability distribution is a useful tool to identify the real effect of tested factors and interactions.
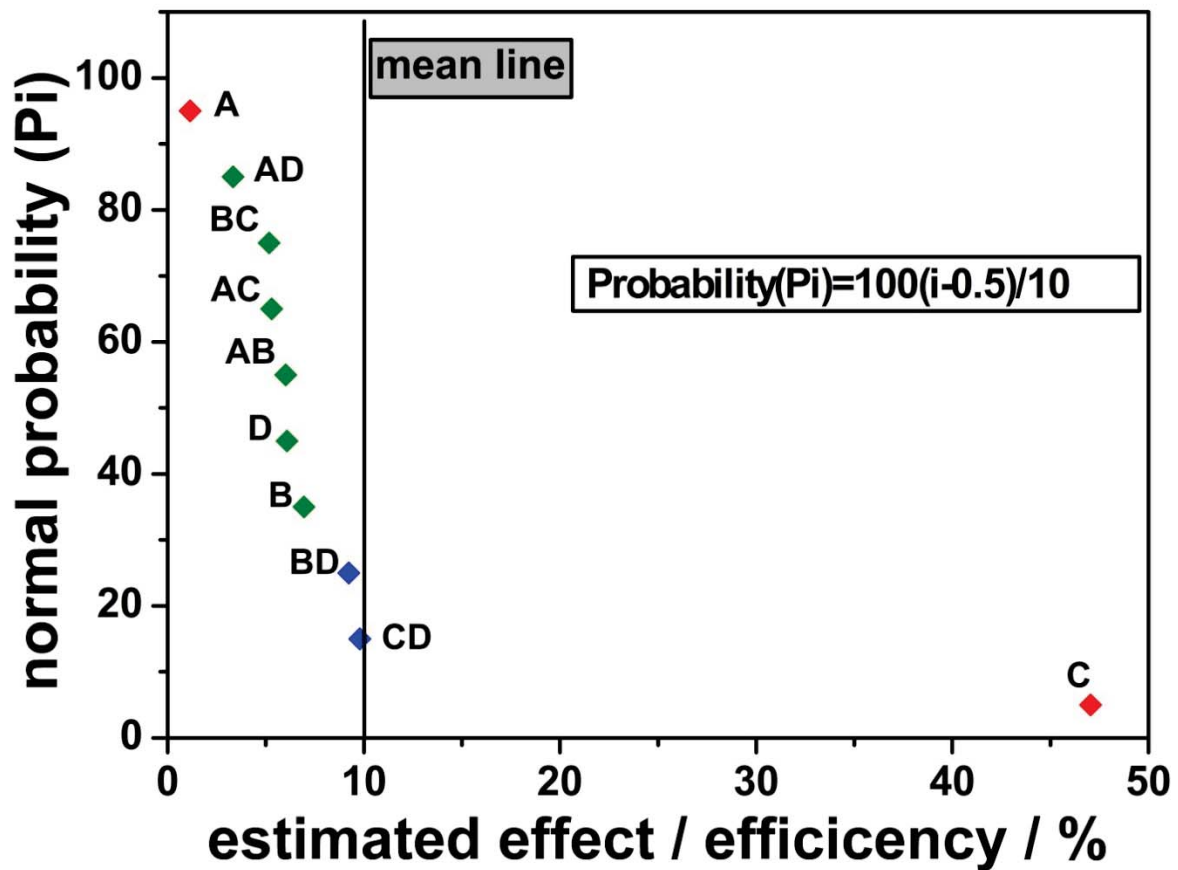

Fig. 3-29: Normal probability distribution of individual and interactions effect on protection of steel CR4 in salt water by using inhibitor Oleoylsarcosine (O).

3.7.4 Response surface methodology (RSM)

Second order model of RSM is applied to optimize a complex effect during the process by a mathmatically way and build a predictor model to obtain the optimum response from tested

levels of variables. There are sequentially steps that have to be done to implement this technique. The implementation proceedings of RSM are: build the empirical model, stattic simulation, predict the optimum response, and experimentally confirmation of theoretical result.

3.7.4.1 Empirical model

The experimental model used here was build depending on Eq. 2-2 for second order model. In the current regression model only individual and double interaction effects were considered and the interaction of more than two variables are neglected. Minitab17 program was used to implement the 27 orthognal array of BBD and estimate regression coefficients which are listed in Table 3-13 (see appendix II).

Table 3-13: Regression coefficient of the prediction model for second order model of RSM.

No.	Coefficient	Coefficient Estimated	Coefficient symbol
1	A	74.23	ß°
2	B	0.44	ß1
3	C	-2.53	ß2
4	D	-23.52	ß3
5	E	-3.05	ß4
6	F	-0.23	ß11
7	G	2.86	ß22
8	H	-6.07	ß33
9	I	-1.52	ß44
10	J	2.58	ß12
11	K	-2.65	ß13
12	L	1.67	ß14
13	M	-1.86	ß23
14	N	0.72	ß24
15	O	-1.26	ß34

With regression coefficients that are listed in Table 3-13 and the regression equation obtained by Minitab 17 program, the empirical model in Eq. 2-2 can be rewritten in the following manner:

Predicted Efficiency % = $74.23 + 0.44 \times A - 2.53 \times B - 23.53 \times C - 3.05 \times D - 0.23 \times A^2 + 2.86 \times B^2 - 6.07 \times C^2 - 1.52 \times D^2 + 2.58 \times AB - 2.65 \times AC + 1.67 \times AD - 1.86 \times BC + 0.72 \times BD - 1.26 \times CD$ Eq. 3-8

The multiple coefficients (R^2) of the suggested predictor model obtained by Minitab 17 program equal to 89.23 % which refers to the current proposed model has a good acceptability (see appendix II). The maximum error obtained by the differences between the actual and predicted efficiency was 10.55 % which gives a good agreement to use the proposed model here (compare Table 3-14).

Table 3-14: The actual experimental and predicted efficiency according to the proposed model.

Experiment no.	Eff.% - Experimentally	Eff.% - Predicted	Error
1	85.20	81.52	2.59
2	77.99	71.30	4.72
3	66.77	77.25	7.41
4	69.87	77.34	5.28
5	89.11	91.95	2.00
6	92.06	88.37	2.60
7	39.94	47.42	5.28
8	37.86	38.81	0.67
9	70.05	76.74	4.73
10	52.40	67.32	10.55
11	85.57	74.29	7.97
12	74.59	71.54	2.15
13	92.86	95.21	1.66
14	50.15	51.88	1.23
15	91.96	93.87	1.35
16	41.80	43.09	0.91
17	91.98	88.36	2.55
18	54.26	46.61	5.40
19	94.35	94.54	0.13
20	46.03	42.20	2.70
21	86.46	81.86	3.25
22	80.63	74.33	4.45
23	76.51	75.36	0.81
24	73.55	70.70	2.01
25	74.23	74.23	0
26	74.23	74.23	0
27	74.23	74.23	0

3.7.4.2 Static simulation of RSM

To understand the alterations of response in given direction the simulation of RSM was used by adjusting tested variables. Response surface plot displays this simulation in three dimensional graphs (Fig. 3- 30). In this analysis tool only two factors can be combined in one plot when they are across from lower to upper levels and other two variables are hold at middle level (0).
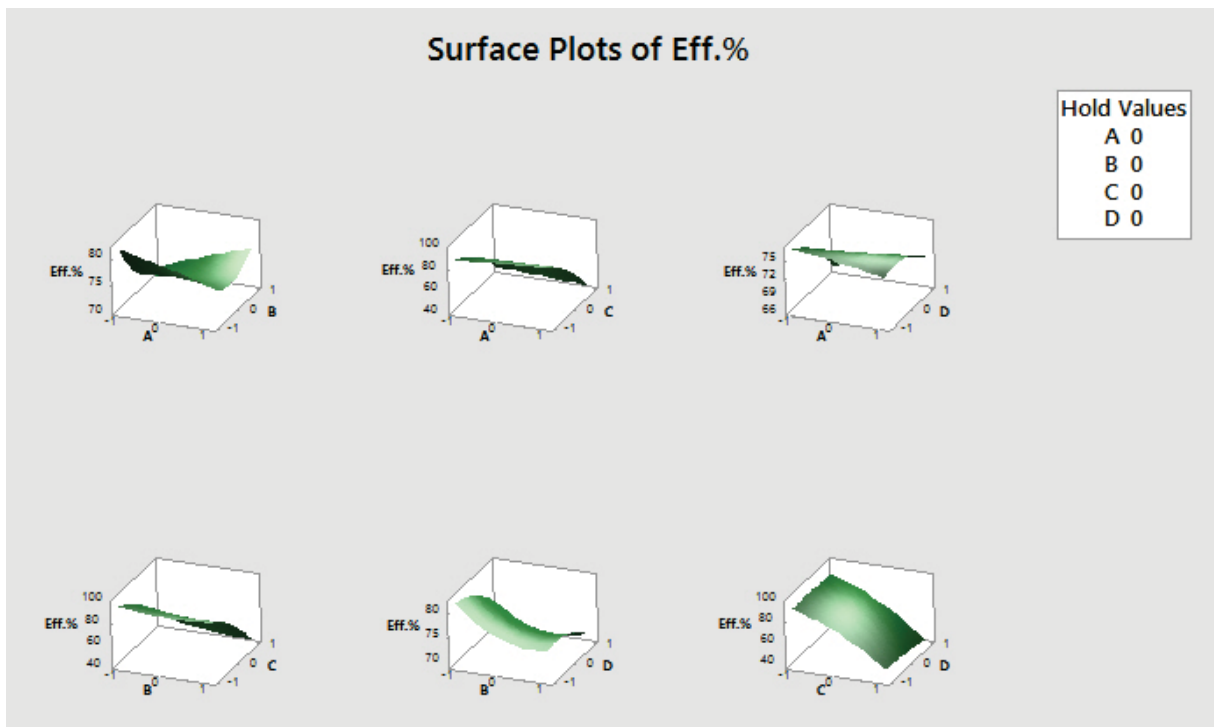

Fig. 3-30: 3-dimensions of surface response plot for pair interaction of tested variables on the protection process. Each plot displays interaction effect of two factors when they are crossed from lower to upper level and other two variables are hold at zero level.

For more visibility and understanding of results obtained in response surface the contour lines in two dimensions graph was used (Fig. 3-31). Contour plots of AB, AD, and BD in Fig. 3-31 refers to that there is no interaction effect when two variables in each contour changed at the same time from lower to upper level because they are influence in same way on the response. In contour plots of AC, BC, and CD (Fig. 3-31), the interaction effect is clear when two factors in each contour crossed during levels. When A and B are located at lower level (-1) in the same time they deliver satisfying efficiencies up to 90 % and up to 70 % at mid and upper levels (contour plot of BA). For A and C, the highest efficiency was up to 90 % when

inhibitor concentration changed from middle to upper level and temperature (C) located at lower level then started to decrease to less than 50 % when C crossed from lower to upper level (contour plot of CA). Changed factor A from lower to middle level with upper level of D gave efficiency up to 60 % and increased to up to 70 % with changed for A crossed from lower to upper level with lower and middle levels of D (contour plot of DA). Efficiency was around 90 % when dip coating time (B) changed from lower to upper level and temperature (C) located at lower level then it is decreased to less than 50 % when C crossed to upper level (contour plot of CB). Efficiency was up to 70 % at all levels of dip coating time (B) and NaCl content (D) except a little region of middle level of B with upper level of D (contour plot of DB). The last contour plot of DC shows the maximum efficiency was up to 90 % when temperature (C) located at lower level and NaCl concentration changed from lower to upper level then it is decreased to less than 50 % when C crossed from middle to upper level and at the same time D changed from lower to upper level.
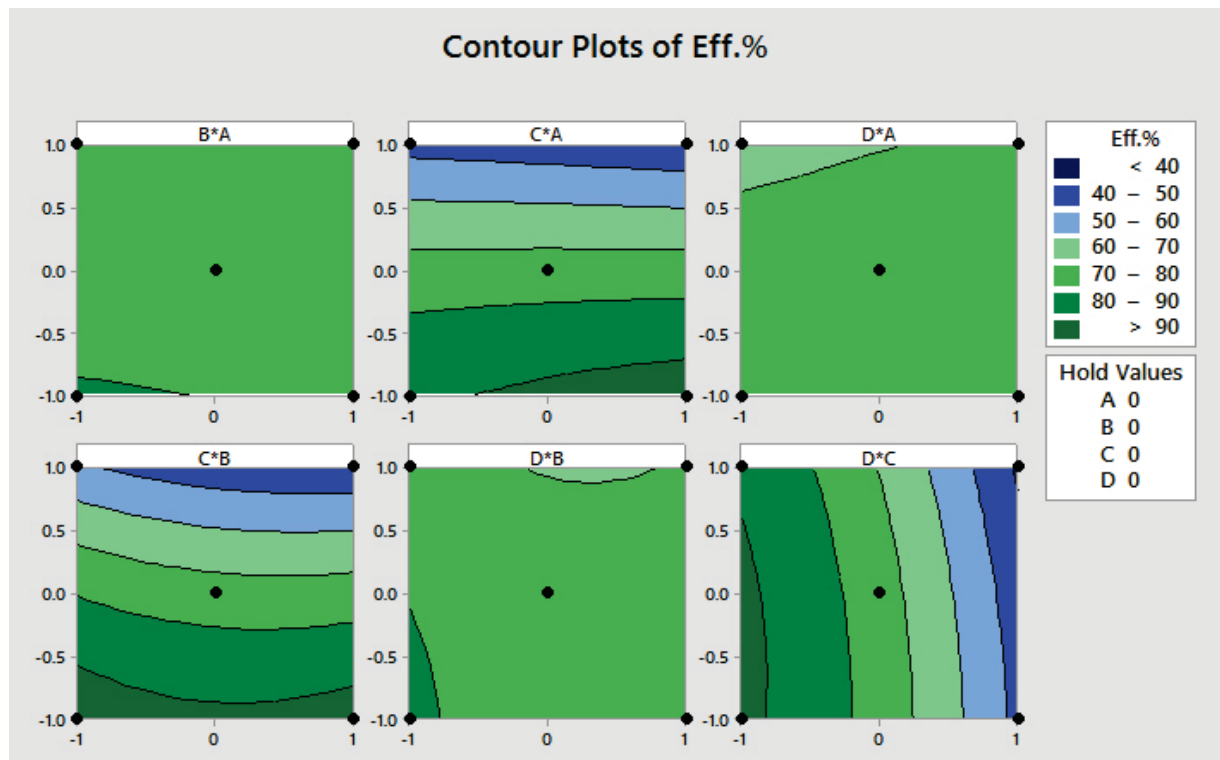

Fig. 3-31: 2- dimensional plots of contour response for pair interaction of tested variables on the protection process. Each plot displays interaction effect of two factors when they are crossed from lower to upper level and other two variables are hold at zero level.

3.6.4.3 Predicting optimum efficiency

The point that gives an optimum response of the process is called the stationary point and it can be obtained by Minitab 17 program (Fig. 3-32). The best tested levels of each variable to give a maximum efficiency were; upper level (+1) for inhibitor concentration (A) and dip coating time (B), lower level (-1) for temperature, and 0.1919 for NaCl concentration (D) which is equal to a real value of upper level (0.2 M) see Table 2-4.
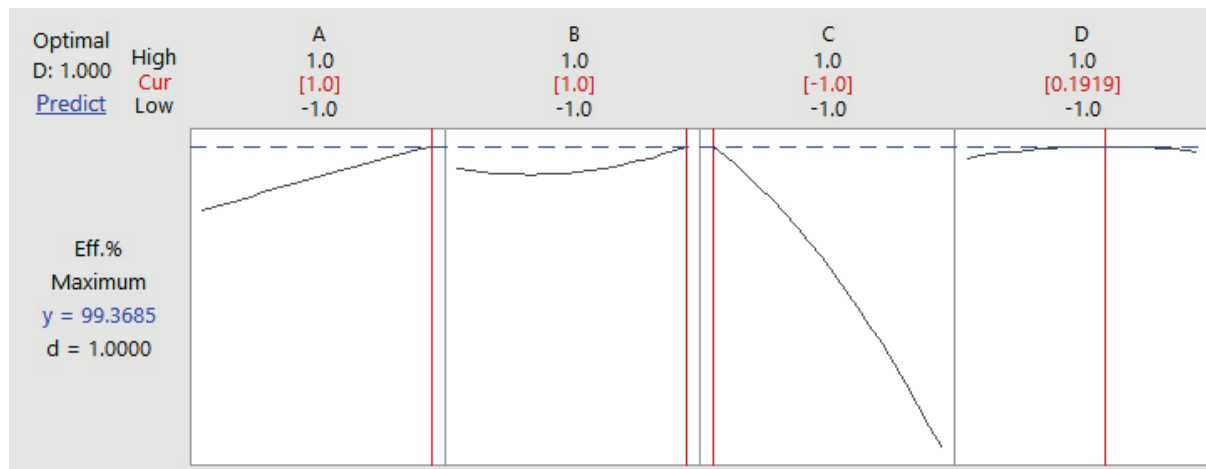
Fig. 3-32: Prediction of best tested levels that result in optimum efficiency of protection steel CR4 in salt water by proposed predictor model RSM supported with Minitab 17 program.

The optimum efficiency predicted by the current proposed predictor model, implemented with Minitab17 program, was 99.3 % according to regression equation (Eq. 3-8) after restitution level values that are found as the best combination (+1, +1, -1, 0.1919) see Eq. 3-9.

Predicted Efficiency % = 74.23 + 0.44 × (1) - 2.53 × (1) -23.53 × (-1) - 3.05 × (0.1919) - 0.23 × $(1)^2$ + 2.86 × $(1)^2$ - 6.07 × $(-1)^2$ -1.52 × $(0.1919)^2$ + 2.58 × (1×1) - 2.65 × (1×-1) + 1.67 × (1×0.1919) - 1.86 × (1×-1) + 0.72 × (1×0.1919) - 1.26 × (-1×0.1919) = 99.3   Eq. 3-9

The optimum efficiency of protection that predicted theoretically is 99.3 % according to the combined levels (A = 75 mmol/L (+1), B = 30 min (+1), C = 25°C (-1), D = 0.1919 ~ 0.2 NaCl (+1)). Predicted efficiency value is higher than the maximum experimental efficiency (94.3 %) in experiment #19 (compare Table 3-11).

3.7.5 Experimental confirmation

The predicted optimum efficiency depending on the combination of levels obtained by RSM supported with Minitab 17 program is not included in design of experiment. The predicted theoretically result was confirmed experimentally of the combination obtained in optimization (A (+1), B (+1), C (-1), and D (+1)). Fig. 3-33 shows the anodic and cathodic polarization for actual experiment #19 and the predicted one confirmed experimentally compared to steel CR4 blank. The result with the error between theoretically and experimentally is summarized in Table 3-15.
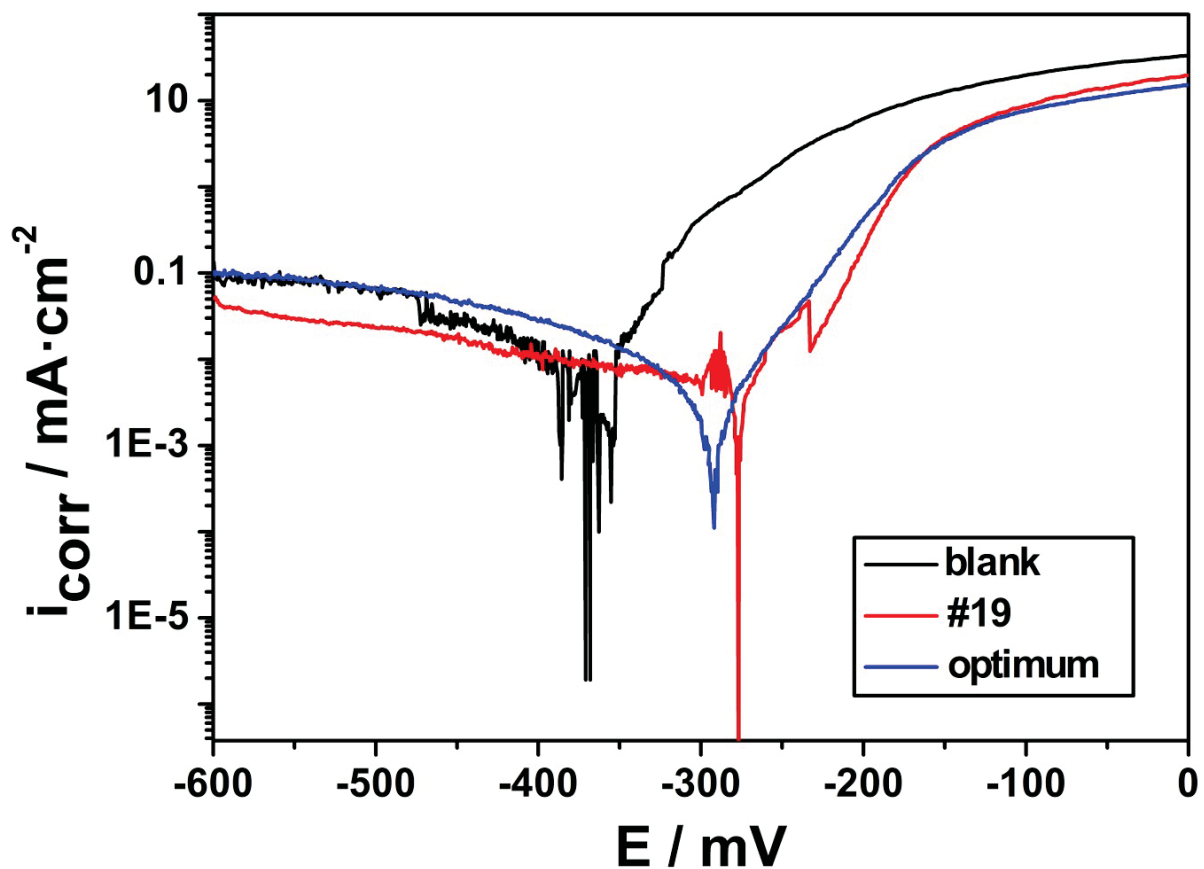
Fig. 3-33: Anodic and cathodic polarization curves for actual experiment #19 and predicted test with combination (+1,+1,-1,+1) confirmed experimentally compared to steel CR4 blank. Blank is displays in black, #19 in red and predicted one in blue.

The experimental test that is predicted according to the proposed model gives efficiency higher than the maximum efficiency value obtained in the 27 individual experiments in BBD (Fig. 3-33 and Table 3-15).

Table 3-15: Results of the theoretical prediction and experimental confirmation of optimum efficiency depending on combination levels (+1, +1, -1, +1).

Method	Theoretically	Experimentally	Error (%)
RSM	99.3 %	97.2 %	2.1

The error value in Table 3-15 shows a good confirmation and acceptability of the proposed predictor model used in the current work as the error is just 2.1 %.

Chapter four

Conclusion

Conclusion

In the current study four different sarcosine derivatives were tested as corrosion inhibitors for a green and sustainable protection of steel CR4 in salt water by electrochemical and weight loss measurements and in tab water with spray corrosion tests as more realistic application. Additionally Oley-Imidazole (OI) a commercial available inhibitor was evaluated for synergistic effects on the efficiency of the most naturally based compound Cocolysarcosine (C) which contains the mixture of coconut oil hydrocarbon chain lengths (C_8-C_{18}). Corrosion behavior and stability of the protective film are investigated with different concentrations of present inhibitors as well as for different dip coating times.

Different aqueous working media (phosphate buffer, boric buffer, 0.1 M NaCl, distilled water, and tab water) were tested by potentiodynamic polarization (PP) measurements to find the most stable system for the current investigation. The results obtained by the survey of open circuit potential (OCP) revealed that 0.1 M NaCl is the best media for the current system showing a stable free potential together with a good conductivity. The OCP-evaluation for different grinding grades applied to steel CR4 and subsequent coating with selected inhibitors revealed no differences as a result by the grade of grinding. OCP tests indicate a time of 20-30 min is sufficient to hold uncoated and inhibitor coated samples in the test solutions to reach a steady state of potential.

The present inhibitors compromise of a small polar group which is able to adsorb on the steel CR4 surface and an organic unpolar chain which is forming the hydrophobic barrier. Because the overall compound is insoluble in the aqueous media, different organic solvents for dip coating were tested via PP. The present investigation showed the most suitable solvent is toluene, because it has a neglectible effect on the protection process and no detectable change in current density and corrosion potential occurred. Therefore it was chosen here to dissolve the present compounds resp. inhibitors.

According to the current results obtained by polarization evaluation the tested compounds act as mixed type inhibitors decreasing both the anodic and cathodic polarization. Furthermore increase of inhibitor concentration fostered the protection efficiency. More inhibitor molecules absorbed on the steel CR4 surface with higher concentration. The best inhibitor throughout all tested concentrations and dip coating times and even in all evaluation systems was substance Oleoylsarcosine (O) followed by Myristoylsarcosine (M). Generally, the efficiency improvement for all evaluated compounds was large with increasing concentration

81

from 25 to 50 mmol/L while for concentrations higher than 50 mmol/L it was less, especially for the most effective inhibitor O.

In weight loss measurements, the highest efficiency was 86 % at 100 mmol/L and 78 % at 25 mmol/L for inhibitor O. For M the efficiency was 75 % and 68 % at 100 and 25 mmol/L respectively. Sarcosine L has only acceptable effects at 75 and 100 mmol/L and less than 50 % at 25 and 50 mmol/L. Compounds C and OI showed individually only insignificant effects at all tested concentrations with efficiencies less than 50 %.

For polarization evaluation, inhibitor O revealed again best maximum efficiencies up to 97 % with 100 mmol/L and 87 % at 25 mmol/L. The second best inhibitor was M with efficiencies over 63 % at all studied concentrations and up to 82 % at 100 mmol/L. The efficiency was a slightly more than 50 % at 75 and 100 mmol/L for L while it gave less than 50 % at 25 and 50 mmol/L. Single compounds C and OI resulted in efficiencies less than 50 % at all tested concentrations.

The results obtained by electrochemical impedance spectroscopy (EIS) showed for O and M an enlargement in the semicircle curves of impedance with increasing compound concentration. The efficiency of O and M to increase the resistance of charge transfer at highest concentration was 84 % and 70 % respectively. Impedance spectra revealed a process which is controlled by charge transfer and diffusion process. Inhibitor L has an insignificant effect to increase the charge transfer resistance with efficiencies less than 50 % at 25 and 50 mmol/L and a bit more than 50 % at 75 and 100 mmol/L. Sarcosine C increased the real impedance but at same time the imaginary impedance was very low at 25 and 50 mmol/L and showed a semicircle curve of impedance with efficiencies 48 % and 41 % at 75 and 100 mmol/L respectively. Compound OI showed already insufficient results of only 46 % at 50 mmol/L.

For synergistic effects, compound OI improved the protection efficiency of C when used in combination (C+OI, 1:1 molar ration). The efficiency increased from less than 50 % up to 91 % in PP, up to 85 % in EIS, and up to 83 % in WL at highest concentrations. The synergist OI showed only small efficiency improvements of the mixed system when combined with L or M. The mixtures improved from 46 % to 60 % and from 70 % to 72 % for L and M respectively, while it negatively affected inhibitor O with a significant decrease from 95 % down to 78 %.

Second synergist Methyl-Imidazoline (MI) was evaluated by potentiodynamic polarization measurements and revealed negative effects on inhibitors L, M, and O. It decreased the efficiencies to lower values in combination compared to the individual results; especially for

M and O. Worth mentioning is just a small positive effect of MI on sarcosine C which slightly increased from 35 % to 42 %.

The results for variable dip coating times (1, 2.5, 5, 10, and 30 min) revealed that the efficiency increased gradually until 10 min up to 95 %, 70 %, and 86 % for O, M, and combination C+OI respectively. Arrangements with L, C, and OI resulted in efficiencies less than 50 % for all studied times but 10 min immersion showed still the highest effect. After 10 min of dip coating time there was no significant enhancement detectable in protection. Therefore, 10 min was chosen as the optimal time for the use of dip coating in the current system.

For more realistic environment and longer duration a spray corrosion measurement was conducted. Parameters for studied compounds were 50 mmol/L for dip solutions and 10 min for dip coating time. After 24 h the best inhibitor to reduce corrosion on steel CR4 surface was O with an efficiency more than 99 % followed by M and L with efficiencies 79 % and 72 % respectively. Compounds C and OI showed efficiencies less than 20 % after 24 h, but if applied in a synergistic combination the efficiency of C+OI improved to 80 % protection.

To sum up the obtained results, all evaluation systems used (WL, PP, EIS, and spray corrosion measurements) are in a good overall agreement and show an identical order in the efficiency of compounds.

Box-Behnken design (BBD) was used to analyze the influence of four different independent variables with three levels for each one on the protection of steel CR4 in salt water by using most effective inhibitor O. Response surface methodology (RSM) is an optimization method depending on BBD and supported with Minitab 17 program and was used to find the best level combination for an optimum efficiency result. The results showed that BBD is a good systematic control tool to investigate the optimum effect of different variables on the current corrosion protection by using inhibitors. According to the acquired data temperature and inhibitor concentration revealed largest individual effects on the present process. For interaction effects they were in following order: (inhibitor concentration and temperature - AC) > (dip coating time and temperature - BC) > (inhibitor concentration and NaCl concentration - AD).

For optimization, results of RSM indicated the best combination concerning levels for studied variables to give an optimum efficiency is upper level (+1) for inhibitor concentration, immersion time, and NaCl concentration while lower level (-1) for dip coating time. The optimum efficiency predicted by proposed prediction model was 99.3 %. This is somehow higher than the maximum efficiency obtained by the real experiments of BBD. The error

between predicted and experimentally efficiency was calculated to 2.1 % which refers to an excellent acceptability for the method applied here.

Acknowledgment

References

[1] M.G. Fontana, N.D. Greene, "Corrosion Engineering", 2nd edition, McGraw - Hill, N.Y., USA, 1978.

[2] B. N. Popov, Corrosion Engineering: Principles and Solved Problems, 1st edition, Edited by Copyright © Elsevier B.V., 2015.

[3] Z. Ahmad, Principles of Corrosion Engineering and corrosion Control, 1st Edition, Butterworth-Heinemann, UK, 2006.

[4] Corrosion of metals and alloys - Basic terms and definitions (ISO 8044:1999/DAM 1:2012); German version EN ISO 8044/prA1, 2012.

[5] M.G. Fontana, Corrosion engineering, 3rd edition, McGraw - Hill, N.Y., USA, 1986.

[6] C.B. Fischer, T. Hecken, D. Willems, Beobachtung von Korrosionsphänomenen mit alltäglichen Ressourcen, Poster presentation, MNU Bundeskongress, Freiburg, April, 2012.

[7] R.N. Gun, Duplex Stainless Steel: Microstructure, properties and applications, Abington Publishing, England, UK, 2003.

[8] Peter Maaß, Peter Peißker (editors), Handbook of Hot-dip Galvanization, WILEY-VCH, Weinheim, 2011.

[9] M. Stern, A.L. Geary, Electrochemical polarization: I. A theoretical analysis of the shape of polarization curves, Electrochem. Soc. Vol. 104, No. 1 (1957) 56-63.

[10] R.W. Revie (editor), " Uhlig's Corrosion Handbook", 3rd Edition, Part 1: Corrosion failure analysis with case histories, WILEY-VCH, USA, 2011.

[11] S.N. Popova, B.N. Popov, R.E. White, Determination of corrosion properties of lacquered tinplate in citrate solutions by DC and AC electrochemical methods, Corrosion Vol. 46, No. 12 (1990) 1007-1014.

[12] D.A. Jones, Polarization in high resistivity media, Corros. Sci. 8 (1968) 19-27.

[13] J.R. Park, D.D. MacDonald, The fast-growth mechanism of magnetite on carbon steel in oxidizing high-temperature aqueous solutions, Corrosion Vol. 45, No. 7 (1989) 563-571.

[14] R.L. Leroy, Evaluation of corrosion rates from nonlinear polarization data, J. Electrochem. Soc. 124 (1977) 1006-1012.

[15] W.R. Revie, H.H. Uhlig, Corrosion and Corrosion Control, 4th edition, WILEY-VCH, USA, 2006.

[16] L.H. Madkour, A.M. Hassanien, M.M. Ghoneim, S.A. Eid, Inhibition effect of hydantion compounds on the corrosion of iron in nitric and sulfuric acid solutions, Monatshefte für

References

Chemie 132 (2001) 245-258.

[17] H.-J. Bargel, Grundlagen der Metall- und Legierungskunde, Werkstoffkunde, G. Schulze (editor), D-Berlin Heidelberg: Springer-Verlag, 2012.

[18] E. Gileadi, Physical Etrochemistry: Fundamental, Techniqes and Applications, WILEY-VCH, Weinheim, 2015.

[19] S. Pathan, S. Ahmad, Synergistic effect of linseed oil based terborne alkyd and 3-isocynatoropyl triethoxysilane: highly transparent, mechanically robustthermally stable, hydrophobic, anticorrosive coatings, ACS Sustainable Chem. Eng. 6 (2016) 3062-3075.

[20] V.S. Saji, A review on recent patents in corrosion inhibitors, Recent Patents on Corros. Sci. 2 (2010) 6-12.

[21] C.G. Dariva and A. Galio, Developmemts in corrosion protection, M. Aliofhazraei, (Eds.), Corrosion Inhibitors - Principles, Mechanisms and Applications, Ch. 16, DOI: 10.5772/57010, 2014.

[22] P. Agarwal, D. Landolt, Corrosion Inhibitors, Part 5, Metrohm Autolab B.V., Application Note COR05, 2011.

[23] S.K. Sharma, Green Corrosion Chemistry and Engineering: Opportunities and Challenges, 1st edition, Wiley-VCH, 2012.

[24] M. Adamu, L.E. Umoru, O.O. Ige, Effect of toluene and dioctylphthalate on rebar corrosion of medium carbon steel in seawater and cassava fluid, J. Miner. Mater. Charact. Eng. 2 (2014) 1-7.

[25] T. Ibrahim and M.A. Zour, Corrosion inhibition of mild steel using fig leaves extract in hydrochloric acid solution, Int. J. Electrochem. Sci. 6 (2011) 6442-6455.

[26] S.E. Kaskah, M. Pfeiffer, H. Klock, H. Bergen, G. Ehrenhaft, P. Ferreira, G. Gollnick, C.B. Fischer, Surface protection of low carbon steel with *N*-acyl sarcosine derivatives as green corrosion inhibitors, Surf. Interfaces 9 (2017) 70-78.

[27] G.S. Frankel, Fundamentals of corrosion kinetics (Chapter 2) Active protective coatings, Springer, Dordrecht (2016) 17-32, DOI: org/10.1007/978-94-017-7540-3_2.

[28] A. Popova, M. Ghristov, A. Zwetanova, Effect of the molecular structure on the inhibitor properties of azoles on mild steel corrosion in 1 M hydrochloric acid, Corros. Sci. 49 (2007) 2131-2143.

[29] S. Papavinsam, "Corrosion Handbook", 2nd edition: 59 Corrosion inhibitors, Wiley-VCH, USA, 2000.

[30] V.J. Drazic, D.M. Drazic, Adsorption of inhibitors on a corroding iron surface, J. Serb. Chem. Soc. 56 (1991) 753-757.

References

[31] V.J. Drazic, D.M. Drazic, Competitive adsorption of water, sulfuric acid inhibition species on a corroding iron surface, J. Serb. Chem. Soc. 57 (1992) 917-926.

[32] L. Vracar, D.M. Drazic, Influence of chloride ion adsorption on hydrogen evolution reaction on iron, J. Electroanal. Chem. 339 (1992) 269-279.

[33] D.M. Drazic, L. Vracar, V.J. Drazic, The kinetics of inhibitor adsorption on iron, Electrochim. Acta. 39 (1994) 1165-1170.

[34] M. L. D. Vracar, M. Drazic, Anomalous temperature dependence of the hydrogen evolution reaction on iron, J. Electroanal. Chem. 256 (1989) 171-178.

[35] Lj.M. Vracar, D.M. Drazic, Adsorption and corrosion inhibitive properties of some organic molecules on iron electrode in sulfuric acid, Corros. Sci. 44 (2002) 1669-1680.

[36] N.A. Negm, N. G. Kandile, E.A. Badr, M.A. Mohammed, Gravimetric and electrochemical evaluation of environmentally friendly non-ionic corrosion inhibitors for carbon steel in 1 M NaCl, Corros. Sci. 65 (2012) 94-103.

[37] J.M. Roque, T. Pandiyan, J. Cruz, E. Garcı´a-Ochoa, DFT and electrochemical studies of tris(benzimidazole-2-ylmethyl) amine as an efficient corrosion inhibitor for carbon steel surface, Corros. Sci. 50 (2008) 614-624.

[38] A.A. Rahim and J. Kassim, Recent development of vegetal tannins in corrosion protection of iron and steel, Recent Pat. Mater. Sci. 1 (2008) 223-231.

[39] F.B. Waanders, S.W. Vorster and A.J. Geldenhuys, Biopolymer corrosion inhibition of mild steel: Electrochemical/Mössbauer results, Proc. Hyperfine Interactions 139/140 (2002) 133-139.

[40] S.W. Dean Jr., R. Derby, G.T. Vondembussche, Inhibitor types, Mater. Perform. 20 (1981) 47-51.

[41] L. Wang, Evaluation of 2-mercaptobenzimidazole as corrosion inhibitor for mild steel in phosphoric acid, Corros. Sci. 43 (2001) 2281-2289.

[42] M.A. Quraishi, R. Sardar, Aromatic triazoles as corrosion inhibitors for mild steel in acidic environments, Corrosion 58 (2002) 748-755.

[43] F. Bentiss, M. Lebrini, H. Vezin, M. Lagrenee, Experimental and theoritacal study of 3-pyridyl-substituted 1,2,4-thiadiazole and 1,3,4-thiadiazole as corrosion inhibitors of mild steel in acidic media, Mater. Chem. Phys. 87 (2004) 18-23.

[44] E.A. Noor, The inhibition of mild steel corrosion in phosphoric acid solutions by some N-heterocyclic compounds in the salt form, Corros. Sci. 47 (2004) 33-35.

[45] M.M. Singh, R.V. Rastogi, B.N. Upadhyay, Inhibition of copper corrosion in aqueous sodium chloride solution by various forms of the piperidine moiety, Corrosion 50 (1994) 620-

References

625.

[46] W. Su, B. Tang, F. Fu, S. Huang, S. Zhao, L. Bin, J. Ding, C. Chen, A new insight into resource recovery of excess sewage sludge: Feasibility of extracting mixed amino acids as an environment-friendly corrosion inhibitor for industrial pickling, J. Hazard. Mater. 279 (2014) 38-45.

[47] N.O. Eddy, Experimental and theoretical studies on some amino acids and their potential activity as inhibitors for the corrosion of mild steel, part 2, J. Adv. Res. 2 (2011) 35-47.

[48] M.A. Pech-Canul, L.P. Chi-Canul, Investigation of the inhibitive effect of N-phosphono-methyl-glycine on the corrosion of carbon steel in neutral solutions by electrochemical techniques, Corrosion 55 (1999) 948-956.

[49] E. Kálmán, F.H. Karman, J. Telegdi, B. Varhegyi, J. Balla, T. Kiss, Inhibition efficiency of N-containing carboxylic and carboxy-phosphonic acids, Corros. Sci. 35 (1993) 1477-1482.

[50] E. Rocca, J. Steinmetz, Inhibition of lead corrosion with saturated linear aliphatic chain monocarboxylates of sodium, Corros. Sci. 43 (2001) 891-902.

[51] G. Boisier, A. Lamure, N. Pébère, N. Portail, M. Villatte, Corrosion protection of AA2024 sealed anodic layers using the hydrophobic properties of carboxylic acids, Surf. Coat. Technol. 203 (2009) 3420-3426.

[52] G.T. Hefter, N.A. North, S.H. Tan, Organic corrosion inhibitors in neutral solutions; Part 1-Inhibition of steel, copper, and aluminum by straight chain carboxylates, Corrosion 53 (1997) 657-667.

[53] D. Lahem, M. Poelman, F. Atmani, M.G. Olivier, Synergistic improvement of inhibitive activity of dicarboxylates in preventing mild steel corrosion in neutral aqueous solution, Corros. Eng., Sci. Technol. 47 (2012) 463-471.

[54] X. Li, S. Deng, H. Fu, G. Mu, Inhibition effect of 6-benzylaminopurine on the corrosion of cold rolled steel in H_2SO_4 solution, Corros. Sci. 51 (2009) 620-634.

[55] H.D. Lece, K.C. Emregul, O. Atakol, Difference in the inhibitive effect of some Schiff base compounds containing oxygen, nitrogen and sulfur donors, Corros. Sci. 50 (2008) 1460-1468.

[56] S.A. Abed El-Maksoud, The influence of some arylazobenzoyl acetonitrile derivatives on the behavior of carbon steel in acidic media, Appl. Surf. Sci. 206 (2003) 129-136.

[57] M.A. Veloz, I.G. Martinz, Effect of some pyridine derivatives on the corrosion behavior of carbon steel in an environment like NACE TM0177, Corrosion 62 (2006) 283-292.

[58] A. Ouchrif, M. Zegmour, B. Hammouti, S. El-Kadiri, A. Ramdani, 1,3-Bis(3-hyroxymethyl-5-methyl-1-pyrazole) propane as corrosion inhibitor for steel in 0.5 M H_2SO_4

References

solution, Appl. Surf. Sci. 252 (2005) 339-344.

[59] A. Chetouani, B. Hammouti, T. Benhadda, M. Daoudi, Inhibitive action of bipyrazolic type organic compounds towards corrosion of pure iron in acidic media, Appl. Surf. Sci. 249 (2005) 375-385.

[60] A. Popova, M. Christov, T. Deligeorigiev, Influence of the molecular structure on the inhibitor properties of benzimidazole derivatives on mild steel corrosion in 1 M hydrochloric acid, Corrosion 59 (2003) 756-764.

[61] A. Popova, M. Christov, S. Raicheva, E. Sokolova, Adsorption and inhibitive properties of benzimidazole derivatives in acid mild steel corrosion, Corros. Sci. 46 (2004) 1333-1350.

[62] I.B. Obot, N.O. Obi-Egbedi, 2, 3-Diphenylbenzoquinoxaline: A new corrosion inhibitor for mild steel in sulfuric acid, Corros. Sci. 52 (2010) 282-285.

[63] N. Ochoa, F. Moran, N. Pébère, B. Tribollet, Influence of flow on the corrosion inhibition of carbon steel by fatty amines in association with phosphonocarboxylic acid salts, Corros. Sci. 47 (2005) 593-604.

[64] N. Ochoa, F. Moran, N. Pébère, Influence of flow on the corrosion inhibition of carbon steel by fatty amines in association with phosphonocarboxylic acid salts, J. Appl. Electrochem. 34 (2004) 487-493.

[65] N. Ochoa, G. Baril, F. Moran, N. Pébère, Study of the properties of a multi-component inhibitor used for water treatment in cooling circuits, J. Appl. Electrochem. 32 (2002) 497-504.

[66] V.S. Sastri, Challenges in Corrosion, JOHN WILEY & SONS, INC., USA, 2015.

[67] A. Ostovari, S.M. Hoseinieh, M. Peikari, S.R. Shadizadeh, S.J. Hashemi, Corrosion inhibition of mild steel in 1 M HCl solution by henna extract: A comparative study of the inhibition by henna and its constituents (Lawsone, Gallic acid, α-D-Glucose and Tannic acid, Corros. Sci. 51 (2009) 1935-1949.

[68] G. Trabanelli, V. Carassiti, Mechanism and phenomenology of organic inhibitors, in: M.G. Fontaine, R.W. Stachle (Ed.), Advances in corrosion science and technology, Vol. I, Plenum press, New York-London, 1970, pp. 147-205.

[69] R. Solmaz, G. Kardas, B. Yazici, M. Erbil, Adsorption and corrosion inhibitive properties of 2-amino-5-mercapto-1,3,4-thiadiazole on mild steel in hydrochloric acid media, Colloids Surf. 312 (2008) 7-17.

[70] H.H. Uhlig, R.W. Revie, Corrosion and corrosion control, 3rd edition, WILEY-VCH, N.Y., USA, 1985.

[71] L. Zhao, H.K. Teng, Y.S. Yang and X. Tan, Corrosion inhibition approach of oil

References

production systems in offshore oilfields, Mater. Corros. 9 (2004) 684-688.

[72] F. Moyo, R. Tandlich, B.S. Wilhelm and S. Balaz, Sorption of hydrophobic organic compounds on natural sorbents and organoclays from aqueous and non-aqueous solutions: A mini-review, Int. J. Environ. Res. Public Health 11 (2014) 5020-5048.

[73] A. Frignani, G. Trabanelli, C. Wrubl, A. Mollica, N-Lauroyl sarcosine sodium salt as a corrosion inhibitor for type 1518 carbon steel in neutral saline environments, Corros. Sci. 52 (1996) 177-182.

[74] S. Lanigan, Final report on the safety assessment of cocoyl sarcosine, lauroyl sarcosine, myristoyl sarcosine, oleoyl sarcosine, stearoyl sarcosine, sodium cocoyl sarcosinate, sodium lauroyl sarcosinate, sodium myristoyl sarcosinate, ammonium cocoyl sarcosinate, and ammonium lauroyl sarcosinate, Int. J. Toxicol. 20 (2001) 1-14.

[75] G.A. Saiensky, M.G. Cobb, Corrosion-inhibitor orientation on steel, Ind. Eng. Chem. Prod. Res. Dev. 25 (1985) 133-140.

[76] Comparisons of response surface designs, NIST/SEMATECH e-Handbook of Statistical Methods, http://www.itl.nist.gov/div898/handbook/.

[77] R.B. Penteado, T.G. Hagui, J.C. Faria, M.B. Silva, M.V. Ribeiro, Application of Taguchi methodin process improvement of turning of a Superalloy NIMONIC 80A, 015-0713.

[78] T. Rakic, I.K. Vujanovic, M. Jovanovic, B.J. Stojanovic, D. Ivanovic, Comparision of full factorial design, central composite design, and box-behnken design in chromatographic method development for the determination of fluconazole and its impurities, Anal. Lett. 47 (2014) 1334-1347.

[79] M. Mourabet, A. El Rhilassi, H. El Boujaady, M. Bennani-Ziatni, R. El Hamri, A. Taitai, Removal of fluorid from aqueous solution by adsorption on apatitic tricalcium phosphate using box-behnken design and desirability function, Appl. Surf. Sci. 258 (2012) 4402-4410.

[80] H. Rushing, A. Karl, J. Wisnowski, Design and analysis of experiments by Douglas Montgomery, SAS Insitute Inc., USA, 2013.

[81] S.L.C. Ferreira, R.E. Bruns, H.S. Ferreira, G.D. Matos, J.M. David, G.C. Brandao, E.G.P. da Silva, L.A. Portugal, P.S. dos Reis, A.S. Souza, W.N.L. dos Santos, Box-behnken design: An alternative for the optimization of analytical methods, Analytica Chemica Acta. 597 (2007) 179-186.

[82] S.S. Kumar, S.K. Malyan, A. Kumar and N.R. Bishnoi, Optimization of fenton's oxidation by box-behnken design of response surface methodology for landfill leachate, J. Mater. Environ. Sci. 7 (12) (2016) 4456-4466.

[83] M. Ahmadi, F. Ghanbari, Optimizing COD removal from greywater by photoelectro-

persulfate process using box-behnken design: assessment of effluent quality and electrical energy consumption, Environ. Sci. Pollut. Res. (DOI 10.1007/s11356-016-7139-6).

[84] V.B. Magdum, V.R. Naik, Evaluation and optimization of machining parameter for turning of EN 8 steel, International Journal of Engineering Trends and Technology (IJETT), Vol 4 issue 5, 2013.

[85] E. Rupi and R. Mawonike, Response surface methodology for process monitoring of soft drink: A case of delta beverages in Zimbabwe, Journal of Mathematics and Statistical Science (2015) 213-233.

[86] H.R.F. Masoumi, A. Kassim, M. Basri and D.K. Abdullah, Determining optimum condition for Lipase-Catalyzed synthesis of triethanolamine (TEA)-Based esterquat cationic surfactant by a Taguchi robust design method, Molecules 16 (2011) 4672-4680.

[87] M.J. Qureshi, F.F. Phin and S. Patro, Enhanced solubility and dissolution rate of clopidogrel by nanosuspension: Formulation via high pressure homogenization technique and optimization using Box-Behnken design response surface methodology, J. Appl. Pharm. Sci.7 (2017) 106-113.

[88] A.I. Khuri, Response surface methodology and its application in agricultural and food sciences, Biom. Biostat Int. J. 5 (2017) 1-11 (DOI: 10.15406/bbij.2017.05.00141).

[89] M. Li, C. Feng, Z. Zhang, R. Chen, Q. Xue, C. Gao, N. Sugiura, Optimization of process parameters for electrochemical nitrate removal using Box-Behnken design, Electrochim. Acta 56 (2010) 265-270.

[90] W.J. Hill, W.G. Hunter, Response surface methodology: A Review, Technical report, University of Wisconsin, 1966.

[91] L. Olivi (editor), Response surface methodology, Handbook for nuclear science and technology, Commission of the European Communities, 1984.

[92] R.H. Myers, D.C. Montgomery and C.M. Anderson-Cook, Response surface methodology, Process and product optimization using designed experiments, 3rd edition, WILEY-VCH, 2008

[93] B. Nakhai, J.S. Neves, The challenges of six sigma in improving service quality, International Journal of Quality & Reliability Management Vol. 26 No. 7 (2009) 663-684.

[94] G.E.P. Box, W.G. Hunter and J.S. Hunter, Statistics for experimenters, An introduction to design, data analysis and model building, WILEY-VCH, USA, 1978.

[95] M.A. Bezerra, R.E. Bruns, S.L.C. Ferreira, Statistical design-principal component analysis optimization of a multiple response procedure using cloud point extraction and simultaneous determination of metals by ICP OES, Anal. Chim. Acta 580 (2006) 251-257.

References

[96] Massart, Handbook of chemometrics and qualimetrics, Vol 20B, 1st Edition, Part B.

[97] N.K. Mondal, A. Samanta, S. Dutta and S. Chattoraj, Optimization of Cr(VI) biosorption onto aspergillus niger using 3-level Box-Behnken design: Equilibrium, kinetic, thermodynamic and regeneration studies, J. Genet. Eng. Biotechnol. 15 (2017) 151-160. (http://dx.doi.org/10.1016/j.jgeb.2017.01.006).

[98] H. Chen, D. Ma, Y. Li, Y. Liu and Y. Wang, Optimization the process of microencapsulation of bifidobacterium bifidum BB01 by Box-Behnken design, Acta universitatis cibiniensis series E: Food Technology, (DOI: https://doi.org/10.1515/aucft-2016-0012).

[99] S.P. Dwivedi, S. Kumar and A. Kumar, Effects of turning parameters on dimensional deviation of A356/5% SiC composite using Box-Behnken design and genetic algorithm, Frontiers in Manufacturing Engineering Vol. 2, No. 1 (2014) 8-14.

[100] C. Wegst, M.Wegst, Stahlschlüssel, Verlag Stahlschlüssel Wegst GmbH, 22. Auflage - edition 2010.

[101] European Committee for Standardization. Corrosion tests in artificial atmospheres - Salt spray tests (DIN EN ISO 9227:2006). Brussels, 2006.

[102] European Committee for Standardization. Paints and varnishes - Standard panels for testing (DIN EN ISO 1514:2005-02). Brussels, 2004.

[103] P. Bommersbach, C. Alemany-Dumont, J.P. Millet, and B. Normand, Formation and behaviour study of an environment-friendly corrosion inhibitor by electrochemical methods, Electrochemic Acta. 51 (2005) 1076-1084.

[104] Glycine, N-coco acyl derivs., sodium salts (INCI name: Sodium Cocoyl Glycinate), Full public report, NICNAS, Australia, 2010.

[105] HAMPOSYL N-Acyl Sarcosinate Surfactants are anionic surfactants available in several acid and salt grades, Product information, Chattem Chemicals, Inc. An Elcat Company.

[106] S.E. Kaskah, G. Ehrenhaft, J. Gollnick, C.B. Fischer, Concentration and coating time effects of *N*-acyl sarcosine derivatives for corrosion protection of low carbon steel CR4 in salt water - Defining a suitable application window, submitted to Corros. Eng., Sci. Technol.

[107] S.E. Kaskah, G. Ehrenhaft, J. Gollnick, C.B. Fischer, Oley Imidazole used as synergist to enhance the inhibition efficiency of the nature Cocoylsarcosine for low carbon steel in aqueous solution, submitted to ACS Sustainable Chemistry & Engineering.

[108] A. Edwards, C. Osborne, S. Webster, D. Klenerman, M. Joseph, P. Ostovar and M. Doyle, Mechanistic studies of the corrosion inhibitor oleic imidazoline, Corros. Sci. 36

References

(1994) 315-325.

[109] S.M. Tawfik, N.A. Negm, Vanillin-derived non-ionic surfactants as green corrosion inhibitors for carbon steel in acidic environments, Res. Chem. Intermed. 42 (2016) 3579-3607.

[110] S.M. Tawfik, A.A. Bd-Elaal, I. Aiad, Three gemini cationic surfactants as biodegradable corrosion inhibitors for carbon steel in HCl solution, Res. Chem. Intermed. 42 (2016) 1101-1123.

[111] ImageJ homepage: http://rsb.info.nih.gov/ij/.

[112] Origin 8.1 SR2, home page: http://www.originlab.com/.

[113] F. Mounir, R. Salghi, S. Jodeh, S. El Issami, L. Bazzi, *Argania spinose* (L.) as a source of new and efficient green corrosion inhibitor for copper in acidic medium: a comparative study of three green compounds, Int. J. Corros. Scale Inhib. 5 (2016) 159-171.

[114] K.F. Khaled, Studies of iron corrosion inhibition using chemical, electrochemical and computer simulation techniques, Electrochim. Acta 55 (2010) 6523-6532.

[115] H. Vashisht, S. Kumar, I. Bahadur, G. Singh, Evaluation of (2-hydroxyethyl) triphenyl phosphonium bromide as corrosion inhibitor for mild steel in sulphuric acid, Int. J. Electrochem. Sci. 8 (2013) 684-699.

[116] T. Jacobsen, K. West, Diffusion impedance in planar, cylindrical and spherical symmetry, Electrochim. Acta 40 (1995) 255-262.

[117] Zia, A.; Mukhopadhyay, S. Electrochemical sensing: Carcinogens in Beverages, Smart Sensors, Measurement and Instrumentation 20, Ch 2: Impedance spectroscopy and experimental setup. DOI 10.1007/978-3-319-32655-9_2.

[118] Sorkhabi, H. A.; Asghari, E.; Ejbari, P. Electrochemical studies of adsorption and inhibitive performance of basic yellow 28 dye on mild steel corrosion in acid solutions. *Acta Chim. Slov.* 2011, 58, 270-277.

[119] F. Bentiss, M. Bouanis, B. Mernari, M. Traisnel, H. Vezin, M. Lagrenée, Understanding the adsorption of 4*H*-1,2,4-triazole derivatives on mild steel surface in molar hydrochloric acid, Appl. Surf. Sci. 253 (2007) 3696-3704.

[120] M. Heydari, M. Javidi, Corrosion inhibition and adsorption behaviour of an amido-imidazoline derivative on API 5L X52 steel in CO_2-saturated solution and synergistic effect of iodide ions, Corros. Sci. 61 (2012) 148-155.

Appendix I

Details of macro implemented to split the image color values into three color channels (blue, green and red). Macro was used during image processing via ImageJ to determine corrosion area and spots in spray corrosion test.
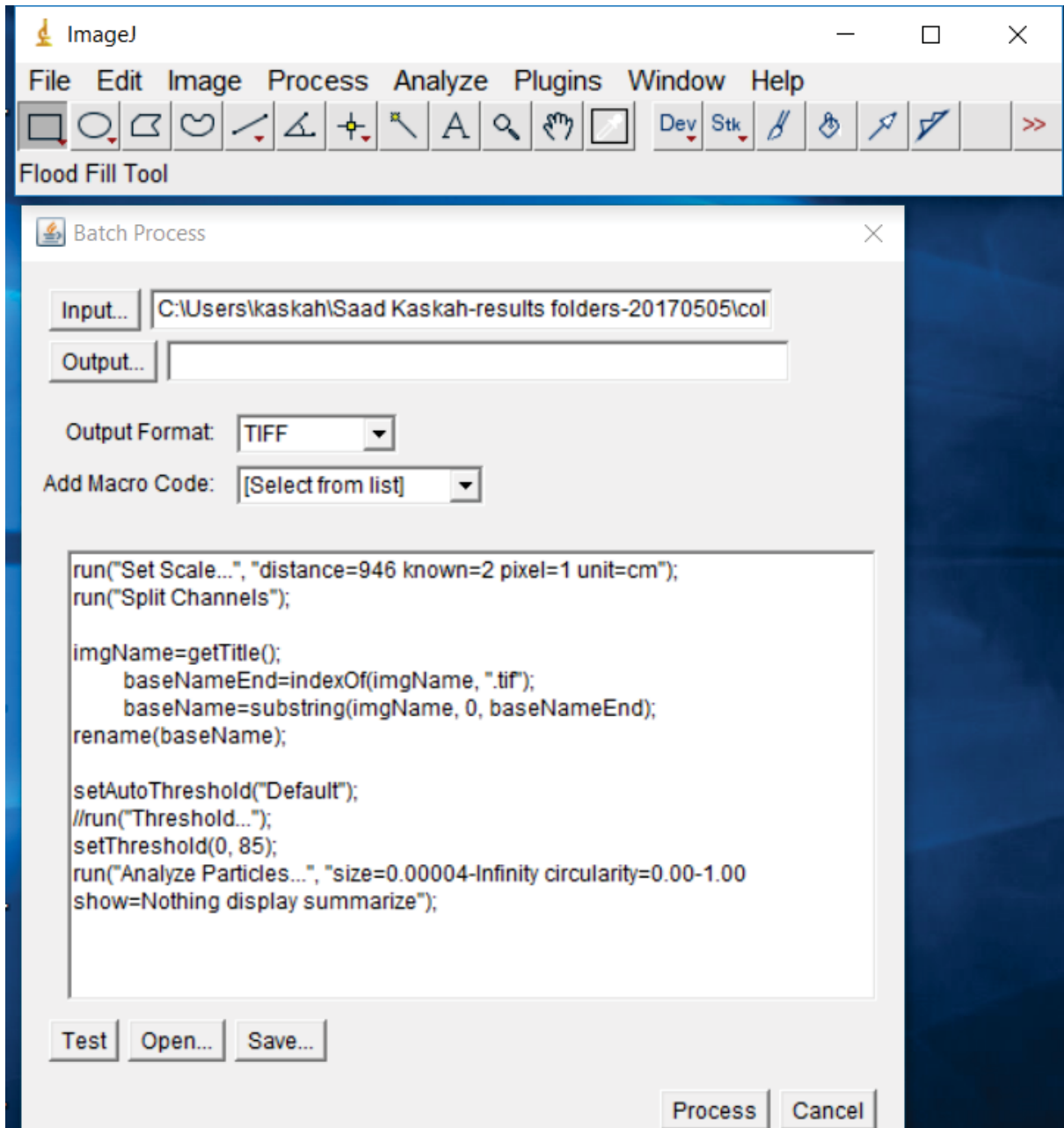
Appendix II

Details of optimization by response surface method (RSM) implementation in Minitab17 based on Box-Behnken Design (BBD)

Box-Behnken Design
Design Summary

Factors:	4	Replicates:	1
Base runs:	27	Total runs:	27
Base blocks:	1	Total blocks:	1
Center points: 3			

Response Surface Regression: Efficiency / % versus A, B, C, D
Analysis of Variance

Source	DF	Adj SS	Adj MS	F-Value	P-Value
Model	14	7264.74	518.91	7.10	0.001
Linear	4	6830.80	1707.70	23.37	0.000
A	1	2.34	2.34	0.03	0.861
B	1	76.96	76.96	1.05	0.325
C	1	6640.17	6640.17	90.89	0.000
D	1	111.33	111.33	1.52	0.241
Square	4	345.89	86.47	1.18	0.367
A*A	1	0.28	0.28	0.00	0.951
B*B	1	43.50	43.50	0.60	0.455
C*C	1	196.37	196.37	2.69	0.127
D*D	1	12.35	12.35	0.17	0.688
2-Way Interaction	6	88.05	14.67	0.20	0.970
A*B	1	26.57	26.57	0.36	0.558
A*C	1	28.09	28.09	0.38	0.547
A*D	1	11.12	11.12	0.15	0.703
B*C	1	13.88	13.88	0.19	0.671
B*D	1	2.06	2.06	0.03	0.869
C*D	1	6.33	6.33	0.09	0.774
Error	12	876.72	73.06		
Lack-of-Fit	10	876.72	87.67	*	*
Pure Error	2	0.00	0.00		
Total	26	8141.45			

Model Summary

S	R-sq	R-sq(adj)	R-sq(pred)
8.54750	89.23%	76.67%	37.97%

Appendix

Coded Coefficients

Term	Coef	SE Coef	T-Value	P-Value	VIF
Constant	74.23	4.93	15.04	0.000	
A	0.44	2.47	0.18	0.861	1.00
B	-2.53	2.47	-1.03	0.325	1.00
C	-23.52	2.47	-9.53	0.000	1.00
D	-3.05	2.47	-1.23	0.241	1.00
A*A	-0.23	3.70	-0.06	0.951	1.25
B*B	2.86	3.70	0.77	0.455	1.25
C*C	-6.07	3.70	-1.64	0.127	1.25
D*D	-1.52	3.70	-0.41	0.688	1.25
A*B	2.58	4.27	0.60	0.558	1.00
A*C	-2.65	4.27	-0.62	0.547	1.00
A*D	1.67	4.27	0.39	0.703	1.00
B*C	-1.86	4.27	-0.44	0.671	1.00
B*D	0.72	4.27	0.17	0.869	1.00
C*D	-1.26	4.27	-0.29	0.774	1.00

Regression Equation in Uncoded Units

Efficiency / %   =   74.23 + 0.44 A - 2.53 B - 23.52 C - 3.05 D - 0.23 A*A + 2.86 B*B - 6.07 C*C
- 1.52 D*D + 2.58 A*B - 2.65 A*C + 1.67 A*D - 1.86 B*C + 0.72 B*D - 1.26 C*D

Fits and Diagnostics for Unusual Observations

Obs	Efficiency / %	Fit	Resid	Std Resid	
10	52.40	67.32	-14.92	-2.70	R
11	85.57	74.30	11.27	2.04	R

R Large residual

Response Optimization: Efficiency / %
Parameters

Response	Goal	Lower	Target	Upper	Weight	Importance
Efficiency / %	Maximum	37.86	94.35		1	1

Solution

Solution	A	B	C	D	Efficiency / % Fit	Composite Desirability
1	1	1	-1	0.191919	99.3685	1

Appendix

Multiple Response Prediction

Variable	Setting
A	1
B	1
C	-1
D	0.191919

Response	Fit	SE Fit	95% CI	95% PI
Efficiency / %	99.37	9.76	(78.11, 120.63)	(71.10, 127.63)

Settings

Variable	Setting
A	-1
B	-1
C	0
D	0

Prediction

Fit	SE Fit	95% CI	95% PI
81.5238	6.52826	(67.2999, 95.7476)	(58.0898, 104.958)

Settings

Variable	Setting
A	-1
B	1
C	0
D	0

Prediction

Fit	SE Fit	95% CI	95% PI
71.3038	6.52826	(57.0799, 85.5276)	(47.8698, 94.7377)

Settings

Variable	Setting
A	1
B	-1
C	0
D	0

Prediction

Fit	SE Fit	95% CI	95% PI
77.2521	6.52826	(63.0282, 91.4760)	(53.8181, 100.686)

Appendix

Settings

Variable	Setting
A	1
B	1
C	0
D	0

Prediction

Fit	SE Fit	95% CI	95% PI
77.3421	6.52826	(63.1182, 91.5660)	(53.9081, 100.776)

Settings

Variable	Setting
A	0
B	0
C	-1
D	-1

Prediction

Fit	SE Fit	95% CI	95% PI
91.9521	6.52826	(77.7282, 106.176)	(68.5181, 115.386)

Settings

Variable	Setting
A	0
B	0
C	-1
D	1

Prediction

Fit	SE Fit	95% CI	95% PI
88.3754	6.52826	(74.1515, 102.599)	(64.9415, 111.809)

Settings

Variable	Setting
A	0
B	0
C	1
D	-1

Prediction

Fit	SE Fit	95% CI	95% PI
47.4204	6.52826	(33.1965, 61.6443)	(23.9865, 70.8544)

Appendix

Settings

Variable	Setting
A	0
B	0
C	1
D	1

Prediction

Fit	SE Fit	95% CI	95% PI
38.8137	6.52826	(24.5899, 53.0376)	(15.3798, 62.2477)

Settings

Variable	Setting
A	-1
B	0
C	0
D	-1

Prediction

Fit	SE Fit	95% CI	95% PI
76.7496	6.52826	(62.5257, 90.9735)	(53.3156, 100.184)

Settings

Variable	Setting
A	-1
B	0
C	0
D	1

Prediction

Fit	SE Fit	95% CI	95% PI
67.3229	6.52826	(53.0990, 81.5468)	(43.8890, 90.7569)

Settings

Variable	Setting
A	1
B	0
C	0
D	-1

Prediction

Fit	SE Fit	95% CI	95% PI
74.2979	6.52826	(60.0740, 88.5218)	(50.8640, 97.7319)

Appendix

Settings

Variable	Setting
A	1
B	0
C	0
D	1

Prediction

Fit	SE Fit	95% CI	95% PI
71.5413	6.52826	(57.3174, 85.7651)	(48.1073, 94.9752)

Settings

Variable	Setting
A	0
B	-1
C	-1
D	0

Prediction

Fit	SE Fit	95% CI	95% PI
95.2112	6.52826	(80.9874, 109.435)	(71.7773, 118.645)

Settings

Variable	Setting
A	0
B	-1
C	1
D	0

Prediction

Fit	SE Fit	95% CI	95% PI
51.8896	6.52826	(37.6657, 66.1135)	(28.4556, 75.3235)

Settings

Variable	Setting
A	0
B	1
C	-1
D	0

Prediction

Fit	SE Fit	95% CI	95% PI
93.8712	6.52826	(79.6474, 108.095)	(70.4373, 117.305)

Appendix

Settings

Variable	Setting
A	0
B	1
C	1
D	0

Prediction

Fit	SE Fit	95% CI	95% PI
43.0996	6.52826	(28.8757, 57.3235)	(19.6656, 66.5335)

Settings

Variable	Setting
A	-1
B	0
C	-1
D	0

Prediction

Fit	SE Fit	95% CI	95% PI
88.3633	6.52826	(74.1395, 102.587)	(64.9294, 111.797)

Settings

Variable	Setting
A	-1
B	0
C	1
D	0

Prediction

Fit	SE Fit	95% CI	95% PI
46.6167	6.52826	(32.3928, 60.8405)	(23.1827, 70.0506)

Settings

Variable	Setting
A	1
B	0
C	-1
D	0

Prediction

Fit	SE Fit	95% CI	95% PI
94.5467	6.52826	(80.3228, 108.771)	(71.1127, 117.981)

Appendix

Settings

Variable	Setting
A	1
B	0
C	1
D	0

Prediction

Fit	SE Fit	95% CI	95% PI
42.2	6.52826	(27.9761, 56.4239)	(18.7661, 65.6339)

Settings

Variable	Setting
A	0
B	-1
C	0
D	-1

Prediction

Fit	SE Fit	95% CI	95% PI
81.86	6.52826	(67.6361, 96.0839)	(58.4261, 105.294)

Settings

Variable	Setting
A	0
B	-1
C	0
D	1

Prediction

Fit	SE Fit	95% CI	95% PI
74.3333	6.52826	(60.1095, 88.5572)	(50.8994, 97.7673)

Settings

Variable	Setting
A	0
B	1
C	0
D	-1

Prediction

Fit	SE Fit	95% CI	95% PI
75.36	6.52826	(61.1361, 89.5839)	(51.9261, 98.7939)

Appendix

Settings

Variable	Setting
A	0
B	1
C	0
D	1

Prediction

Fit	SE Fit	95% CI	95% PI
70.7033	6.52826	(56.4795, 84.9272)	(47.2694, 94.1373)

Settings

Variable	Setting
A	0
B	0
C	0
D	0

Prediction

Fit	SE Fit	95% CI	95% PI
74.23	4.93490	(63.4778, 84.9822)	(52.7255, 95.7345)

Settings

Variable	Setting
A	0
B	0
C	0
D	0

Prediction

Fit	SE Fit	95% CI	95% PI
74.23	4.93490	(63.4778, 84.9822)	(52.7255, 95.7345)

Settings

Variable	Setting
A	0
B	0
C	0
D	0

Prediction

Fit	SE Fit	95% CI	95% PI
74.23	4.93490	(63.4778, 84.9822)	(52.7255, 95.7345)

Appendix III

Anodic and cathodic polarization curves for 25 experiments designed by Box-Behnken design (BBD).